# EFFECT OF INFLAMMATION ON CEFADROXIL PHARMACOKINETICS IN BRAIN AND KIDNEY AND PHARMACOMETRIC MODELING OF PEPT2-MEDIATED DISPOSITION OF GLYCYLSARCOSINE IN BRAIN

**by**

**Yea Min Huh**

A dissertation submitted in partial fulfillment
of the requirements for the degree of
Doctor of Philosophy
(Pharmaceutical Sciences)
in The University of Michigan
2013

Doctoral Committee:

Professor David E. Smith, Chair
Professor Gordon L. Amidon
Associate Research Scientist Meihua R. Feng
Professor Richard F. Keep

## DEDICATION

To my beloved husband Peter Keumseok Koh
for his understanding and endless support,
and my daughter Emma Sevin Koh
for giving me all the happiness everyday

To my parents Mr. Goo-Young Huh and Mrs. Sook-Ja Jung
for their constant love and support

## ACKNOWLEDGMENTS

First of all, I would like to gratefully and sincerely thank my advisor, Dr. David E. Smith, for his guidance and support throughout the whole of my doctoral study. He has always inspired me with his clear vision and critical thinking. His mentorship was not by giving me a direct answer, but by providing me with all the resources needed to find the right direction and allow me to think independently. I believe what I have learned from him during the doctoral study will become the cornerstone for my growing as a true scientist. That is why I owe him a great debt of gratitude.

I would also like to thank all of my committee members: Dr. Richard F. Keep, Dr. Gordon L. Amidon, and Dr. Meihua R. Feng. Dr. Keep has always brought me all the valuable suggestions with his deep knowledge on renal physiology and the central nervous system, which became a big asset for my doctoral research. I sincerely appreciate his guidance and constructive advice. Dr. Amidon, a master in the Pharmaceutical Sciences, came up with all the critical questions, always inspiring me to think about my research in a variety of angles. I also appreciate Dr. Feng for introducing me to Pharmametrics and helping me to learn the statistical modeling. Her guidance led me to choose starting my post-graduate career as a pharmacometrician.

I would like to express my sincere gratitude to all the current and previous members in Dr. Smith's laboratory: Yongjun Hu, Yehua Xie, Xiaomei Chen, Bei Yang, Maria M. Posada, Shupei Wu, Ke Ma, Naoki Nishio, and Scott M. Hynes. Because of their friendship and support, I was able to enjoy my life as a PhD student, even

though sometimes things were not going as smoothly as I had planned. I would especially like to thank Yongjun for teaching me all the experimental techniques and Scott for allowing me to have access to his data for the modeling project.

I also have to thank my friends, current and past students in the department of Pharmaceutical Sciences: Dr. Yajun Liu, Byum-Seok Koh, Oluseyi Adeniyi, Hanna Song, Rae-Sung Chang, Dr. Nahyung Kim, Dr. Juhee Lee, Dr. Jason Baik, Dr. Kefeng Sun, Dr. Kyung-Ah Min, and Dr. Meong-Cheol Shin for their true friendship and help.

I would like to give my special thanks to the wonderful staff in the College of Pharmacy: Maria Herbel, Jeanne Getty, Gail Benninghoff, Mark Nelson, Antoinette, Hopper, and Patrina Hardy for all of their help during my doctoral study. I also would like to thank the department of Pharmaceutical Sciences at the University of Michigan and all the financial support including Amidon Fellowship, Fred W. Lyons Fellowship, Warner/Lambert Fellowship, and Graduate Student Instructorship funding from the College of Pharmacy. Owing to these generous support mechanisms, I was able to continue my studies in the highly academic atmosphere of the University of Michigan without any financial difficulties.

Last, but not least, I sincerely express my deepest gratitude to my parents, Mr. Goo-Young Huh and Mrs. Sook-Ja Jung, for their love, endless support, and encouragement. I also would like to sincerely thank my husband, Peter Keumseok Koh, who has always been a pillar of strength. I cannot think of going through all this time as a PhD student without his endless support and love. I give special thanks to my daughter, a sweet little angel, who always gives me all the happiness.

## TABLE OF CONTENTS

## LIST OF TABLES

## LIST OF FIGURES

## ABSTRACT

The first objective of this dissertation was to investigate the effect of lipopolysaccharide (LPS) – induced inflammation on the systemic pharmacokinetics, tissue distribution, and renal clearance of the PEPT2 substrate cefadroxil. The results demonstrated that blood, CSF and tissue cefadroxil concentrations were markedly increased and tissue-to-blood concentration ratios were decreased by 4.6-fold in choroid plexus and by 2.5-fold in kidney during LPS-induced inflammation. The mRNA expression of PEPT2, OAT1, OAT3 and MRP4 in kidney was mildly reduced in LPS-treated mice without significant changes of transporter expression in choroid plexus. Renal clearance of cefadroxil was substantially decreased by LPS treatment. GFR was reduced by 3-fold in LPS-treated mice, but no significant differences were observed in the fractional reabsorption of cefadroxil and renal secretion normalized by GFR. These findings demonstrate that LPS-induced inflammation has a dramatic effect on the renal excretion of cefadroxil. It appears that changes in transporter expression has played a minor role during LPS treatment and that renal dysfunction, associated with reductions in GFR, is responsible for the substantial increase in cefadroxil plasma concentrations.

The second objective of this dissertation was to develop a population pharmacokinetic model to quantitatively determine the significance of PEPT2 in the efflux kinetics of glycylsarcosine (GlySar) at the blood-cerebrospinal fluid barrier.

The profiles of GlySar in blood, CSF, and kidney were best described by a four-compartment model. The estimated systemic elimination clearance and volume of distribution in the central and peripheral compartments for wild-type versus PEPT2 knockout mice were 0.236 vs 0.449 ml/min, 3.79 vs 4.75 ml and 5.75 vs 9.18 ml, respectively. Total CSF efflux clearance was 4.3 fold higher for wild-type mice compared to knockout animals. NONMEM parameter estimates indicated that 77% of CSF efflux clearance was mediated by PEPT2 and the remaining 23% was mediated by diffusional and bulk clearances.

In conclusion, the findings of this study will help to optimize dosing regimens for renally excreted drugs in severe inflammatory states and for PEPT2 drug substrates for treating CNS diseases in patients whose PEPT2 function is disrupted.

# CHAPTER 1 RESEARCH OBJECTIVES

Over the past half century, it has been increasingly reported that drug absorption and disposition can be altered during an inflammatory response because of changes in plasma proteins, drug metabolizing enzymes and drug transporters. Decreased plasma proteins and downregulated drug metabolizing enzymes during inflammation seem to contribute to increased unbound drug concentrations in plasma and decreased elimination of a drug, respectively. Compared to the well-known impairment of drug-metabolizing enzymes during inflammation, inflammatory-mediated regulation of drug transporters has been reported relatively recently, especially for ATP-binding cassette (ABC) and solute carrier (SLC) transporters. Regulation of ABC and SLC transporters during inflammation has been reported to affect the intestinal absorption, target site distribution, and elimination of drugs through biliary or renal routes. Also, it has been recently demonstrated that peptide transporter 2 (PEPT2) mRNA expression is upregulated in the choroid plexus, in response to peripheral inflammation by lipopolysaccharide treatment, indicating that the PEPT2 gene may also be regulated by inflammatory stimuli. Although inflammation-induced changes in drug kinetics and dynamics have been intensively studied over the past 30 years, the mechanism of these changes has not been fully characterized. This information may be especially critical for drugs with a narrow therapeutic index.

PEPT2 belongs to the proton-coupled oligopeptide transporter (POT) family and plays an important role not only in transporting di- and tripeptides across biological membranes, but also in affecting the pharmacokinetics and pharmacodynamics of peptides/mimetics and peptide-like drugs. Four functional POTs have been identified in human, namely PEPT1, PEPT2, PHT1, and PHT2. Among them, PEPT2 is abundantly expressed and functionally relevant in the kidney and brain. In kidney, PEPT2 is localized to the apical membrane of proximal tubule epithelial cells and is involved in the reabsorption of peptidomimetic drugs such as cefadroxil, enalapril, bestatin, and valacyclovir. In addition to kidney, PEPT2 is localized to astrocytes, ependyma, and epithelial cells of the choroid plexus in brain. It seems that PEPT2 plays an important role in the pharmacokinetics and therapeutic outcome of peptidomimetic drugs at the central nervous system (CNS). Previous studies have demonstrated that PEPT2 facilitates the efflux of substrates (e.g., glycylsarcosine, carnosine, and cefadroxil) from CSF to blood. Therefore, PEPT2 drug substrates, such as the α–amino-containing β-lactam antibiotics, are limited in their use for the treatment of CNS diseases. Since PEPT2 is involved in the elimination and distribution of peptidomimetic drugs, inflammation-mediated changes in this transporter may induce significant alterations in the kinetics and dynamics for a variety of drugs.

Genetically modified animal systems provide a unique opportunity to understand the in vivo role and importance of target proteins in the presence of other drug transporters. Our laboratory has generated PEPT2 knockout mice and successfully demonstrated that the distribution and elimination of PEPT2 drug

substrates are significantly altered when the PEPT2 gene is ablated. By comparing the pharmacokinetic profiles of PEPT2 knockout mice with wild-type animals, it is possible to quantify the importance of this transporter in the disposition of peptidomimetic drugs. The PEPT2 gene is polymorphically expressed in humans with single nucleotide polymorphisms (SNPs) and some genetic variants showing a complete loss of functional activity. It is also possible that PEPT2 expression and/or function may be altered in disease conditions such as inflammation. Therefore, quantitative information about PEPT2-mediated changes in drug disposition during inflammation will help to optimize the dose of peptidomimetic drugs with narrow therapeutic indices for patients whose PEPT2 function is disrupted because of genetic and/or pathophysiological reasons.

With this in mind, we hypothesized that: 1) the expression and functional activity of drug transporters, including PEPT2 and OATs, are altered during inflammation, thereby, affecting the disposition of peptidomimetic drugs; and 2) quantitative information about the importance of PEPT2 in brain distribution kinetics of peptides and peptidomimetic drugs can be obtained using a PEPT2 gene knockout mouse model.

To test the first hypothesis, cefadroxil was used as a model compound. Cefadroxil is a first-generation aminocephalosporin antibiotic with a broad spectrum of antibacterial activity. Previous studies by our group have shown that cefadroxil is a substrate of PEPT2 and that its *in vivo* disposition is mainly influenced by PEPT2. PEPT2 plays an important role in the tubular reabsorption of cefadroxil in kidney and in limiting the exposure of the drug in CSF due to its

function as an efflux pump in choroid plexus. Cefadroxil is also a substrate of the OATs, which are responsible for tubular active secretion of numerous drugs in kidney. Moreover, cefadroxil is highly stable, not metabolized in the body, and predominantly eliminated via renal excretion. Therefore, cefadroxil can be a useful model compound for studying how inflammation-mediated changes in pharmacokinetic determinants, including drug transporters, may affect the disposition of peptidomimetic drugs. Specific aims related to the first hypothesis are: (i) to determine if cefadroxil exhibits changes in disposition during lipopolysaccharide (LPS) - induced acute inflammation; (ii) to understand the mechanism underlying any changes observed in cefadroxil pharmacokinetics during LPS-induced acute inflammation; and (iii) to evaluate possible changes in the expression levels or functional activity of PEPT2 and OATs during any inflammation-mediated changes in cefadroxil pharmacokinetics.

The second hypothesis was investigated using previously generated data on the pharmacokinetics of glycylsarcosine (GlySar), a model PEPT2 substrate, in blood, CSF and kidney of wild-type and PEPT2 knockout mice. Our laboratory reported previously that GlySar concentrations in blood and kidney tissue were significantly lower, whereas CSF concentrations were significantly higher in PEPT2 knockout mice compared to wild-type animals. Based on these findings, we decided to develop a model, which describes the distribution kinetics of GlySar in blood, CSF and kidney, and to quantify the importance of PEPT2 in the distribution kinetics of GlySar especially at the blood-CSF barrier. To describe CSF pharmacokinetics, a nonlinear-mixed effects modeling (NONMEM) method was considered. In clinical

trials, CSF data contain a large degree of variation since limited CSF samples are only available in each subject. NONMEM provides a unique opportunity in this case to address different sources of variability and identify major origins of variability. By parameterizing all the distribution mechanisms in CSF pharmacokinetics, NONMEM can additionally allow us to quantitatively analyze the importance of each distribution mechanism. Therefore, specific aims related to the second hypothesis are: (i) to develop a suitable model that can describe the distribution kinetics of GlySar in blood, CSF and kidney of wild-type and PEPT2 knockout mice using NONMEM; and (ii) to evaluate the relative importance of PEPT2 in the efflux pathways of GlySar at the blood-CSF barrier.

Results of this dissertation are novel in investigating how changes in pharmacokinetic determinants during inflammatory response play a role in the altered disposition of cefadroxil. Moreover, our results also provide quantitative information about the importance of PEPT2 in the CSF efflux pathways of peptidomimetic drugs at the blood-CSF barrier. Overall, our findings will help guide optimized dosing regimens of renally excreted PEPT2 drug substrates during severe inflammation and minimize CNS side effects for patients whose PEPT2 functional activity is disrupted.

# CHAPTER 2 BACKGROUND AND LITERATURE REVIEW

## INFLAMMATION-MEDIATED CHANGES IN DRUG PHARMACOKINETICS

During recent half century, it has been increasingly reported that many pharmacokinetic determinants are modified under inflammation states such as plasma protein binding, drug metabolizing enzymes and drug transporters (Figure 2.1). These changes can induce significant alterations in absorption, distribution, metabolism and elimination of a drug, so that dose adjustment would be necessary to meet both efficacy and safety concerns of a drug. Even though changes in pharmacokinetics during inflammatory response has been largely reported, there is still a lack of knowledge about the full spectrum of how inflammation-associated changes in various drug disposition mechanisms are involved in inducing altered pharmacokinetic and pharmacodynamic properties of a drug. This information may be especially critical for drugs with a narrow therapeutic index.

### Changes in Absorption

In severe inflammation, such as hyperdynamic sepsis, local blood flow dysregulation has been reported, which can induce significant reduction in perfusion of muscles, skin and splanchnic organs (Gavin et al., 1994). Therefore, absorption from the site of decreased blood flow becomes incomplete and circulatory status is also disrupted (Power et al., 1998). Many drugs are

recommended to be administered intravenously because of the poor absorption from oral, transdermal, subcutaneous and intramuscular routes in severe inflammation. Gut hypomotility, a lower gastrointestinal pH during sepsis can also cause variability in oral bioavailability. On the other hand, an oral drug with extensive first-pass metabolism may exhibit increased bioavailability during inflammation when the hepatic dysfunction is observed in patients (Verbeeck and Horsmans, 1998).

### Changes in Distribution

Several determinants of drug distribution have reported to undergo changes during inflammation, including tissue perfusion, tissue permeability and protein binding. These changes can alter volume of distribution for the administered drug and induce corresponding increase or decrease of drug concentrations in plasma.

It has been reported that cardiac output is redistributed during severe inflammation moving aside from less vital organs to vital organs such as heart and brain. This redistributed blood induces decreased blood flow in microcirculation causing impaired tissue perfusion and drug distribution into certain tissues. Several studies have identified the impact of reduced tissue perfusion on drug distribution during inflammation. When gentamicin was given to septic animals intravenously, gentamacin concentrations in peripheral small vessels were significantly lower than central venous concentrations (Flournoy et al., 1983, Beller et al., 1983, Hinshaw et al., 1984). Roberts et al. also reported that subcutaneous tissue concentrations of piperacillin were 1-5-fold lower than plasma concentrations in septic patients (Roberts et al., 2009). Therefore, higher dose of antibiotics would be necessary for

the septic patients with impaired tissue perfusion to achieve the target concentrations in tissue.

Fluid shift because of the increased tissue permeability is also commonly observed during severe inflammation such as septic shock. During an inflammation, endothelial damage is promoted by various endogenous mediators, which results in increased capillary permeability (Bochud and Calandra, 2003, Bone, 1991, Glauser et al., 1991). The capillary leak leads to fluid shift from the intravascular space to the interstitial space called a 'third spacing' phenomenon. This process can increase volume of distribution for hydrophilic drugs having relatively small volume of distribution such as beta-lactam antibiotics, which results in significant reduction in plasma and tissue concentration of drugs (Joynt et al., 2001, Lipman et al., 2001). For example, it has been reported that gentamicin volume of distribution was increased in hyperdynamic state of sepsis, whereas this changes in volume was not observed in hypodynamic state of sepsis (Tang et al., 1999). Therefore, changes in volume of distribution during inflammation need to be monitored for hydrophilic anitibiotics to adjust the dose to maintain drug concentrations above the minimum inhibitory concentration (MIC).

Changes in plasma protein binding during inflammation are associated with alterations in concentrations of the plasma proteins, competition with endogenous substances for the binding site of proteins, and conformational changes of plasma proteins (De Paepe et al., 2002). It has been reported that concentration of $\alpha_1$-acid glycoprotein, the major binding plasma protein for basic drugs, is increased during severe inflammation (Lamy, 1989). Increased concentration of $\alpha_1$-acid glycoprotein

will be reflected in decrease of unbound drug concentration in plasma and tissue distribution. On the other hand, decreased concentration of serum albumin, which commonly binds to acidic and neutral drugs, is often observed during an inflammatory response (Ruot et al., 2002, Moshage et al., 1987, Don and Kaysen, 2004). This will lead to the increase in unbound drug concentration of highly bound drugs and corresponding increase in tissue distribution. It has been also demonstrated that endogenous metabolites are significantly accumulated and conformation of albumin molecule is changed during sepsis associated with hepatic and renal failure, resulting in significant decrease of drug binding to plasma proteins (Bodenham et al., 1988, Elston et al., 1993). These changes can also increase the unbound drug concentrations especially for highly protein-bound drugs.

### Changes in Metabolism

Hepatic metabolism is the major elimination route for various drugs. Hepatic clearance (CL) can be expressed using the venous equilibrium model:

$$CL = \frac{Q_H \bullet f_u \bullet CL_{\text{int}}}{Q_H + f_u \bullet CL_{\text{int}}}$$

where $Q_H$ represents hepatic blood flow, $f_u$ represents unbound fraction of a drug in blood, and $CL_{int}$ represents intrinsic clearance, describing intrinsic ability of hepatic enzymes in metabolizing drugs. Therefore, changes in each of the three parameters during inflammation can induce alteration of hepatic metabolism. The impact of each parameter on drug metabolism especially depends on whether the drug is a high extraction or a low extraction compound. On the other hand, hepatic

metabolism of the drugs with an intermediate extraction ratio can be influenced by all the three parameters.

Drugs with a high extraction ratio have an extensive intrinsic metabolism in the liver ($f_u \bullet CL_{int} >> Q_H$) and hepatic clearance of these drugs primarily depends on hepatic blood flow ($CL \approx Q_H$). Therefore, any changes in hepatic blood flow during inflammation can affect hepatic metabolism of highly extracted compounds. Animal studies have shown that hepatic blood flow is either increased or not changed during hyperdynamic sepsis, whereas hypodynamic phase induces a reduction of hepatic blood flow (Wang et al., 1991a, Wang et al., 1991b, Wang et al., 1992, Wang et al., 1993, Bersten et al., 1992, Wyler et al., 1969, Ayuse et al., 1995). A few clinical studies are available to show altered pharmacokinetics of highly extracted drugs during inflammation. Macnab et al. reported that morphine clearance was significantly reduced in patients with septic shock, which may be attributable to the reduced liver blood flow (Macnab et al., 1986). Groeger et al. also showed that substantial reduction in naloxone clearance in septic patients seemed to be associated with decreased hepatic perfusion (Groeger and Inturrisi, 1987).

Hepatic clearance of drugs with a low extraction ratio is primarily dependent on the unbound fraction of drugs and intrinsic metabolizing activity of hepatic enzymes, since those drugs have a low intrinsic metabolism in the liver ($f_u \bullet CL_{int} << Q_H$ and $CL \approx f_u \bullet CL_{int}$). Therefore, changes in unbound fraction or hepatic enzyme activity can induce alterations in hepatic metabolism of low extraction drugs. It has been previously discussed that protein bindings are altered during inflammation. For example, concentration of $\alpha_1$-acid glycoprotein, the major binding plasma

protein for basic drugs, is reported to be increased during severe inflammation. Therefore, hepatic clearance of clindamycin, which highly binds to $\alpha_1$-acid glycoprotein and has a low extraction ratio, was significantly decreased during hyperdynamic sepsis partly due to the increased protein binding (Mann et al., 1987).

Reduced hepatic enzyme activity is also commonly observed during inflammation. Possible underlying mechanism is associated with decreased efficiency of hepatic enzymes or decreased enzyme expression (Power et al., 1998, Bodenham et al., 1988, Pentel and Benowitz, 1984). Reduced organ perfusion and hypoxia during severe inflammation can disrupt the efficiency of hepatic enzymes, which leads to decreased metabolism of low extraction drugs (Park, 1996). Moreover, downregulation of drug metabolizing enzymes during inflammation has been intensively studied over the past 20 years and is now well identified. Cytokines released during inflammation is reported to modify the function of gene transcription factors such as PXR and NF-κB, resulting in repression of most cytochrome P450 genes (Figure 2.2.) (Morgan et al., 2008). Other proposed mechanism is associated with increased nitric oxide production during inflammation by cytokine-mediated stimulation of nitric oxide synthase 2, which leads to inhibition of P450 activities or downregulation of P450 gene expression (Aitken et al., 2006). This inflammation-induced decrease of P450 enzymatic activity can induce severe drug toxicity because of the decreased clearance of drugs. For example, when children were infected with influenza virus, inflammatory cytokines released responding to the virus induced significant loss of CYP1A2, which resulted

in large accumulation of theophylline given to the young patients and corresponding increase in drug toxicity such as convulsions (Kraemer et al., 1982).

### Changes in Elimination

Kidney is the major eliminating organ for a variety of both parent drug and metabolites. Changes in renal elimination during inflammation have been relatively well studied compared to biliary excretion or pulmonary excretion. Renal excretion of a drug can be either increased or decreased during inflammatory response. The hyperdynamic phase of sepsis is characterized by an increased cardiac output resulting in increased renal blood flow and a corresponding increase of glomerular filtration rate (GFR). As a result, renal clearance of a drug being predominantly renally excreted can be significantly increased exhibiting low drug concentrations in plasma (Udy et al., 2010). For example, β-lactam antibiotics are mainly renally excreted drugs and subtherapeutic plasma concentrations of a drug have been largely reported in critically ill patients with sepsis because of the increased GFR (Lipman et al., 2003, Wells and Lipman, 1997). More frequent dosing or continuous infusion of beta-lactam antibiotics is recommended for these patients to maintain the drug concentrations above the minimum inhibitory concentration (MIC) (Lipman et al., 2001).

On the other hand, substantial reduction in GFR is commonly observed in hypodynamic septic shock associated with lowered cardiac output leading to a significant reduction in clearance of drugs (Pentel and Benowitz, 1984). Reduced GFR by inflammatory stimuli has also been well demonstrated from the animal models (Schmidt et al., 2007, Wang et al., 2003, Wang et al., 2008). Renal

dysfunction associated with reduced GFR can be reflected as substantial increase in plasma concentrations of a drug. This information is especially critical for drugs with a narrow therapeutic index. For example, aminoglycoside antibiotics are mainly renally excreted drugs with a narrow therapeutic range. In acute renal failure developed during sepsis, a high risk of oto- and nephrotoxicity for aminoglycoside has been reported because of the reduced clearance. Therefore, reducing the dose or increasing the dosing interval of aminoglycoside should be considered for septic patients with renal dysfunction not to exceed the therapeutic range of the drug (Jellett and Heazlewood, 1990, St Peter et al., 1992).

Impacts of inflammation on nonrenal drug elimination such as biliary or pulmonary excretion have not been extensively studied. However, it is speculated that biliary and pulmonary drug excretions are theoretically decreased during severe inflammation, since hepatic obstruction of bile flow and acute respiratory distress syndrome have been reported in patients with septic shock (Verbeeck and Horsmans, 1998, Wheeler and Bernard, 1999).

### Changes in Drug Transporters during Inflammation

Compared to the well-established impairment of drug metabolizing enzyme during inflammation, inflammation-mediated regulation of drug transporters was recognized relatively recently. Since drug transporters play an important role in absorption from the GI tract, distribution into target sites, and elimination through biliary and renal routes, changes in drug transporters during inflammation can induce significant alterations in drug pharmacokinetics. Downregulated mRNA and protein expression of ATP binding cassette (ABC) transporters such as PGP and

MRPs has been reported during inflammatory response in brain, liver, and intestine, thereby affecting brain efflux, biliary clearance and intestinal absorption of drug substrates (Hartmann et al., 2002, Piquette-Miller et al., 1998, Hartmann et al., 2001, Tang et al., 2000). It has been also demonstrated that mRNA and protein expression of solute carrier (SLC) transporters such as OATs and OATP2 are downregulated in brain, liver and kidney, which was translated into significant reduction in renal clearance of a substrate, para-amino hippurate (Goralski et al., 2003, Hocherl et al., 2009). More recent study has also shown that peptide transporter 2 (PEPT2) mRNA expression is upregulated in choroid plexus responding to the peripheral inflammation by LPS treatment (Marques et al., 2009).

The mechanisms underlying inflammation-mediated regulation of drug transporters are still not fully characterized. However, it seems that proinflammatory cytokines such as IL-6 and IL-1β are involved in inflammation-mediated downregulation of ABC transporters (Hartmann et al., 2001, Hartmann et al., 2002). It has been reported that proinflammatory cytokines induces transcription factors which play a role in suppressing expression of the ABC transporters (Sukhai et al., 2000, Ho and Piquette-Miller, 2007). More recent study showed that nuclear hormone receptor, pregnane X recepter (PXR), is involved in downregulatory gene expression of hepatic drug transporters during inflammation (Teng and Piquette-Miller, 2005). PXR activation responding to hormones and xenobiotics is known to mediate an induction of several genes for drug transporters and P450 genes. Also, it has been observed that PXR expression is downregulated during inflammatory response (Morgan et al., 2008). Therefore, endotoxin or IL-6

mediated downregulation of MRP2 expression was observed in PXR (+/+) mice, whereas this was not observed in PXR (-/-) mice (Teng and Piquette-Miller, 2005).

## PROTON-COUPLED OLIGOPEPTIDE TRANSPORTER

The peptide transporters PEPT1 and PEPT2 belong to the Proton-Coupled Oligopeptide Transporters (POT) and are responsible for the cellular uptake of di- and tripeptides in the organism. There are four members in the POT family in mammals: PEPT1 (SLC15A1), PEPT2 (SLC15A2), PHT1 (SLC15A4) and PHT2 (SLC15A3). Expression cloning techniques in the mid-1990s allowed POTs encoding genes to be identified. PEPT1 was firstly cloned from a rabbit intestinal cDNA library (Fei et al., 1994) and PEPT2 was next identified and cloned from a human kidney cDNA library (Liu et al., 1995). PHT1 and PHT2 were cloned more recently from a rat brain cDNA library (Yamashita et al., 1997, Sakata et al., 2001) and have been demonstrated *ex vivo* to recognize not only di- and tripeptides, but also L-histidine, which differs from PEPT1 and PEPT2. However, after their cloning, no further studies have been done on their substrate specificity and nothing is known about their pharmaceutical and pharmacological relevance (Brandsch et al., 2008). The protein sequences of PHT1 and PHT2 show very weak similarity to PEPT1 and PEPT2 (32% and 27%, respectively), while PEPT1 and PEPT2 have about 50% of sequence homology (Botka et al., 2000).

PEPT1 and PEPT2 have 700-730 amino acid residues and contain twelve transmembrane domains and a large extracellular loop between the ninth and tenth transmembrane domains (Figure 2.3) (Daniel and Kottra, 2004). Both amino and carboxy termini face the cytoplasmic side. The construction of chimeras of PEPT1

and PEPT2 has provided evidence that the four $NH_2$-terminal transmembrane regions and domains 7-9 play an important role in determining the substrate affinity (Doring et al., 1996, Fei et al., 1998, Terada et al., 2000). It is also revealed that transmembrane domain 5 of human PEPT1 forms a part of the substrate translocation pathway (Kulkarni et al., 2003a) and the extracellular end of transmembrane domain 7 provides the basis for channel opening and substrate translocation (Kulkarni et al., 2003b). Also, site-directed mutagenesis studies have identified residues that are important for transport characteristics. For example, histidine 57 in the second transmembrane domain has been demonstrated to be involved in binding and translocation of $H^+$ during the conformational change of the protein when transporting peptides in a cotransport mode (Uchiyama et al., 2003). It has also been shown that tyrosine 56, 64, and 167 are involved in substrate affinity and substrate translocation (Chen et al., 2000, Aronson et al., 1982). However, the three dimensional structures of these transporter proteins are still unknown.

The driving force of peptide transporters is an inwardly directed electrochemical $H^+$ gradient. There is an acidic microclimate at the epithelia of intestine and kidney and this $H^+$ gradient is established and maintained by the apical $Na^+/H^+$ antiporter, NHE3 (Aronson et al., 1982). The driving force of $Na^+/H^+$ antiporter is the inwardly directed $Na^+$ gradient established by basolateral $Na^+$-$K^+$-ATPase. Peptide transporters, which are $H^+$/peptide cotransporters, transport peptides against a concentration gradient using an inwardly directed electrochemical $H^+$ gradient, thereby accumulating peptides inside of cells. However,

it is still unclear how the accumulated peptides are effluxed through the basolateral membrane and whether there are any other driving forces contributing to this basolateral efflux of the peptides (Figure 2.4).

The expression of peptide transporters in mammalian tissues is unique for the different POTs. PEPT1 is functionally expressed in the brush border membrane of epithelial cells of the small intestine (rat and human) (Ogihara et al., 1996, Groneberg et al., 2001) and S1 segments of the early convoluted proximal tubule of rat kidney (Shen et al., 1999). PEPT1 expression and function at the extrahepatic biliary duct have also been elucidated (Knutter et al., 2002). On the other hand, PEPT2 is predominantly localized in S3 segments of the latter proximal tubule of rat kidney (Groneberg et al., 2004). It also has been detected in the lung, brain (specifically in astrocytes, sub-ependymal cells, ependymal cells and choroid plexus), and mammary gland (Groneberg et al., 2004, Meredith and Boyd, 2000, Berger and Hediger, 1999). The tissue distribution of peptide transporters is summarized in Table 2.1.

PEPT1 displays low-affinity and high-capacity, whereas PEPT2 has high-affinity and low-capacity. Both transporters have exceptionally broad substrate specificity. They generally accept all possible di- and tripeptides in a stereospecific manner, while amino acids and tetrapeptides are unable to be transported. However, preferred structural features of PEPT1 and PEPT2 exist: (1) a peptide backbone of 2-3 amino acid residues which can be replaced by a ketomethylene group, (2) L-amino acids, (3) a trans conformation of peptide bonds, (4) a free N-terminal α-amino group, (5) an acidic or hydrophobic function at the C-terminus,

and (6) the presence of hydrophobic side chains (Brandsch et al., 2008, Kamal et al., 2008). In addition to natural di- and tripeptides, foreign compounds are also able to be recognized by peptide transporters, including amino β-lactam antibiotics (especially, cephalosporin and penicillin classes), certain angiotensin-converting enzyme inhibitors, renin inhibitors, antitumor agents such as bestatin, dopamine receptor antagonists such as sulpride and various amino acid ester prodrugs (e.g. Valcyclovir) (Rubio-Aliaga and Daniel, 2002, Brandsch et al., 2008, Biegel et al., 2006). The differences in substrate recognition between PEPT1 and PEPT2 have also been studied. The main differences are the following (Biegel et al., 2006):

- PEPT2 generally accepts the same substrates as PEPT1, but it has a higher affinity and lower capacity.
- PEPT2 has a higher binding affinity for the substrates with more hydrophobicity. This was not applicable to PEPT1.
- PEPT2 has higher affinities for the β-lactam antibiotics containing an α-amino group than PEPT1.
- Tripeptides with a charged amino acid in position 3 exhibit low binding affinities to PEPT2 and high binding affinities to PEPT1.
- PEPT2 has more specific and confined requirements for substrate recognition in general.

Recent studies have found that peptide transporters are regulated under a variety of conditions. The regulation of peptide transporters can be classified as physiological, pathological, and pharmacological regulations (Adibi, 2003, Terada and Inui, 2007). In terms of physiological factors, oligopeptides (Walker et al.,

1998), various hormones such as thyroid hormone, insulin and leptin (Thamotharan et al., 1999, Buyse et al., 2001, Ashida et al., 2002), cytokines (interferon-γ and tumor necrosis factor-α) (Buyse et al., 2003, Vavricka et al., 2006), development (Shen et al., 2001, Hussain et al., 2002), and diurnal rhythm (Pan et al., 2002, Pan et al., 2003, Pan et al., 2004) are known to regulate intestinal PEPT1. For example, leptin has been shown to increase PEPT1-mediated transport activity with a short-term exposure (Buyse et al., 2001). In terms of pathological factors, the expression of intestinal PEPT1 in rats was mainly regulated at the transcriptional level under various nutritional metabolic conditions (high-protein diet (Erickson et al., 1995, Shiraga et al., 1999), fasting (Pan et al., 2003, Erickson et al., 1995), and diabetes (Gangopadhyay et al., 2002)), whereas regulation of protein expression level was reported under the chronic renal failure (Shimizu et al., 2005). It has also proven that patients having intestinal disease such as Crohn's disease and ulcerative colitis exhibit up-regulated PEPT1 mRNA and protein expression in colon (Merlin et al., 2001). Lastly, pharmacological studies have shown that the mRNA expression of PEPT1 was up-regulated by agents such as pentazocine (Fujita et al., 1999) and 5-fluorouracil (Tanaka et al., 1998, Inoue et al., 2005). Compared to intensive studies about PEPT1 regulation, there is little data available on how PEPT2 is regulated under various conditions. Using a cell culture model, it has been found that PEPT2 is regulated by intracellular $Ca^{2+}$ (Wenzel et al., 1999) and epidermal growth factor (Bravo et al., 2004). Moreover, hypothyroidism (Doring et al., 2005) and thyroidectomy (Lu and Klaassen, 2006) of rats were reported to increase mRNA and protein expression levels of renal PEPT2.

Inflammation-mediated regulation of drug transporters has been previously focused on ABC transporters. However, a few studies have reported that peptide transporters are also changed during inflammatory response in either expression or functional level. In inflammatory bowel disease (IBD) patients, PEPT1 expression in colon, which does not express PEPT1 in normal condition, was shown to be upregulated (Merlin et al., 2001). Transcriptional upregulation of PEPT1 has also been reported in small intestine responding to *Crystosporidium Parvum* induced malnutrition (Barbot et al., 2003). On the other hand, PEPT1 mRNA expression of small intestine was significantly decreased when rats were treated with LPS (Shu et al., 2002). A recent study also reported that LPS-induced peripheral inflammation upregulated PEPT2 mRNA expression in choroid plexus (Marques et al., 2009).

After genetic information of people has been available, individual treatment and personalized dosing regimen are becoming important. Genetic information of peptide transporters can contribute to the personalized medicine since pharmacokinetics of peptidomimetic drugs can be changed by the genetic variability of peptide transporters. Several reports have already revealed that PEPT1 and PEPT2 genes are polymorphically expressed in humans using different genomic DNA sample collections. Non-synonymous PEPT1 single nucleotide polymorphisms (SNPs) have been reported from Zhang's and Anderle's studies (Anderle et al., 2006, Zhang et al., 2004). However, characterization of the variants revealed no significant differences in substrate transport. It seems that a high evolutionary pressure on PEPT1 prevents the survival of mutations which may result in severe loss of function (Brandsch et al., 2008). PEPT2 gene was also found to be polymorphically

expressed in humans with single nucleotide polymorphisms (Pinsonneault et al., 2004, Terada et al., 2004). Unlike PEPT1, genetic variant R57H of PEPT2 showed complete loss of GlySar transport activity (Terada et al., 2004). Therefore, it is possible that genetic variability in PEPT2 gene affects the pharmacokinetic profiles of peptide-like drugs.

## CHOROID PLEXUS STRUCTURE AND FUNCTION

### Choroid Plexus Anatomy and Physiology

The choroid plexuses, located in the four ventricles of the brain, form a barrier between the cerebrospinal fluid (CSF) and the blood compartment. They play an important role in the formation and regulation of CSF. The CSF is formed in the choroid plexuses and secreted out of the ventricles into the subarachnoid space. Due to this production of CSF, the concentration of compounds that are either produced endogenously or passively diffused from outside of the brain can be kept low in the CSF (Smith et al., 2004).

The choroid plexus is composed of a single layer of cuboidal epithelial cells surrounding the central stroma. The apical side of epithelial cells forms numerous microvilli and some cilia. Underneath the microvilli, the adjacent epithelial cells are linked by tight junctions. Compared to the Blood Brain Barrier (BBB), the tightness of the epithelial cells appears not that complete, thereby making a much leakier barrier with an electrical resistance of about 150-175$\Omega \bullet cm^2$ (that of the BBB is about 8000$\Omega \bullet cm^2$) (Smith et al., 2004, Smith and Rapoport, 1986). Therefore, it is possible that this relatively leaky barrier tissue contributes to a great potential of

the choroid plexus for transporting drugs from blood to the brain compartment. Moreover, fenestrated endothelium of the plexus parenchyma also contributes to this enhanced paracellular pathway. The capillaries within the choroid plexus parenchyma are fenestrated, which differ from those of the BBB, so that they allow free movement of molecules across the endothelial cells through fenestrations and intercellular gaps (Figure 2.5) (Engelhardt and Sorokin, 2009).

Epiplexus cells or Kolmer cells are closely associated with the epithelial microvilli in the choroid plexus. They show typical ultrastructural features of active macrophages. Although their exact origin is still not fully understood, there is evidence that they comes from monocytic origin and may serve as barrier-associated antigen presenting cells, which may be associated with immunosurveillance of the central nervous system (CNS) (Engelhardt and Sorokin, 2009).

### Drug Transport at the Choroid Plexus

There are several kinds of regulatory mechanisms that could affect the exchange processes across the blood-CSF barrier in the choroid plexus; tight junctions which link the choroid plexus epithelial cells, metabolic processes limiting movements of molecules between blood and CSF, and inwardly or outwardly directed transporter proteins.

First, the presence of tight junctions restricts the paracellular route across the blood-CSF barrier. These tight junctions particularly restrict the transport of polar compounds, which are not substrates for transporters.

Second, the choroid plexus is a major site of drug metabolism in the brain and this feature modulates the cerebral biodisposition of drugs. It expresses a variety of enzymes that degrades drug molecules such as cytochrome P-450-dependent monooxygenases, epoxide hydrolase, carboxy-, amino-, and endopeptidases. The large GSH concentration and antioxidant enzyme activities also contribute to keeping oxidant species at the low steady-state level in the choroid plexus. The cellular and regional distribution of drug metabolizing enzymes in the brain is heterogenous, with the blood-brain interfaces bearing special drug metabolic capacities (Ghersi-Egea et al., 1995, Ghersi-Egea et al., Strazielle and Ghersi-Egea, 2000). Due to the high activity of these enzymes involved in drug biotransformation and reactive species inactivation, the choroid plexuses appear unique among all brain structures (Strazielle et al., 2004).

Third, the choroid plexus possesses a variety of transporter proteins that act as physical barriers to allow either inward or outward movement of molecules across the blood-CSF barrier (BCSFB). Inwardly directed basolateral transporter proteins can facilitate entry of molecules (e.g., nutrients) into the CSF, whereas outwardly directed apical transporter proteins can increase the elimination of undesired molecules (e.g., drugs and CSF-borne endogenous metabolites) into the blood. The main drug transporters in the choroid plexus belong to two superfamilies of transporters, the solute carrier (SLC) family including OAT1-3, OATP3, and PEPT2, and the ATP-binding cassette (ABC) carrier family including P-gp and MRP1. Other transporter proteins displaying relatively narrow substrate specificity, such as the nucleoside transporters, are also present in the choroid plexus. Their

distributions are polarized and thereby allow efficient movement of drug substrates across the BCSFB (Figure 2.6) (Keep and Smith, 2011).

### Role of the Choroid Plexus in Drug Delivery into the Brain

Even though the regulatory mechanisms previously discussed can restrict the drug transport across the BCSFB, it is possible that the choroid plexus plays a more important role in delivery of certain drugs into the brain than BBB, which is usually the major site of drug molecule exchange between the brain and blood, due to the following reasons. First, the choroid plexus epithelial cells have a large surface area because of the basolateral infoldings and numerous apical microvilli, thereby serving a large surface for exchange of drug molecules between the CSF and the blood compartment. Second, the weak tight junctions linking epithelial cells of choroid plexus allow having relatively high permeability compared to the BBB. Highly polar drugs, which are mainly transported through paracellular pathway, can be more easily transported through the BCSFB than through the BBB. For example, stavudine (D4T), a highly hydrophilic drug, can slowly but significantly diffuse into the CSF, while being excluded at the BBB (Thomas and Segal, 1998). Third, the choroid plexus constitutes a direct access to the ventricles, ependyma and subependymal tissue, leptomeninges, velae, outerlayers of pial vessels, and perivascular spaces (Ghersi-Egea et al., 1996a, Ghersi-Egea et al., 1996b). For the treatment of infectious diseases such as meningitidis or AIDS, perivascular spaces and meningeal areas are important target. Moreover, antiretroviral agents should reach macrophagic cells primarily found in the subarachnoid spaces and periventricular spaces, especially during the early phase of the infection (Atwood et

al., 1993). Therefore, the choroid plexus can be a useful target for drug delivery to the brain in several CNS diseases.

### Role of PEPT2 in Drug Delivery in the Choroid Plexus

Peptides have been regarded as a potential target for several CNS disorders. Therefore, peptide agonists and antagonists have been proposed as useful agents in the treatment of Alzheimer's disease, cerebral acquired immunodeficiency syndrome, stroke and so on (Partridge, 1991). Choroid plexus can be used as an entry of these peptides drug into the interstitial fluid of the brain. However, it is possible that the polarized expression of PEPT2 on the apical side of the choroid plexus membrane restricts the residence of the drugs inside the CNS compartment. PEPT2 is expressed at the apical side of the epithelium in choroid plexus and plays a role as an efflux pump at the BCSFB, continuously pumping out the drug molecules from CSF to the blood (Figure 2.6). Therefore, choroid plexus is believed to be the predominant site for elimination of β-lactam antibiotics from the CSF (Suzuki et al., 1997). For example, aminocephalosporins are transported to the CSF through the paracellular or CSF bulk flow pathway in choroid plexus at a reasonable amount, but are rapidly removed by the efflux system of PEPT2. When whole tissue uptake study was performed using choroid plexus of wild type and PEPT2 knockout mice with cefadroxil as a model compound, the cefadroxil uptake into choroid plexus was substantially reduced in PEPT2 null mice as compared to wild type controls under physiological conditions (Ocheltree et al., 2004). Therefore, drugs with no or minimal affinity for PEPT2 (e.g., cefuroxime, moxalactaam, cefotaxime, ceftriaxone, cefepime, and ceftizoxime) are more likely to be useful for treating CNS diseases

such as meningitis. These drugs all lack an α-amino group, which is one of the key substrate-recognition criteria for PEPT2 (Smith et al., 2004). Understanding the role and substrate specificity of PEPT2 in the choroid plexus will play a critical role for future drug design to treat the CNS diseases.

## Choroid Plexus Drug Transport in CNS Diseases

It has been reported that choroidal drug transport systems are altered in CNS diseases. These alterations come from two types of changes, morphological changes and functional changes of transporter proteins. For morphological changes, loss of the apical microvilli, severe vacuolization and mitochondria alterations have been reported in experimental autoimmune encephalomyelitis (EAE), the model for the study of multiple sclerosis (Engelhardt et al., 2001). Similar alterations of choroid plexus microvilli have also been reported in other animal models of CNS diseases, such as intraventricular injection of lipopolysaccharide (LPS) (Endo et al., 1998), transient forebrain ischemia (Johanson et al., 2000), and murine influenza virus encephalomyelitis (Miyoshi et al., 1973). However, these changes of the choroid plexus can be recovered rapidly (Johanson et al., 2000, Davet et al., 1998) and the tight junctions of the choroid plexus appear relatively resistant to different types of stress, such as EAE and anti-orthostatic restraints (Masseguin et al., 2001, Wolburg et al., 2001).

The functional changes of the choroid plexus in CNS diseases have not been extensively studied yet, but there are several evidence to indicate that functional changes of the choroid plexus itself and transporter proteins of it can contribute to altered drug transport. First, multiple signaling agents such as pro-inflammatory

cytokines are produced by brain cells during neuroinflammation or neuroinfection and, thus, there can be interactions between drugs and endogenous substrates for both choroid plexus transporters and metablic enzymes, allowing choroidal drug transport to be changed (Strazielle et al., 2004). Second, the active transcellular clearance of organic anion (phenol red) in the choroid plexus was strongly impaired by exposure to the inflammatory stimuli, tumor necrosis factor α (TNFα) and interleukin 1 (IL1) without any alteration of the structural integrity of the epithelium (Strazielle et al., 2003). Third, the CSF level of penicillins was increased upon induction of experimental meningitis in animals and in bacterial meningitis of human (Spector and Lorenzo, 1974). This result agrees with the reduced uptake of benzylpenicillin (BPC) in the choroid plexus of rats with experimental inflammation (Han et al., 2002). A nitric oxide (NO) production is reported to be associated with this functional impairment of BPC transport in LPS-induced inflammation. Overall, these data indicate that the altered function of transporter proteins in CNS diseases can contribute to changes in the pharmacokinetics of drugs in the brain.

The morphology of the choroid plexus and its function of secreting CSF are significantly deteriorated in aging and neurodegenerative diseases. In Alzheimer's disease, a strong thickening of basal membranes has been reported together with a major atrophy of the epithelium, stroma fibrosis and frequent immune complex deposition. These changes can also lead to strongly impaired CSF and protein secretion as well as the function of transporter proteins, thereby altering drug pharmacokinetics in CSF (Preston, 2001, Serot et al., 2003).

## CEFADROXIL

### Chemical Structure and Pharmacological Properties of Cefadroxil

Cefadroxil is a first-generation amino-cephalosporin antibiotic with a broad spectrum of antibacterial activity. While older drugs of cephalosporins have shown a short half-life and rapid renal clearance, cefadroxil could overcome these drawbacks by chemical manipulations, placing a *para*-hydroxy group on the aromatic ring of cephalexin (Figure 2.7). It has good water solubility and fair degree of lipid solubility. Its apparent pKa's are 2.64, 7.30 and 9.69 at 35°C (Connors et al., 1986).

The mechanism of bactericidal activity is similar as penicillins, inhibiting the enzymatic reactions necessary for the production of a stable bacterial cell wall (Tanrisever and Santella, 1986). Cefadroxil binds to specific penicillin-binding proteins (PBPs), which are located inside of the bacterial cell wall, causing the inhibition of cross-linking of peptydoglycan, a basic step of bacterial cell wall synthesis. This inhibition interrupts the equilibrium between degradation and formation of new bonds and then cell lysis was induced by bacterial autolysins, a bacterial cell wall autolytic enzyme (Brunton et al., 2006).

Cefadroxil is broadly effective in Gram-positive and Gram-negative bacterial infections; it is active against most Gram-positive cocci, except enterococci and methicillin-resistant staphylococci, whereas only *Escherichia coli, Klebsiella pneumoniae* and *Proteus mirabilis* of Gram-negative enteric bacilli are susceptible to this drug. It has been shown that cefadroxil can cure infections of many tissues,

including upper and lower respiratory tract, urinary tract, skin, and soft tissues. Since it is widely distributed to body tissues and fluids, cefadroxil can be useful treatment for infections of such a variety of tissues. Especially, cefadroxil is highly effective in the treatment of upper and lower respiratory tract infections such as sinusitis otitis media, acute bronchitis and lung abscesses (Quintiliani, 1986).

The side effects of cefadroxil are usually mild and can be easily recovered. The most common side effects are nausea, vomiting, diarrhea and upset stomach. Hypersensitivity reactions such as skin rashes and dermatitis have also been rarely reported. Therefore, it is contraindicated for patients with known allergic reactions to other cephalosporin antibiotics (Queener et al., 1986).

### Pharmacokinetic Properties of Cefadroxil

The pharmacokinetic profile of cefadroxil showed complete absorption from the gastrointestinal tract, wide distribution into body tissues, and slower rate of excretion than other oral cephalosporins (Tanrisever and Santella, 1986, Nightingale, 1980). Food does not affect the absorption of cefadroxil and, therefore, it can be administered regardless of food intake. Cefadroxil is extensively distributed to body tissues because of its good water solubility and a fair degree of lipid solubility. Approximately 20% of the drug is reported to be bound to plasma proteins. Cefadroxil is not metabolized in the body and, therefore, it is mainly eliminated via renal excretion. It has been reported that 88 to 93% of the administered dose was recovered in the urine within 24 hours (Nightingale, 1980). Therefore, elimination of cefadroxil is substantially reduced in patients with

impaired renal function (Leroy et al., 1982). The half-life is about 1.5 hours, which is longer than that of other oral cephalosporins of the same generation.

### Transport Mechanism of Cefadroxil

Cefadroxil exists as a zwitterion at physiological pH and because of this hydrophilic feature; it is more likely to be transferred across the cell epithelium by drug transporters. Previous studies have shown that cefadroxil is a substrate of several drug transporters, including organic anion transporters (OATs), organic anion transporting peptides (OATPs), peptide transporters (PEPT1 and PEPT2) and multidrug resistance-associated protein 4 (MRP4) (Table 2.2). Since antibacterial activity of cefadroxil depends on drug exposure at target site, full characterization of molecular mechanism on drug transport across different tissues may help us to understand the characteristics of cefadroxil disposition in the body.

In small intestine, it has been reported that PEPT1 plays a critical role in the absorption of cefadroxil (Inui et al., 1988). PEPT1 exhibits strong expression level in the apical membrane of small intestine epithelial cells and cefadroxil is known to be a substrate of peptide transporters, PEPT1 and PEPT2. Therefore, when PEPT1 gene knockout mice were used for pharmacokinetic study, oral availability (area under the curve, AUC) of cefadroxil was substantially decreased by 10 to 15-fold for PEPT1 knockout mice compared to wild-type animals (Posada and Smith, 2013). A recent study has also demonstrated that MRP3 and MRP4 are involved in transporting cefadroxil across the basolateral membrane of intestinal epithelium after it is transported across the apical membrane by PEPT1 (de Waart et al., 2012). After administration of cefadroxil through jejunum, significant lower cefadroxil

concentration of portal and peripheral blood were found in MRP3/4 knockout mice compared to wild-type mice.

Most cephalosporin antibiotics, including cefadroxil, are mainly renally excreted. OATs are located in the basolateral side of the proximal tubule in human kidney and thought to play an important role in active secretion into the urine (Khamdang et al., 2003). The elimination rate of cefadroxil was significantly reduced when probenecid, an inhibitor of OAT, was co-administered (Shitara et al., 2005). PEPT2 is also extensively localized in the brush-border membrane of proximal tubule and involved in tubular reabsorption of cefadroxil. PEPT2 knockout mice exhibited substantial increase in systemic clearance and corresponding decrease in plasma concentrations of cefadroxil compared with wild-type mice (Shen et al., 2007).

Drug transporters are also involved in cefadroxil exposure to other tissues. In the hepatic uptake of β-lactam antibiotics, OATPs have been identified to play a key role. Multiple OATP transporters (OATP1, OATP2, and OATP4) localized at the basolateral membrane of hepatocyte can accept β-lactam antibiotics, including cefadroxil, as substrates and are responsible for hepatic uptake of those drugs. When tested by Xenopus laevis oocytes expressing OATPs, cefadroxil was transported by OATP2 even though the hepatic uptake was not directly translated into biliary excretion (Nakakariya et al., 2008). On the other hand, cefadroxil distribution to brain is largely controlled by PEPT2, which is expressed in the apical membrane of the choroid plexus epithelial cells. PEPT2 in choroid plexus plays an important role as an efflux pump pumping out drug molecules from CSF into the

blood. Therefore, when PEPT2 function was disrupted, cefadroxil exposure to CSF was substantially increased by approximately 6-fold (Shen et al., 2007).

**Table 2.1.** Unique localization of peptide transporters, PEPT1 and PEPT2, in mammalian tissues. (Adapted from Brandsch et al. 2008)

| Transporter | Organ/tissue | Localization | Demonstration |
|---|---|---|---|
| PEPT1 | Small intestine | Epithelial cells | Function, mRNA, protein |
| | Kidney | S1-segment, Lysosomes | Function, mRNA, protein |
| | Pancreas | Vascular smooth muscle cells, Schwann cells, Exocrine pancreas | Protein |
| | Bile duct | Epithelial cells, extrahepatic | Function, mRNA, protein |
| | Liver | Lysosomes | Function |
| | Blood | Monocytes | Function, mRNA, protein |
| | Adrenal gland | Neuroendocrine cells | Function, mRNA |
| PEPT2 | Kidney | S2-S3 segment | Function, mRNA, protein |
| | Peripheral nervous system | Ganglionic neurons, satellite glial cells | mRNA, protein |
| | Central nervous system | Choroid plexus, Subependymal & ependymal cells, Astroglia, Cerebral cortex | Function, mRNA, protein |
| | Enteric nervous sytem | Neuromuscular layers of gastrointestinal tract, enteric glial cells, tissue-resident macrophages | Function, mRNA, protein |
| | Lung | Bronchia, Alveoli, Small arteries | Function, mRNA, protein |
| | Mammary gland | Ducts and glands | mRNA, protein |

**Table 2.2.** Identified drug transporters that are involved in transporting cefadroxil and corresponding experimental systems used.

| Tissue | Transporters involved | Experimental System used |
|---|---|---|
| Kidney | PEPT2, OAT1-4 | Transfected S2 cells, KO mice, Oocytes |
| Small Intestine | PEPT1, MRP3-4 | Caco-2 cells, Oocytes, KO mice |
| Brain (CP) | PEPT2, OAT3 | Cells, KO mice |
| Liver | OATP2 | Oocytes |

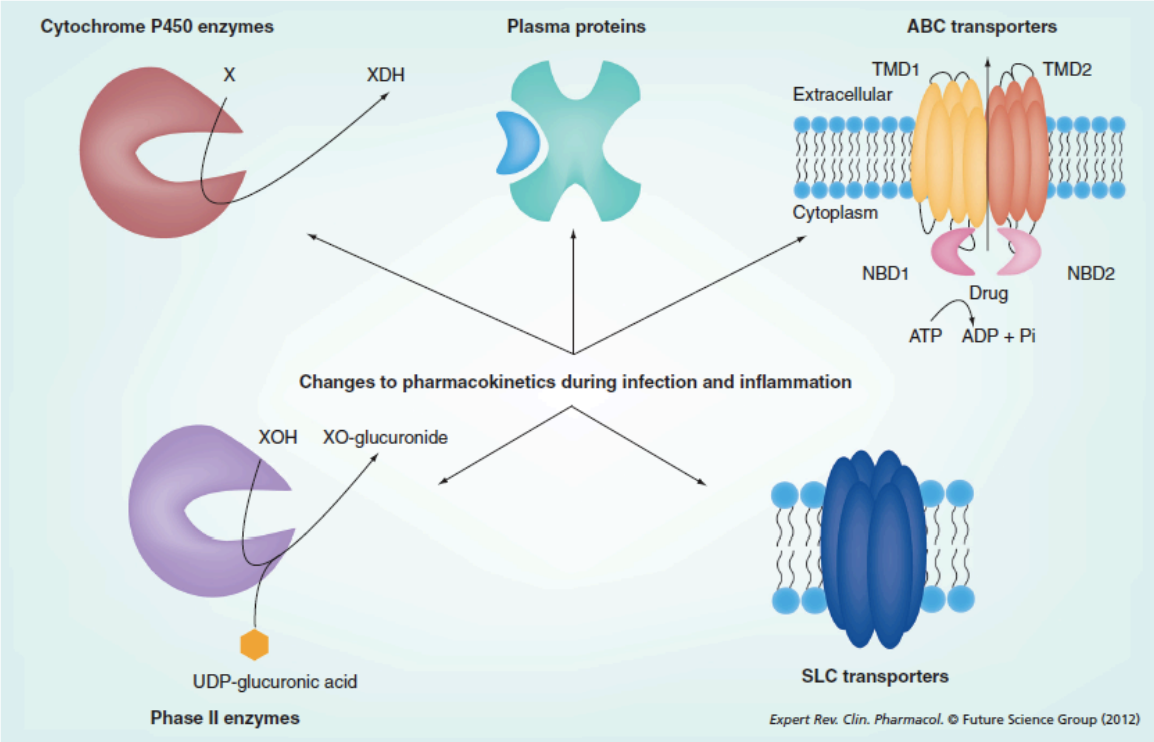


**Figure 2.1.** Determinants of drug pharmacokinetics that are identified to be changed by inflammatory stimuli. ABC: ATP-binding cassette; TMD: Transmembrane domain; NBD: Nucleotide-binding domain; SLC: Solute carrier (Adapted from Alexander et al. 2012).

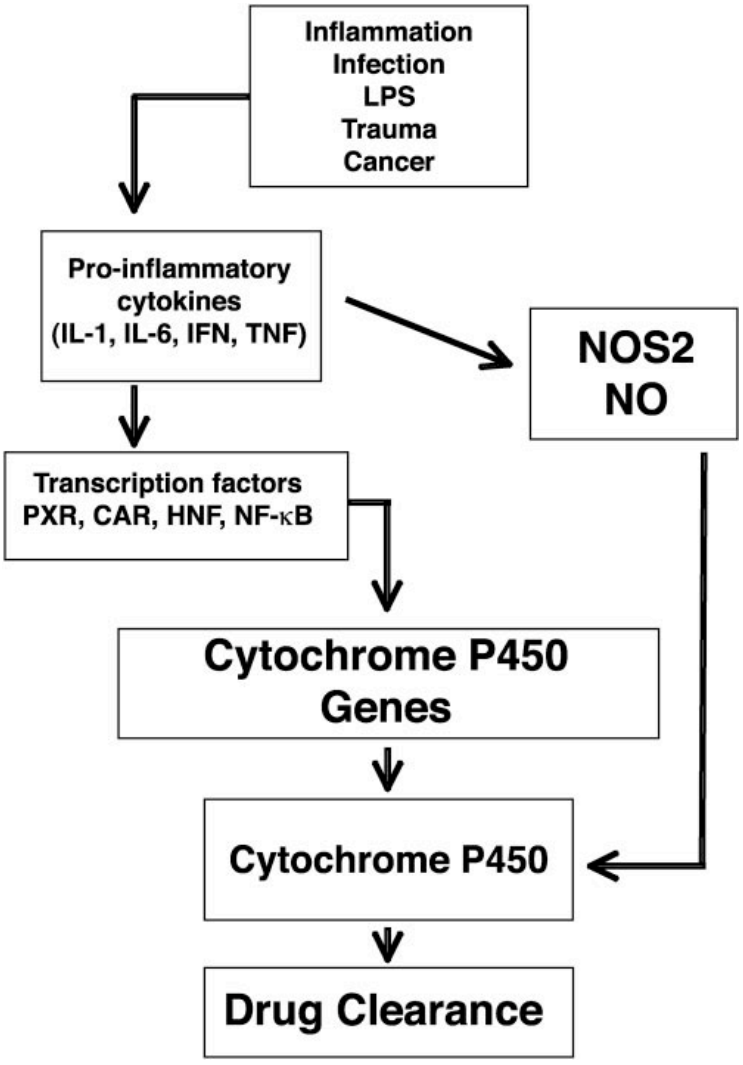


**Figure 2.2.** Proposed mechanism of changes in gene expression of drug metabolizing enzymes during inflammation, leading to the reduction of drug metabolism. NOS: Nitric-oxide synthase; NO: Nitric oxide; HNF: hepatocyte nuclear factor; NF: Nuclear factor (Adapted from Morgan et al. 2008).

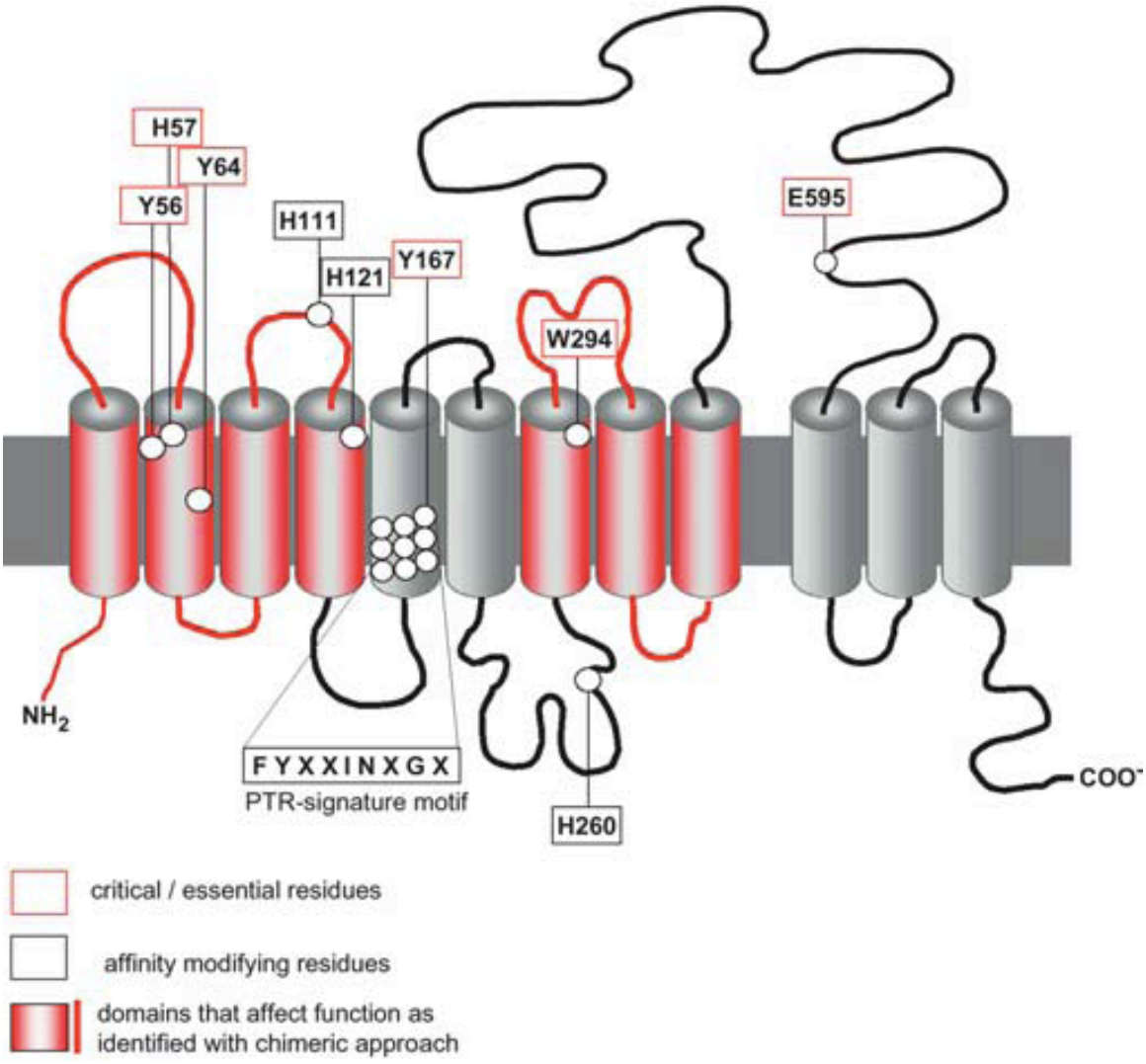


**Figure 2.3.** Membrane topology model of peptide transporter 1 (PEPT1). Protein domains and amino acide residues marked in colors represent the ones play an important role in determining functional characteristics (Adapted from Daniel et al. 2004).

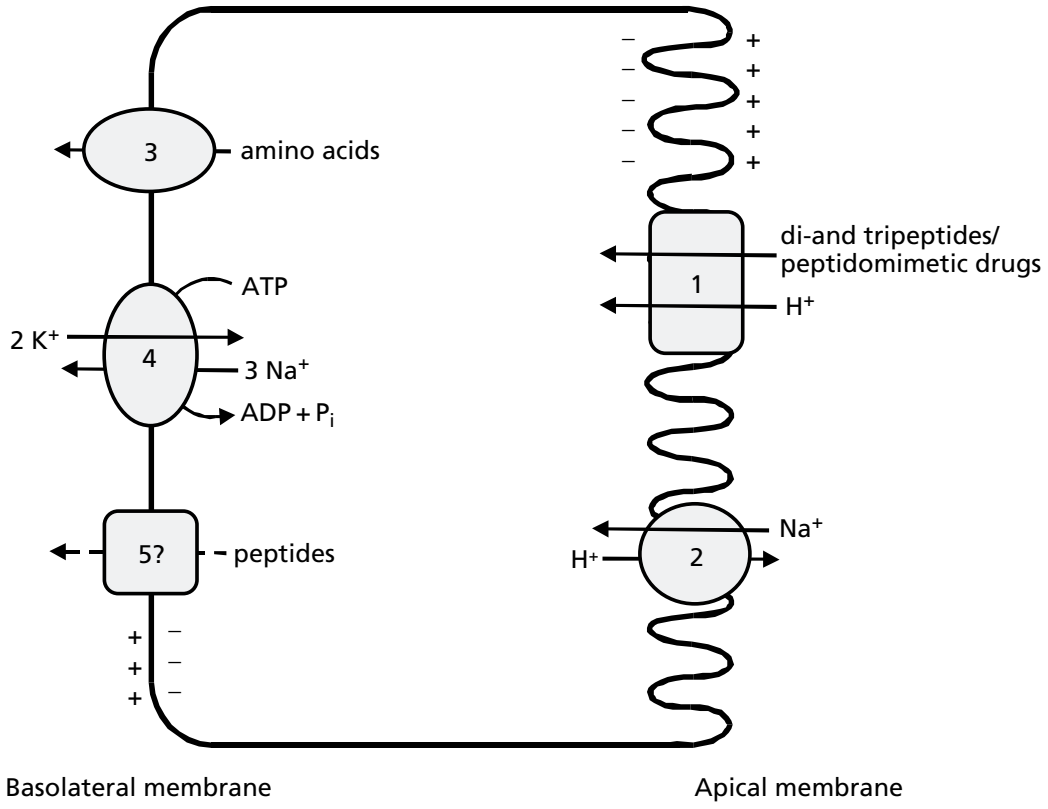


**Figure 2.4.** Schematic representation of peptides transporting mechanisms through intestinal or renal epithelium. 1, peptide transporter 1/2 (PEPT1/2); 2, $Na^+/H^+$ antiporter (NHE3); 3, amino acid transporters; 4, $Na^+/K^+$ ATPase; 5, putative peptide transporter (Adapted from Brandsch et al. 2008).

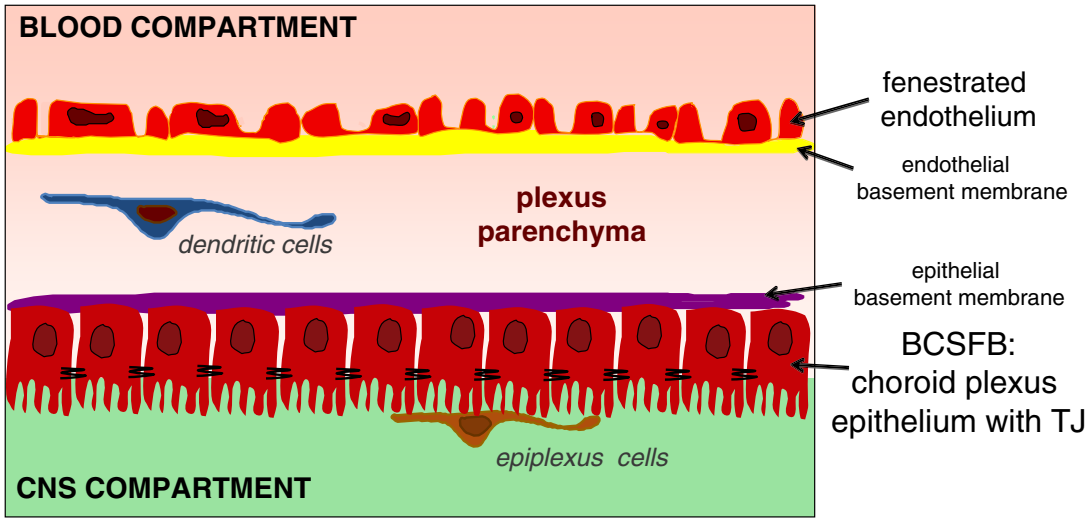


**Figure 2.5.** Schematic figure of the choroid plexus, which forms a barrier between blood and CSF (CNS in the figure) compartments (Adapted from Engelhardt et al. 2009).

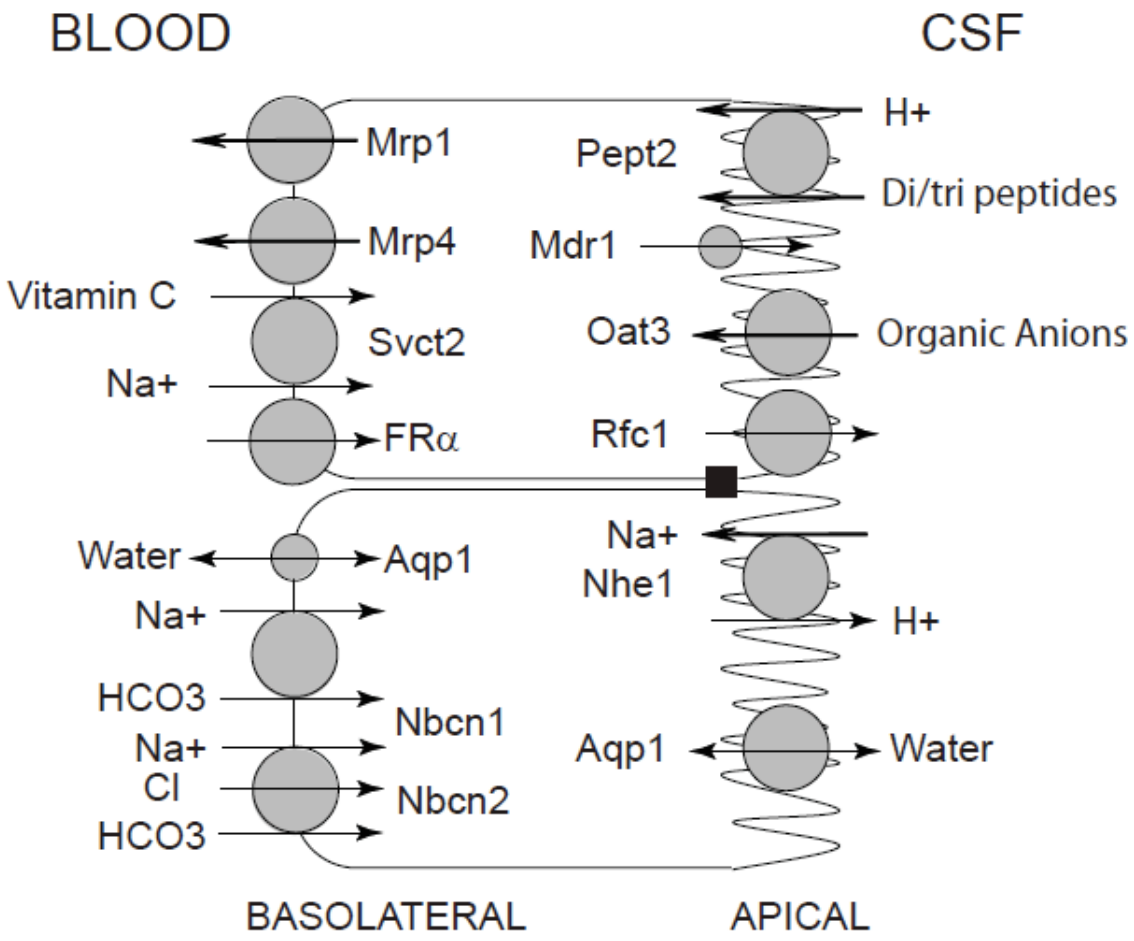


**Figure 2.6.** Schematic diagram of the distribution of drug transporters in the choroid plexus (Adapted from Keep et al. 2011).

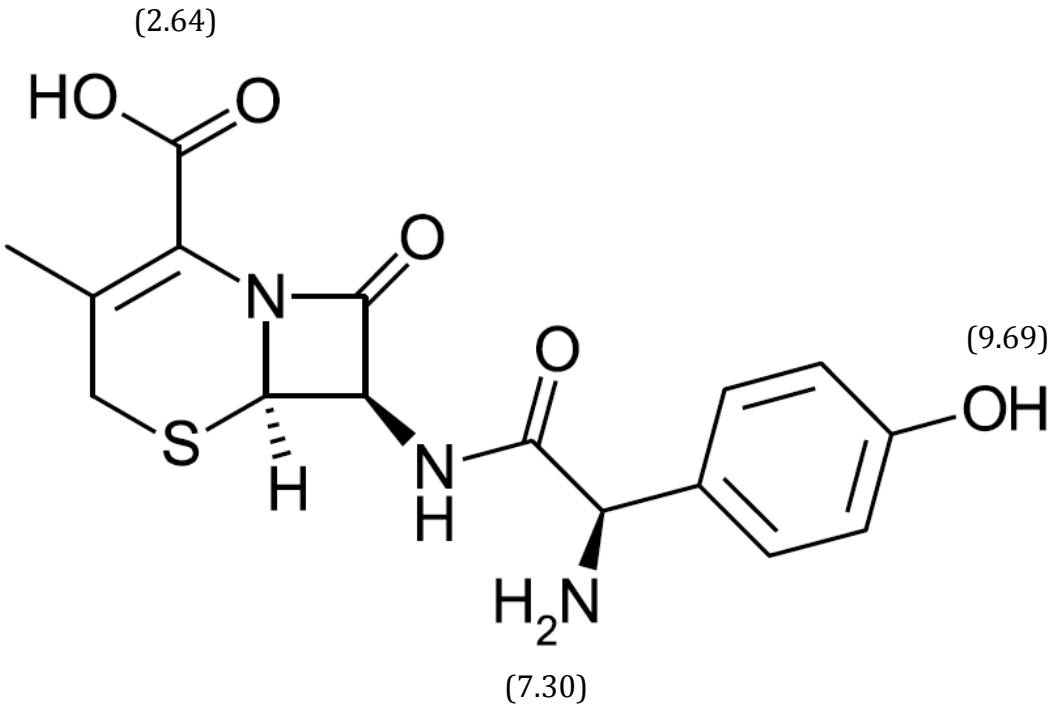


**Figure 2.7.** Chemical structure of cefadroxil (pKa values)

## REFERENCES


ADIBI, S. A. (2003) Regulation of expression of the intestinal oligopeptide transporter (Pept-1) in health and disease. *Am J Physiol Gastrointest Liver Physiol,* 285**,** G779-88.

AITKEN, A. E., RICHARDSON, T. A. & MORGAN, E. T. (2006) Regulation of drug-metabolizing enzymes and transporters in inflammation. *Annu Rev Pharmacol Toxicol,* 46**,** 123-49.

ANDERLE, P., NIELSEN, C. U., PINSONNEAULT, J., KROG, P. L., BRODIN, B. & SADEE, W. (2006) Genetic variants of the human dipeptide transporter PEPT1. *J Pharmacol Exp Ther,* 316**,** 636-46.

ARONSON, P. S., NEE, J. & SUHM, M. A. (1982) Modifier role of internal H+ in activating the Na+-H+ exchanger in renal microvillus membrane vesicles. *Nature,* 299**,** 161-3.

ASHIDA, K., KATSURA, T., MOTOHASHI, H., SAITO, H. & INUI, K. (2002) Thyroid hormone regulates the activity and expression of the peptide transporter PEPT1 in Caco-2 cells. *Am J Physiol Gastrointest Liver Physiol,* 282**,** G617-23.

ATWOOD, W. J., BERGER, J. R., KADERMAN, R., TORNATORE, C. S. & MAJOR, E. O. (1993) Human immunodeficiency virus type 1 infection of the brain. *Clin Microbiol Rev,* 6**,** 339-66.

AYUSE, T., BRIENZA, N., REVELLY, J. P., O'DONNELL, C. P., BOITNOTT, J. K. & ROBOTHAM, J. L. (1995) Alternations in liver hemodynamics in an intact porcine model of endotoxin shock. *Am J Physiol,* 268**,** H1106-14.

BARBOT, L., WINDSOR, E., ROME, S., TRICOTTET, V., REYNES, M., TOPOUCHIAN, A., HUNEAU, J. F., GOBERT, J. G., TOME, D. & KAPEL, N. (2003) Intestinal peptide transporter PepT1 is over-expressed during acute cryptosporidiosis in suckling rats as a result of both malnutrition and experimental parasite infection. *Parasitol Res,* 89**,** 364-70.

BELLER, B. K., ARCHER, L. T., PASSEY, R. B., FLOURNOY, D. J. & HINSHAW, L. B. (1983) Effectiveness of modified steroid-antibiotic therapies for lethal sepsis in the dog. *Arch Surg,* 118**,** 1293-9.

BERGER, U. V. & HEDIGER, M. A. (1999) Distribution of peptide transporter PEPT2 mRNA in the rat nervous system. *Anat Embryol (Berl),* 199**,** 439-49.

BERSTEN, A. D., HERSCH, M., CHEUNG, H., RUTLEDGE, F. S. & SIBBALD, W. J. (1992) The effect of various sympathomimetics on the regional circulations in hyperdynamic sepsis. *Surgery,* 112**,** 549-61.

BIEGEL, A., KNUTTER, I., HARTRODT, B., GEBAUER, S., THEIS, S., LUCKNER, P., KOTTRA, G., RASTETTER, M., ZEBISCH, K., THONDORF, I., DANIEL, H., NEUBERT, K. & BRANDSCH, M. (2006) The renal type H+/peptide symporter PEPT2: structure-affinity relationships. *Amino Acids,* 31**,** 137-56.

BOCHUD, P. Y. & CALANDRA, T. (2003) Pathogenesis of sepsis: new concepts and implications for future treatment. *BMJ,* 326**,** 262-6.

BODENHAM, A., SHELLY, M. P. & PARK, G. R. (1988) The altered pharmacokinetics and pharmacodynamics of drugs commonly used in critically ill patients. *Clin Pharmacokinet,* 14**,** 347-73.

BONE, R. C. (1991) The pathogenesis of sepsis. *Ann Intern Med,* 115**,** 457-69.

BOTKA, C. W., WITTIG, T. W., GRAUL, R. C., NIELSEN, C. U., HIGAKA, K., AMIDON, G. L. & SADEE, W. (2000) Human proton/oligopeptide transporter (POT) genes: identification of putative human genes using bioinformatics. *AAPS PharmSci,* 2**,** E16.

BRANDSCH, M., KNUTTER, I. & BOSSE-DOENECKE, E. (2008) Pharmaceutical and pharmacological importance of peptide transporters. *J Pharm Pharmacol,* 60**,** 543-85.

BRAVO, S. A., NIELSEN, C. U., AMSTRUP, J., FROKJAER, S. & BRODIN, B. (2004) Epidermal growth factor decreases PEPT2 transport capacity and expression in the rat kidney proximal tubule cell line SKPT0193 cl.2. *Am J Physiol Renal Physiol,* 286**,** F385-93.

BRUNTON, L., LAZO, J. & PARKER, K. (2006) *Goodman & Gilman's the pharmacological basis of therapeutics,* New York, McGraw-Hill.

BUYSE, M., BERLIOZ, F., GUILMEAU, S., TSOCAS, A., VOISIN, T., PERANZI, G., MERLIN, D., LABURTHE, M., LEWIN, M. J., ROZE, C. & BADO, A. (2001) PepT1-mediated epithelial transport of dipeptides and cephalexin is enhanced by luminal leptin in the small intestine. *J Clin Invest,* 108**,** 1483-94.

BUYSE, M., CHARRIER, L., SITARAMAN, S., GEWIRTZ, A. & MERLIN, D. (2003) Interferon-gamma increases hPepT1-mediated uptake of di-tripeptides including the bacterial tripeptide fMLP in polarized intestinal epithelia. *Am J Pathol,* 163**,** 1969-77.

CHEN, X. Z., STEEL, A. & HEDIGER, M. A. (2000) Functional roles of histidine and tyrosine residues in the H(+)-peptide transporter PepT1. *Biochem Biophys Res Commun,* 272**,** 726-30.

CONNORS, K. A., AMIDON, G. L. & STELLA, V. J. (1986) *Chemical stability of pharmaceuticals: a handbook for pharmacists,* New York, Wiley.

DANIEL, H. & KOTTRA, G. (2004) The proton oligopeptide cotransporter family SLC15 in physiology and pharmacology. *Pflugers Arch,* 447**,** 610-8.

DAVET, J., CLAVEL, B., DATAS, L., MANI-PONSET, L., MAUREL, D., HERBUTE, S., VISO, M., HINDS, W., JARVI, J. & GABRION, J. (1998) Choroidal readaptation to gravity in rats after spaceflight and head-down tilt. *J Appl Physiol,* 84**,** 19-29.

DE PAEPE, P., BELPAIRE, F. M. & BUYLAERT, W. A. (2002) Pharmacokinetic and pharmacodynamic considerations when treating patients with sepsis and septic shock. *Clin Pharmacokinet,* 41**,** 1135-51.

DE WAART, D. R., VAN DE WETERING, K., KUNNE, C., DUIJST, S., PAULUSMA, C. C. & OUDE ELFERINK, R. P. (2012) Oral availability of cefadroxil depends on ABCC3 and ABCC4. *Drug Metab Dispos,* 40**,** 515-21.

DON, B. R. & KAYSEN, G. (2004) Serum albumin: relationship to inflammation and nutrition. *Semin Dial,* 17**,** 432-7.

DORING, F., DORN, D., BACHFISCHER, U., AMASHEH, S., HERGET, M. & DANIEL, H. (1996) Functional analysis of a chimeric mammalian peptide transporter derived from the intestinal and renal isoforms. *J Physiol,* 497 ( Pt 3)**,** 773-9.

DORING, F., SCHMITT, R., BERNHARDT, W. M., KLAPPER, M., BACHMANN, S., DANIEL, H. & GRONEBERG, D. A. (2005) Hypothyroidism induces expression of the peptide transporter PEPT2. *Biol Chem,* 386**,** 785-90.

ELSTON, A. C., BAYLISS, M. K. & PARK, G. R. (1993) Effect of renal failure on drug metabolism by the liver. *Br J Anaesth,* 71**,** 282-90.

ENDO, H., SASAKI, K., TONOSAKI, A. & KAYAMA, T. (1998) Three-dimensional and ultrastructural ICAM-1 distribution in the choroid plexus, arachnoid membrane and dural sinus of inflammatory rats induced by LPS injection in the lateral ventricles. *Brain Res,* 793**,** 297-301.

ENGELHARDT, B. & SOROKIN, L. (2009) The blood-brain and the blood-cerebrospinal fluid barriers: function and dysfunction. *Semin Immunopathol,* 31**,** 497-511.

ENGELHARDT, B., WOLBURG-BUCHHOLZ, K. & WOLBURG, H. (2001) Involvement of the choroid plexus in central nervous system inflammation. *Microsc Res Tech,* 52**,** 112-29.

ERICKSON, R. H., GUM, J. R., JR., LINDSTROM, M. M., MCKEAN, D. & KIM, Y. S. (1995) Regional expression and dietary regulation of rat small intestinal peptide and amino acid transporter mRNAs. *Biochem Biophys Res Commun,* 216**,** 249-57.

FEI, Y. J., KANAI, Y., NUSSBERGER, S., GANAPATHY, V., LEIBACH, F. H., ROMERO, M. F., SINGH, S. K., BORON, W. F. & HEDIGER, M. A. (1994) Expression cloning of a mammalian proton-coupled oligopeptide transporter. *Nature,* 368**,** 563-6.

FEI, Y. J., LIU, J. C., FUJITA, T., LIANG, R., GANAPATHY, V. & LEIBACH, F. H. (1998) Identification of a potential substrate binding domain in the mammalian peptide transporters PEPT1 and PEPT2 using PEPT1-PEPT2 and PEPT2-PEPT1 chimeras. *Biochem Biophys Res Commun,* 246**,** 39-44.

FLOURNOY, D. J., BELLER, B. K., ARCHER, L. T. & HINSHAW, L. B. (1983) Relationship of serum gentamicin levels and methylprednisolone sodium succinate treatment in baboons challenged with Escherichia coli LD100. *Clin Ther,* 5**,** 417-21.

FUJITA, T., MAJIKAWA, Y., UMEHISA, S., OKADA, N., YAMAMOTO, A., GANAPATHY, V. & LEIBACH, F. H. (1999) sigma Receptor ligand-induced up-regulation of the H(+)/peptide transporter PEPT1 in the human intestinal cell line Caco-2. *Biochem Biophys Res Commun,* 261**,** 242-6.

GANGOPADHYAY, A., THAMOTHARAN, M. & ADIBI, S. A. (2002) Regulation of oligopeptide transporter (Pept-1) in experimental diabetes. *Am J Physiol Gastrointest Liver Physiol,* 283**,** G133-8.

GAVIN, T. J., FABIAN, T. C., WILSON, J. D., TRENTHEM, L. L., PRITCHARD, F. E., CROCE, M. A., STEWART, R. M. & PROCTOR, K. G. (1994) Splanchnic and systemic hemodynamic responses to portal vein endotoxin after resuscitation from hemorrhagic shock. *Surgery,* 115**,** 310-24.

GHERSI-EGEA, J. F., FINNEGAN, W., CHEN, J. L. & FENSTERMACHER, J. D. (1996a) Rapid distribution of intraventricularly administered sucrose into cerebrospinal fluid cisterns via subarachnoid velae in rat. *Neuroscience,* 75**,** 1271-88.

GHERSI-EGEA, J. F., GOREVIC, P. D., GHISO, J., FRANGIONE, B., PATLAK, C. S. & FENSTERMACHER, J. D. (1996b) Fate of cerebrospinal fluid-borne amyloid beta-peptide: rapid clearance into blood and appreciable accumulation by cerebral arteries. *J Neurochem,* 67**,** 880-3.

GHERSI-EGEA, J. F., LEININGER-MULLER, B., CECCHELLI, R. & FENSTERMACHER, J. D. (1995) Blood-brain interfaces: relevance to cerebral drug metabolism. *Toxicol Lett,* 82-83**,** 645-53.

GHERSI-EGEA, J. F., LENINGER-MULLER, B., SULEMAN, G., SIEST, G. & MINN, A. (1994) Localization of drug-metabolizing enzyme activities to blood-brain interfaces and circumventricular organs. *J Neurochem,* 62**,** 1089-96.

GLAUSER, M. P., ZANETTI, G., BAUMGARTNER, J. D. & COHEN, J. (1991) Septic shock: pathogenesis. *Lancet,* 338**,** 732-6.

GORALSKI, K. B., HARTMANN, G., PIQUETTE-MILLER, M. & RENTON, K. W. (2003) Downregulation of mdr1a expression in the brain and liver during CNS inflammation alters the in vivo disposition of digoxin. *Br J Pharmacol,* 139**,** 35-48.

GROEGER, J. S. & INTURRISI, C. E. (1987) High-dose naloxone: pharmacokinetics in patients in septic shock. *Crit Care Med,* 15**,** 751-6.

GRONEBERG, D. A., DORING, F., EYNOTT, P. R., FISCHER, A. & DANIEL, H. (2001) Intestinal peptide transport: ex vivo uptake studies and localization of peptide carrier PEPT1. *Am J Physiol Gastrointest Liver Physiol,* 281**,** G697-704.

GRONEBERG, D. A., FISCHER, A., CHUNG, K. F. & DANIEL, H. (2004) Molecular mechanisms of pulmonary peptidomimetic drug and peptide transport. *Am J Respir Cell Mol Biol,* 30**,** 251-60.

HAN, H., KIM, S. G., LEE, M. G., SHIM, C. K. & CHUNG, S. J. (2002) Mechanism of the reduced elimination clearance of benzylpenicillin from cerebrospinal fluid in rats with intracisternal administration of lipopolysaccharide. *Drug Metab Dispos,* 30**,** 1214-20.

HARTMANN, G., CHEUNG, A. K. & PIQUETTE-MILLER, M. (2002) Inflammatory cytokines, but not bile acids, regulate expression of murine hepatic anion transporters in endotoxemia. *J Pharmacol Exp Ther,* 303**,** 273-81.

HARTMANN, G., KIM, H. & PIQUETTE-MILLER, M. (2001) Regulation of the hepatic multidrug resistance gene expression by endotoxin and inflammatory cytokines in mice. *Int Immunopharmacol,* 1**,** 189-99.

HINSHAW, L. B., BELLER, B. K., CHANG, A. C., FLOURNOY, D. J., LAHTI, R. A., PASSEY, R. B. & ARCHER, L. T. (1984) Evaluation of naloxone for therapy of Escherichia coli shock. Species differences. *Arch Surg,* 119**,** 1410-8.

HO, E. A. & PIQUETTE-MILLER, M. (2007) KLF6 and HSF4 transcriptionally regulate multidrug resistance transporters during inflammation. *Biochem Biophys Res Commun,* 353**,** 679-85.

HOCHERL, K., SCHMIDT, C. & BUCHER, M. (2009) COX-2 inhibition attenuates endotoxin-induced downregulation of organic anion transporters in the rat renal cortex. *Kidney Int,* 75**,** 373-80.

HUSSAIN, I., KELLETT, L., AFFLECK, J., SHEPHERD, J. & BOYD, R. (2002) Expression and cellular distribution during development of the peptide transporter (PepT1) in the small intestinal epithelium of the rat. *Cell Tissue Res,* 307**,** 139-42.

INOUE, M., TERADA, T., OKUDA, M. & INUI, K. (2005) Regulation of human peptide transporter 1 (PEPT1) in gastric cancer cells by anticancer drugs. *Cancer Lett,* 230**,** 72-80.

INUI, K., OKANO, T., MAEGAWA, H., KATO, M., TAKANO, M. & HORI, R. (1988) H+ coupled transport of p.o. cephalosporins via dipeptide carriers in rabbit intestinal brush-border membranes: difference of transport characteristics between cefixime and cephradine. *J Pharmacol Exp Ther,* 247**,** 235-41.

JELLETT, L. B. & HEAZLEWOOD, V. J. (1990) Pharmacokinetics in acute illness. *Med J Aust,* 153**,** 534-41.

JOHANSON, C. E., PALM, D. E., PRIMIANO, M. J., MCMILLAN, P. N., CHAN, P., KNUCKEY, N. W. & STOPA, E. G. (2000) Choroid plexus recovery after transient forebrain ischemia: role of growth factors and other repair mechanisms. *Cell Mol Neurobiol,* 20**,** 197-216.

JOYNT, G. M., LIPMAN, J., GOMERSALL, C. D., YOUNG, R. J., WONG, E. L. & GIN, T. (2001) The pharmacokinetics of once-daily dosing of ceftriaxone in critically ill patients. *J Antimicrob Chemother,* 47**,** 421-9.

KAMAL, M. A., KEEP, R. F. & SMITH, D. E. (2008) Role and relevance of PEPT2 in drug disposition, dynamics, and toxicity. *Drug Metab Pharmacokinet,* 23**,** 236-42.

KEEP, R. F. & SMITH, D. E. (2011) Choroid plexus transport: gene deletion studies. *Fluids Barriers CNS,* 8**,** 26.

KHAMDANG, S., TAKEDA, M., BABU, E., NOSHIRO, R., ONOZATO, M. L., TOJO, A., ENOMOTO, A., HUANG, X. L., NARIKAWA, S., ANZAI, N., PIYACHATURAWAT, P. & ENDOU, H. (2003) Interaction of human and rat organic anion transporter 2 with various cephalosporin antibiotics. *Eur J Pharmacol,* 465**,** 1-7.

KNUTTER, I., RUBIO-ALIAGA, I., BOLL, M., HAUSE, G., DANIEL, H., NEUBERT, K. & BRANDSCH, M. (2002) H+-peptide cotransport in the human bile duct epithelium cell line SK-ChA-1. *Am J Physiol Gastrointest Liver Physiol,* 283**,** G222-9.

KRAEMER, M. J., FURUKAWA, C. T., KOUP, J. R., SHAPIRO, G. G., PIERSON, W. E. & BIERMAN, C. W. (1982) Altered theophylline clearance during an influenza B outbreak. *Pediatrics,* 69**,** 476-80.

KULKARNI, A. A., HAWORTH, I. S. & LEE, V. H. (2003a) Transmembrane segment 5 of the dipeptide transporter hPepT1 forms a part of the substrate translocation pathway. *Biochem Biophys Res Commun,* 306**,** 177-85.

KULKARNI, A. A., HAWORTH, I. S., UCHIYAMA, T. & LEE, V. H. (2003b) Analysis of transmembrane segment 7 of the dipeptide transporter hPepT1 by cysteine-scanning mutagenesis. *J Biol Chem,* 278**,** 51833-40.

LAMY, M. (1989) Acute-phase proteins and protease-antiproteases in the inflammatory reaction. *Fullerton (CA): Society of Critical Care Medicine***,** 193-217.

LEROY, A., HUMBERT, G., GODIN, M. & FILLASTRE, J. P. (1982) Pharmacokinetics of cefadroxil in patients with impaired renal function. *J Antimicrob Chemother,* 10 Suppl B**,** 39-46.

LIPMAN, J., WALLIS, S. C. & BOOTS, R. J. (2003) Cefepime versus cefpirome: the importance of creatinine clearance. *Anesth Analg,* 97**,** 1149-54, table of contents.

LIPMAN, J., WALLIS, S. C., RICKARD, C. M. & FRAENKEL, D. (2001) Low cefpirome levels during twice daily dosing in critically ill septic patients:

pharmacokinetic modelling calls for more frequent dosing. *Intensive Care Med,* 27**,** 363-70.

LIU, W., LIANG, R., RAMAMOORTHY, S., FEI, Y. J., GANAPATHY, M. E., HEDIGER, M. A., GANAPATHY, V. & LEIBACH, F. H. (1995) Molecular cloning of PEPT 2, a new member of the H+/peptide cotransporter family, from human kidney. *Biochim Biophys Acta,* 1235**,** 461-6.

LU, H. & KLAASSEN, C. (2006) Tissue distribution and thyroid hormone regulation of Pept1 and Pept2 mRNA in rodents. *Peptides,* 27**,** 850-7.

MACNAB, M. S., MACRAE, D. J., GUY, E., GRANT, I. S. & FEELY, J. (1986) Profound reduction in morphine clearance and liver blood flow in shock. *Intensive Care Med,* 12**,** 366-9.

MANN, H. J., TOWNSEND, R. J., FUHS, D. W. & CERRA, F. B. (1987) Decreased hepatic clearance of clindamycin in critically ill patients with sepsis. *Clin Pharm,* 6**,** 154-9.

MARQUES, F., SOUSA, J. C., COPPOLA, G., FALCAO, A. M., RODRIGUES, A. J., GESCHWIND, D. H., SOUSA, N., CORREIA-NEVES, M. & PALHA, J. A. (2009) Kinetic profile of the transcriptome changes induced in the choroid plexus by peripheral inflammation. *J Cereb Blood Flow Metab,* 29**,** 921-32.

MASSEGUIN, C., MANI-PONSET, L., HERBUTE, S., TIXIER-VIDAL, A. & GABRION, J. (2001) Persistence of tight junctions and changes in apical structures and protein expression in choroid plexus epithelium of rats after short-term head-down tilt. *J Neurocytol,* 30**,** 365-77.

MEREDITH, D. & BOYD, C. A. (2000) Structure and function of eukaryotic peptide transporters. *Cell Mol Life Sci,* 57**,** 754-78.

MERLIN, D., SI-TAHAR, M., SITARAMAN, S. V., EASTBURN, K., WILLIAMS, I., LIU, X., HEDIGER, M. A. & MADARA, J. L. (2001) Colonic epithelial hPepT1 expression occurs in inflammatory bowel disease: transport of bacterial peptides influences expression of MHC class 1 molecules. *Gastroenterology,* 120**,** 1666-79.

MIYOSHI, K., WOLF, A., HARTER, D. H., DUFFY, P. E., GAMBOA, E. T. & HSU, K. C. (1973) Murine influenza virus encephalomyelitis. I. Neuropathological and immunofluorescence findings. *J Neuropathol Exp Neurol,* 32**,** 51-71.

MORGAN, E. T., GORALSKI, K. B., PIQUETTE-MILLER, M., RENTON, K. W., ROBERTSON, G. R., CHALUVADI, M. R., CHARLES, K. A., CLARKE, S. J., KACEVSKA, M., LIDDLE, C., RICHARDSON, T. A., SHARMA, R. & SINAL, C. J. (2008) Regulation of drug-metabolizing enzymes and transporters in infection, inflammation, and cancer. *Drug Metab Dispos,* 36**,** 205-16.

MOSHAGE, H. J., JANSSEN, J. A., FRANSSEN, J. H., HAFKENSCHEID, J. C. & YAP, S. H. (1987) Study of the molecular mechanism of decreased liver synthesis of albumin in inflammation. *J Clin Invest,* 79**,** 1635-41.

NAKAKARIYA, M., SHIMADA, T., IROKAWA, M., KOIBUCHI, H., IWANAGA, T., YABUUCHI, H., MAEDA, T. & TAMAI, I. (2008) Predominant contribution of rat organic anion transporting polypeptide-2 (Oatp2) to hepatic uptake of beta-lactam antibiotics. *Pharm Res,* 25**,** 578-85.

NIGHTINGALE, C. (1980) Pharmacokinetics of the oral cephalosporins in adults. *J Int Med Res,* 8**,** 2-8.

OCHELTREE, S. M., SHEN, H., HU, Y., XIANG, J., KEEP, R. F. & SMITH, D. E. (2004) Mechanisms of cefadroxil uptake in the choroid plexus: studies in wild-type and PEPT2 knockout mice. *J Pharmacol Exp Ther,* 308**,** 462-7.

OGIHARA, H., SAITO, H., SHIN, B. C., TERADO, T., TAKENOSHITA, S., NAGAMACHI, Y., INUI, K. & TAKATA, K. (1996) Immuno-localization of H+/peptide cotransporter in rat digestive tract. *Biochem Biophys Res Commun,* 220**,** 848-52.

PAN, X., TERADA, T., IRIE, M., SAITO, H. & INUI, K. (2002) Diurnal rhythm of H+-peptide cotransporter in rat small intestine. *Am J Physiol Gastrointest Liver Physiol,* 283**,** G57-64.

PAN, X., TERADA, T., OKUDA, M. & INUI, K. (2003) Altered diurnal rhythm of intestinal peptide transporter by fasting and its effects on the pharmacokinetics of ceftibuten. *J Pharmacol Exp Ther,* 307**,** 626-32.

PAN, X., TERADA, T., OKUDA, M. & INUI, K. (2004) The diurnal rhythm of the intestinal transporters SGLT1 and PEPT1 is regulated by the feeding conditions in rats. *J Nutr,* 134**,** 2211-5.

PARK, G. R. (1996) Molecular mechanisms of drug metabolism in the critically ill. *Br J Anaesth,* 77**,** 32-49.

PARTRIDGE, W. M. (1991) *Peptides as potential neuropharmaceuticals in disorders of the brain,* New York, Raven Press.

PENTEL, P. & BENOWITZ, N. (1984) Pharmacokinetic and pharmacodynamic considerations in drug therapy of cardiac emergencies. *Clin Pharmacokinet,* 9**,** 273-308.

PINSONNEAULT, J., NIELSEN, C. U. & SADEE, W. (2004) Genetic variants of the human H+/dipeptide transporter PEPT2: analysis of haplotype functions. *J Pharmacol Exp Ther,* 311**,** 1088-96.

PIQUETTE-MILLER, M., PAK, A., KIM, H., ANARI, R. & SHAHZAMANI, A. (1998) Decreased expression and activity of P-glycoprotein in rat liver during acute inflammation. *Pharm Res,* 15**,** 706-11.

POSADA, M. M. & SMITH, D. E. (2013) Relevance of PepT1 in the intestinal permeability and oral absorption of cefadroxil. *Pharm Res,* 30**,** 1017-25.

POWER, B. M., FORBES, A. M., VAN HEERDEN, P. V. & ILETT, K. F. (1998) Pharmacokinetics of drugs used in critically ill adults. *Clin Pharmacokinet,* 34**,** 25-56.

PRESTON, J. E. (2001) Ageing choroid plexus-cerebrospinal fluid system. *Microsc Res Tech,* 52**,** 31-7.

QUEENER, S. F., J.A., W. & S.W., Q. (1986) *Beta-lactam antibiotics for clinical use,* New York, M. Dekker.

QUINTILIANI, R. (1986) Efficacy of a twice-daily regimen of cefadroxil in the treatment of respiratory tract infections. *Drugs,* 32 Suppl 3**,** 43-9.

ROBERTS, J. A., ROBERTS, M. S., ROBERTSON, T. A., DALLEY, A. J. & LIPMAN, J. (2009) Piperacillin penetration into tissue of critically ill patients with sepsis-Bolus versus continuous administration? *Critical Care Medicine,* 37**,** 926-933 10.1097/CCM.0b013e3181968e44.

RUBIO-ALIAGA, I. & DANIEL, H. (2002) Mammalian peptide transporters as targets for drug delivery. *Trends Pharmacol Sci,* 23**,** 434-40.

RUOT, B., BECHEREAU, F., BAYLE, G., BREUILLE, D. & OBLED, C. (2002) The response of liver albumin synthesis to infection in rats varies with the phase of the inflammatory process. *Clin Sci (Lond),* 102**,** 107-14.

SAKATA, K., YAMASHITA, T., MAEDA, M., MORIYAMA, Y., SHIMADA, S. & TOHYAMA, M. (2001) Cloning of a lymphatic peptide/histidine transporter. *Biochem J,* 356**,** 53-60.

SCHMIDT, C., HOCHERL, K., SCHWEDA, F., KURTZ, A. & BUCHER, M. (2007) Regulation of renal sodium transporters during severe inflammation. *J Am Soc Nephrol,* 18**,** 1072-83.

SEROT, J. M., BENE, M. C. & FAURE, G. C. (2003) Choroid plexus, aging of the brain, and Alzheimer's disease. *Front Biosci,* 8**,** s515-21.

SHEN, H., OCHELTREE, S. M., HU, Y., KEEP, R. F. & SMITH, D. E. (2007) Impact of genetic knockout of PEPT2 on cefadroxil pharmacokinetics, renal tubular reabsorption, and brain penetration in mice. *Drug Metab Dispos,* 35**,** 1209-16.

SHEN, H., SMITH, D. E. & BROSIUS, F. C., 3RD (2001) Developmental expression of PEPT1 and PEPT2 in rat small intestine, colon, and kidney. *Pediatr Res,* 49**,** 789-95.

SHEN, H., SMITH, D. E., YANG, T., HUANG, Y. G., SCHNERMANN, J. B. & BROSIUS, F. C., 3RD (1999) Localization of PEPT1 and PEPT2 proton-coupled oligopeptide transporter mRNA and protein in rat kidney. *Am J Physiol,* 276**,** F658-65.

SHIMIZU, Y., MASUDA, S., NISHIHARA, K., JI, L., OKUDA, M. & INUI, K. (2005) Increased protein level of PEPT1 intestinal H+-peptide cotransporter upregulates absorption of glycylsarcosine and ceftibuten in 5/6 nephrectomized rats. *Am J Physiol Gastrointest Liver Physiol,* 288**,** G664-70.

SHIRAGA, T., MIYAMOTO, K., TANAKA, H., YAMAMOTO, H., TAKETANI, Y., MORITA, K., TAMAI, I., TSUJI, A. & TAKEDA, E. (1999) Cellular and molecular mechanisms of dietary regulation on rat intestinal H+/Peptide transporter PepT1. *Gastroenterology,* 116**,** 354-62.

SHITARA, Y., SATO, H. & SUGIYAMA, Y. (2005) Evaluation of drug-drug interaction in the hepatobiliary and renal transport of drugs. *Annu Rev Pharmacol Toxicol,* 45**,** 689-723.

SHU, H. J., TAKEDA, H., SHINZAWA, H., TAKAHASHI, T. & KAWATA, S. (2002) Effect of lipopolysaccharide on peptide transporter 1 expression in rat small intestine and its attenuation by dexamethasone. *Digestion,* 65**,** 21-9.

SMITH, D. E., JOHANSON, C. E. & KEEP, R. F. (2004) Peptide and peptide analog transport systems at the blood-CSF barrier. *Adv Drug Deliv Rev,* 56**,** 1765-91.

SMITH, Q. R. & RAPOPORT, S. I. (1986) Cerebrovascular permeability coefficients to sodium, potassium, and chloride. *J Neurochem,* 46**,** 1732-42.

SPECTOR, R. & LORENZO, A. V. (1974) Inhibition of penicillin transport from the cerebrospinal fluid after intracisternal inoculation of bacteria. *J Clin Invest,* 54**,** 316-25.

ST PETER, W. L., REDIC-KILL, K. A. & HALSTENSON, C. E. (1992) Clinical pharmacokinetics of antibiotics in patients with impaired renal function. *Clin Pharmacokinet,* 22**,** 169-210.

STRAZIELLE, N. & GHERSI-EGEA, J. F. (2000) *Chapter 12. Implication of blood-brain interfaces in cerebral drug metabolism and drug metabolite disposition* Saint Lucia, London, OICA International.

STRAZIELLE, N., KHUTH, S. T. & GHERSI-EGEA, J. F. (2004) Detoxification systems, passive and specific transport for drugs at the blood-CSF barrier in normal and pathological situations. *Adv Drug Deliv Rev,* 56**,** 1717-40.

STRAZIELLE, N., KHUTH, S. T., MURAT, A., CHALON, A., GIRAUDON, P., BELIN, M. F. & GHERSI-EGEA, J. F. (2003) Pro-inflammatory cytokines modulate matrix metalloproteinase secretion and organic anion transport at the blood-cerebrospinal fluid barrier. *J Neuropathol Exp Neurol,* 62**,** 1254-64.

SUKHAI, M., YONG, A., KALITSKY, J. & PIQUETTE-MILLER, M. (2000) Inflammation and interleukin-6 mediate reductions in the hepatic expression and transcription of the mdr1a and mdr1b Genes. *Mol Cell Biol Res Commun,* 4**,** 248-56.

SUZUKI, H., TERASAKI, T. & SUGIYAMA, Y. (1997) Role of efflux transport across the blood-brain barrier and blood-cerebrospinal fluid barrier on the disposition of xenobiotics in the central nervous system. *Advanced Drug Delivery Reviews,* 25**,** 257-285.

TANAKA, H., MIYAMOTO, K. I., MORITA, K., HAGA, H., SEGAWA, H., SHIRAGA, T., FUJIOKA, A., KOUDA, T., TAKETANI, Y., HISANO, S., FUKUI, Y., KITAGAWA, K. & TAKEDA, E. (1998) Regulation of the PepT1 peptide transporter in the rat small intestine in response to 5-fluorouracil-induced injury. *Gastroenterology,* 114**,** 714-23.

TANG, G. J., TANG, J. J., LIN, B. S., KONG, C. W. & LEE, T. Y. (1999) Factors affecting gentamicin pharmacokinetics in septic patients. *Acta Anaesthesiol Scand,* 43**,** 726-30.

TANG, W., YI, C., KALITSKY, J. & PIQUETTE-MILLER, M. (2000) Endotoxin downregulates hepatic expression of P-glycoprotein and MRP2 in 2-acetylaminofluorene-treated rats. *Mol Cell Biol Res Commun,* 4**,** 90-7.

TANRISEVER, B. & SANTELLA, P. J. (1986) Cefadroxil. A review of its antibacterial, pharmacokinetic and therapeutic properties in comparison with cephalexin and cephradine. *Drugs,* 32 Suppl 3**,** 1-16.

TENG, S. & PIQUETTE-MILLER, M. (2005) The involvement of the pregnane X receptor in hepatic gene regulation during inflammation in mice. *J Pharmacol Exp Ther,* 312**,** 841-8.

TERADA, T. & INUI, K. (2007) Gene expression and regulation of drug transporters in the intestine and kidney. *Biochem Pharmacol,* 73**,** 440-9.

TERADA, T., IRIE, M., OKUDA, M. & INUI, K. (2004) Genetic variant Arg57His in human H+/peptide cotransporter 2 causes a complete loss of transport function. *Biochem Biophys Res Commun,* 316**,** 416-20.

TERADA, T., SAITO, H., SAWADA, K., HASHIMOTO, Y. & INUI, K. (2000) N-terminal halves of rat H+/peptide transporters are responsible for their substrate recognition. *Pharm Res,* 17**,** 15-20.

THAMOTHARAN, M., BAWANI, S. Z., ZHOU, X. & ADIBI, S. A. (1999) Hormonal regulation of oligopeptide transporter pept-1 in a human intestinal cell line. *Am J Physiol,* 276**,** C821-6.

THOMAS, S. A. & SEGAL, M. B. (1998) The transport of the anti-HIV drug, 2',3'-didehydro-3'-deoxythymidine (D4T), across the blood-brain and blood-cerebrospinal fluid barriers. *Br J Pharmacol,* 125**,** 49-54.

UCHIYAMA, T., KULKARNI, A. A., DAVIES, D. L. & LEE, V. H. (2003) Biophysical evidence for His57 as a proton-binding site in the mammalian intestinal transporter hPepT1. *Pharm Res,* 20**,** 1911-6.

UDY, A. A., ROBERTS, J. A., BOOTS, R. J., PATERSON, D. L. & LIPMAN, J. (2010) Augmented renal clearance: implications for antibacterial dosing in the critically ill. *Clin Pharmacokinet,* 49**,** 1-16.

VAVRICKA, S. R., MUSCH, M. W., FUJIYA, M., KLES, K., CHANG, L., ELORANTA, J. J., KULLAK-UBLICK, G. A., DRABIK, K., MERLIN, D. & CHANG, E. B. (2006) Tumor necrosis factor-alpha and interferon-gamma increase PepT1 expression and activity in the human colon carcinoma cell line Caco-2/bbe and in mouse intestine. *Pflugers Arch,* 452**,** 71-80.

VERBEECK, R. K. & HORSMANS, Y. (1998) Effect of hepatic insufficiency on pharmacokinetics and drug dosing. *Pharm World Sci,* 20**,** 183-92.

WALKER, D., THWAITES, D. T., SIMMONS, N. L., GILBERT, H. J. & HIRST, B. H. (1998) Substrate upregulation of the human small intestinal peptide transporter, hPepT1. *J Physiol,* 507 ( Pt 3)**,** 697-706.

WANG, P., BA, Z. F. & CHAUDRY, I. H. (1991a) Hepatic extraction of indocyanine green is depressed early in sepsis despite increased hepatic blood flow and cardiac output. *Arch Surg,* 126**,** 219-24.

WANG, P., BA, Z. F. & CHAUDRY, I. H. (1991b) Increase in hepatic blood flow during early sepsis is due to increased portal blood flow. *Am J Physiol,* 261**,** R1507-12.

WANG, P., BA, Z. F., TAIT, S. M., ZHOU, M. & CHAUDRY, I. H. (1993) Alterations in circulating blood volume during polymicrobial sepsis. *Circ Shock,* 40**,** 92-8.

WANG, P., ZHOU, M., RANA, M. W., BA, Z. F. & CHAUDRY, I. H. (1992) Differential alterations in microvascular perfusion in various organs during early and late sepsis. *Am J Physiol,* 263**,** G38-43.

WANG, W., JITTIKANONT, S., FALK, S. A., LI, P., FENG, L., GENGARO, P. E., POOLE, B. D., BOWLER, R. P., DAY, B. J., CRAPO, J. D. & SCHRIER, R. W. (2003) Interaction among nitric oxide, reactive oxygen species, and antioxidants during endotoxemia-related acute renal failure. *Am J Physiol Renal Physiol,* 284**,** F532-7.

WANG, W., ZOLTY, E., FALK, S., SUMMER, S., ZHOU, Z., GENGARO, P., FAUBEL, S., ALP, N., CHANNON, K. & SCHRIER, R. (2008) Endotoxemia-related acute kidney injury in transgenic mice with endothelial overexpression of GTP cyclohydrolase-1. *Am J Physiol Renal Physiol,* 294**,** F571-6.

WELLS, M. & LIPMAN, J. (1997) Measurements of glomerular filtration in the intensive care unit are only a rough guide to renal function. *S Afr J Surg,* 35**,** 20-3.

WENZEL, U., DIEHL, D., HERGET, M., KUNTZ, S. & DANIEL, H. (1999) Regulation of the high-affinity H+/peptide cotransporter in renal LLC-PK1 cells. *J Cell Physiol,* 178**,** 341-8.

WHEELER, A. P. & BERNARD, G. R. (1999) Treating patients with severe sepsis. *N Engl J Med,* 340**,** 207-14.

WOLBURG, H., WOLBURG-BUCHHOLZ, K., LIEBNER, S. & ENGELHARDT, B. (2001) Claudin-1, claudin-2 and claudin-11 are present in tight junctions of choroid plexus epithelium of the mouse. *Neurosci Lett,* 307**,** 77-80.

WYLER, F., FORSYTH, R. P., NIES, A. S., NEUTZE, J. M. & MELMON, K. L. (1969) Endotoxin-induced regional circulatory changes in the unanesthetized monkey. *Circ Res,* 24**,** 777-86.

YAMASHITA, T., SHIMADA, S., GUO, W., SATO, K., KOHMURA, E., HAYAKAWA, T., TAKAGI, T. & TOHYAMA, M. (1997) Cloning and functional expression of a brain peptide/histidine transporter. *J Biol Chem,* 272**,** 10205-11.

ZHANG, E. Y., FU, D. J., PAK, Y. A., STEWART, T., MUKHOPADHYAY, N., WRIGHTON, S. A. & HILLGREN, K. M. (2004) Genetic polymorphisms in human proton-dependent dipeptide transporter PEPT1: implications for the functional role of Pro586. J Pharmacol Exp Ther, 310, 437-45.

# CHAPTER 3 IMPACT OF LIPOPOLYSACCHARIDE-INDUCED INFLAMMATION ON THE DISPOSITION OF THE AMINOCEPHALOSPORIN CEFADROXIL


## ABSTRACT

It has been increasingly reported that drug kinetics and dynamics are changed during inflammation states. The purpose of this study was to determine if cefadroxil, an α-amino-containing β-lactam anitibiotic, exhibits changes in drug disposition during lipopolysaccharide (LPS)-induced acute inflammation. Six hour after pretreatment of LPS or normal saline (as a control), mice were administered 1 nmol/g cefadroxil intravenously along with inulin for determining glomerular filtration rate (GFR). Serial blood samples, along with tissue and urine samples, were collected at predetermined time points. In order to determine inflammation-induced changes in GFR, renal tubular secretion and reabsorption, it was necessary to co-administer 70 mg/kg probenecid. Changes in mRNA expression of those transporters involved in cefadroxil disposition in kidney and choroid plexus were also investigated six hour after LPS treatment. The results demonstrated that tissue-to-blood concentration ratios were decreased by 4.6-fold in choroid plexus and by 2.5-fold in kidney during LPS-induced inflammation. The mRNA expression of PEPT2, OAT1, OAT3 and MRP4 in kidney was mildly reduced in LPS-treated mice without significant changes in choroid plexus. Renal clearance of cefadroxil was substantially decreased by LPS treatment (3-fold). GFR was also reduced by 3-fold

in LPS-treated mice, but no significant differences were observed in the fractional reabsorption of cefadroxil and renal secretion once normalized by GFR. These findings demonstrated that LPS-induced inflammation had a dramatic effect on the renal elimination of cefadroxil. It appears that changes in transporter expression has played a minor role during LPS treatment but that renal dysfunction, associated with reductions in GFR, is responsible for the substantial increase in cefadroxil plasma concentration-time profiles.

## INTRODUCTION

Inflammation is a highly complicated biological response to damages by noxious stimuli as a protective mechanism of organisms to remove the harmful stimuli. Over the past half century, it has been largely reported that drug absorption and disposition can be altered during an inflammatory response due to modifications in plasma proteins, drug-metabolizing enzymes, and drug transporters (Cressman et al., 2012). Downregulation in the levels of drug-binding plasma proteins and drug-metabolizing enzymes are now well identified, which is translated into increased plasma concentrations or decreased clearance of drug substrates (Ruot et al., 2002, Moshage et al., 1987, Don and Kaysen, 2004, Morgan et al., 2008, Morgan, 2009). Inflammation-mediated regulation of drug transporters has been also reported relatively recently, especially for ATP-binding cassette (ABC) and solute carrier (SLC) transporters (Morgan et al., 2008, Cressman et al., 2012). ABC transporters, such as P-glycoprotein (Pgp) and multidrug resistance associated proteins (MRPs), are reported to be downregulated during an inflammatory response in brain, liver and intestine, thereby affecting brain efflux, biliary clearance

and intestinal absorption of drug substrates (Morgan et al., 2008). Studies have also shown that organic anion transporting polypeptides (OATPs) and organic anion transporters (OATs) are downregulated in kidney during inflammation, resulting in reduced renal clearance of the substrate p-aminohippurate (PAH) (Hocherl et al., 2009). Although inflammation-induced changes in drug kinetics and dynamics have been intensively studied over the past 30 years, there is still a lack of knowledge concerning the mechanism(s) by which inflammation-associated changes in drug disposition are coordinated. This information may be especially critical for those drugs with a narrow therapeutic index.

Sepsis is a systemic inflammatory response state, commonly caused by bacterial endotoxin. Sepsis is frequently associated with acute renal failure (ARF), characterized by abrupt decline in glomerular filtration rate and tubular function (Thadhani et al., 1996). The mortality rate of sepsis is substantially increased when associated with ARF, resulting in 75% mortality (Levy et al., 1996). The kidney is involved in the elimination pathway for a large variety of drugs. Therefore, renal failure during septic conditions results in a significant decrease of renal clearance and a substantial increase of plasma concentration for many drugs (De Paepe et al., 2002).

Cefadroxil is a first-generation α-amino-containing β-lactam antibiotic with a broad spectrum of antibacterial activity. It has good water solubility and a modest degree of lipid solubility. Clinical studies showed that cefadroxil is widely distributed to body tissues and, therefore, is useful for infections of a variety of tissues (Quintiliani, 1982, Tanrisever and Santella, 1986). Cefadroxil is especially

effective in the treatment of upper and lower respiratory tract infections such as sinusitis otitis media, acute bronchitis and lung abscesses (Quintiliani, 1986). Cefadroxil is not metabolized in the body and is mainly eliminated via renal excretion in intact form. It has been reported that 88 to 93% of the administered dose was recovered in the urine within 24 hours (Nightingale, 1980). Therefore, elimination of cefadroxil is substantially reduced in patients with impaired renal function (Leroy et al., 1982). Previous studies have shown that cefadroxil is a substrate of several drug transporters, including the organic anion transporters (OATs) and peptide transporters (PEPT1 and PEPT2). OATs are expressed in the basolateral side of proximal tubule epithelial cells and PEPTs are localized in the apical side of proximal tubule epithelial cells, thereby playing a key role in active tubular secretion and reabsorption of drug substrates in kidney, respectively (Khamdang et al., 2003, Ganapathy et al., 1995). Therefore, cefadroxil is eliminated from the kidney by a combined process of glomerular filtration, tubular secretion and tubular reabsorption. OATs and PEPTs are also expressed at the apical surface of choroid plexus epithelia in brain, playing a role as an efflux pump for removing drug molecules from the CSF side to the blood side. This may explain in part why β-lactam antibiotics, including cefadroxil, are limited in their use for the treatment of CNS infections.

Lipopolysaccharide (LPS), a major component of bacterial cell wall, is one of the best-characterized models of infection and commonly used to investigate pathophysiology of sepsis in experimental animals. Administration of LPS is known to induce significant reductions in glomerular filtration rate (GFR) and tubular

function, as commonly observed in patients with septic shock (Wang et al., 2008b, Schmidt et al., 2007, Wang et al., 2003, Wang et al., 2008a). It has been also reported that LPS treatment downregulates OAT transcripts and protein expression in kidney, and upregulates PEPT2 transcripts in choroid plexus (Hocherl et al., 2009, Marques et al., 2009). Based on the previous findings that cefadroxil is excreted in the kidney by glomerular filtration, OAT-mediated secretion and PEPT2-mediated reabsorption, and distributed into tissues by OATs and PEPT2, we hypothesized that cefadroxil disposition would be significantly changed by LPS-induced inflammation. Our results are novel in elucidating the mechanism(s) by which LPS-induced inflammation alters the disposition and renal pharmacokinetics of cefadroxil.

## METHODS

### Materials

LPS (from Escherichia coli serotype O111:B4), to induce peripheral inflammation, and unlabeled cefadroxil were purchased from Sigma-Aldrich (St. Louis, MO). [$^{3}$H]Cefadroxil (0.8 Ci/mmol), [$^{14}$C]carboxyl-dextran (1.1 mCi/g), and [$^{14}$C]mannitol were purchased from Moravek Biochemicals (Brea, CA). [$^{14}$C]Carboxyl-inulin (2mCi/g) was obtained from American Radiolabeled Chemicals (Saint Louis, MO). Hyamine hydroxide was obtained from ICN Pharmaceuticals (Costa Mesa, CA) and nylon net filters (100μm) were obtained from Millipore Corporation (Bedford, MA). Primers for PEPT1/2 in the RT-PCR studies were synthesized by Invitrogen Life Technologies (Carlsbad, CA) and primers for OAT1/3

and MRP3/4 were purchased from Abbiotec (San Diego, CA). All other chemicals were obtained from standard sources.

## Animals

All animal studies were performed following the Guide for the Care and Use of Laboratory Animals as adopted and promulgated by the U.S. National Institutes of Health. Wild-type ($PEPT2^{+/+}$) and knockout ($PEPT2^{-/-}$) mice, on a C57BL/6 background, were generated in-house (8 – 10 weeks old). Animals were kept under temperature-controlled conditions with 12-hour light and dark cycles, and given a standard diet along with water ad libitum (Unit for Laboratory animal Medicine, University of Michigan, Ann Arbor, MI)

## Measurement of Pro-Inflammatory Cytokine Levels in Plasma

Mice were given 5mg/kg of LPS intraperitoneally to induce acute peripheral inflammation. Control animals were injected with normal saline. Plasma was collected by heart puncture 6 hour after the administration of LPS and concentrations of TNF-α, IL-1β, and IL-6 were determined using Single-Analyte ELISArray kits (QIAGEN Inc, Valencia, CA).

## Pharmacokinetic and Tissue Distribution Studies

Following the 6 hour pretreatment of LPS or normal saline, mice were anesthetized with sodium pentobarbital (40-60mg/kg i.p.) and then administered 1 nmol/g of [$^3$H]cefadroxil (100 µl; 15 µCi) by tail vein injection. Serial blood samples (~15 µl) were obtained via tail nicks at 0.25, 1, 2, 5, 15, 30, 45, 60, 90, and 120 min. Heparinized blood samples were immediately centrifuged at 3300g for 3 min to

obtain plasma. The radioactivity in plasma samples was determined by a dual-channel liquid scintillation counter (Beckman LS 3801; Beckman Coulter Inc., Fullrton, CA).

For the tissue distribution study, mice were administered [$^{14}$C]dextran (mol. wt. = 70,000) (0.25 μCi/mouse) intravenously 5 min before harvesting the tissues to correct cefadroxil tissue concentrations for the vascular space. After the last blood sample was collected (120 min after intravenous injection of cefadroxil), a CSF sample was taken from the cisterna magna by puncture of the atlantoocipital membrane with a 28-gauge needle. The mouse was immediately decapitated, and tissue samples from choroid plexuses, cerebral cortex, whole kidney, liver, lung, heart, and spleen were collected. Samples were weighed and then solubilized with 1 M hyamine hydroxide, as described by the manufacturer (MP Biomedicals). After solubilization, the level of radioactivity was determined in tissue homogenates after mixing with Ecolite liquid scintillation cocktail. Corrected tissue concentrations of cefadroxil ($C_{tissue,\,corr}$, nmol/g wet tissue) were calculated as:

$$C_{tiss,corr} = C_{tiss} - DS \bullet C_b \quad (1)$$

where $C_{tiss}$ is the uncorrected cefadroxil tissue concentration (nmol/g), DS is the blood volume (ml/g) determined as the dextran space (DS) of tissue samples estimated from dextran concentrations in the final blood sample (Keep et al., 1999), and $C_b$ is the cefadroxil blood concentration (nmol/ml).

## RT-PCR analysis of mRNA

Chroid plexuses from the lateral and fourth ventricles, as well as kidney, were rapidly harvested 6 hour after the pretreatment of LPS or normal saline and stored in RNA*later*® solution. For measuring mRNA of transport proteins in choroid plexus, each sample consisted of nine pooled plexuses from three mice. Total RNA was extracted from mouse tissues with Tri-Reagent (Molecular Research Center, Cincinnati, OH) according to the manufacturer's protocol. RNA was then reverse-transcribed using 200 units of Omniscript reverse transcriptase (QIAGEN Inc., Valencia, CA) and oligo(dT) as a primer. Real-time PCR was performed by TaqMan system for PEPT1/2 and by SYBR green system (ABI®) for OAT1/3 and MRP3/4. PCR was initiated at 95°C for 10 min, followed by 40 cycles (denaturation at 95°C for 15 s, annealing at 60°C for 60 s, and extension at 72°C for 60 s) and terminated by a final extension of 7 min duration.

Target gene mRNA expression was presented as the ratio of target gene to GAPDH housekeeping gene using the following equation (comparative $C_T$ method) (Schmittgen and Livak, 2008):

$$Ratio(T\arg et\ gene/GAPDH) = 2^{\Delta C_T} = 2^{(\Delta C_{T,T\arg et} - \Delta C_T, GAPDH)} \quad (2)$$

where $C_T$ is the threshold cycle for each gene.

## Renal Clearance Studies

Following the 6 hour pretreatment of LPS or normal saline, mice were anesthetized with sodium pentobarbital (40 - 60 mg/kg i.p.) and [$^3$H]cefadroxil (1nmol/g) was then administered by tail vein injection along with [$^{14}$C]inulin (73.6

mg/kg) for determination of GFR. Serial blood samples were collected at 0.25, 1, 2, 5, 15, 30, 45, 60, 90, and 120 min, after which the plasma was obtained after centrifugation of blood. A urine sample was collected directly from the bladder at 120 min. Renal pharmacokinetics of cefadroxil was investigated in the presence and absence of an OAT inhibitor, probenecid, to separate the estimation of fractional reabsoprtion and active tubular secretion of cefadroxil during inflammation. Probenecid (70 or 150 mg/kg) was administered intraperitoneally 45 min prior to, at time zero, and 45 min and 90 min after the co-injection of [$^{3}$H]cefadroxil and [$^{14}$C]inulin. Radioactivity of plasma and urine samples was determined by a dual-channel liquid scintillation counter, as described previously.

**Plasma Protein Binding of Cefadroxil**

The unbound fraction of cefadroxil in plasma of control and LPS treated mice was measured by an ultrafiltration method, as described previously by Shen et al (2007). Blank plasma aliquots from mice were spiked with cefadroxil to produce standard concentrations of 0.01, 0.1, 1, and 10 μM. To measure the effect of probenecid, protein binding of 1 μM cefadroxil plasma sample was also measured in the presence of probenecid (0.1, 1, and 10 mM). After incubation at 37°C for 15 min, plasma samples (200 μl) was loaded into Amicon Ultra–30K devices and centrifuged at 14,000g for 25 min at 37°C, following the manufacturer's protocol. The unbound fraction was calculated by dividing the cefadroxil concentration in ultrafiltrate by that in the original plasma sample.

## Pharmacokinetics of Cefadroxil

Cefadroxil plasma concentration versus time data were best described by a two-compartment model with a weighting factor of 1/predicted value (WinNonlin version 5.2.1; Pharsight Inc, Mountain View, CA):

$$C(t) = C_1 \times e^{-\lambda_1 t} + C_2 \times e^{-\lambda_2 t} \quad (3)$$

where C(t) is the cefadroxil plasma concentration at time t, and $C_1$ and $C_2$ are the coefficients associated with exponents of $\lambda_1$ and $\lambda_2$, respectively. The quality of the fit was determined by Akaike Information Criterion (AIC) values and visual inspection of residual plots. Area under the plasma concentration-time curve (AUC), terminal half-life ($t_{1/2}$), elimination rate constant from the central compartment ($K_{10}$), mean residence time (MRT), volume of distribution steady state ($Vd_{SS}$), volume of the central compartment ($V_1$), and total body clearance (CL) were determined by standard methods from WinNonlin.

## Renal Pharmacokinetics of Cefadroxil

The renal clearances of cefadroxil ($CL_R$) and inulin (GFR) were calculated by the following equations:

$$\begin{aligned} CL_R &= Ae_{cefadroxil(0–120)} / AUC_{cefadroxil(0–120)} \\ GFR &= Ae_{inulin(0–120)} / AUC_{inulin(0–120)} \end{aligned} \quad (4)$$

where $Ae_{(0\text{-}120)}$ is the total amount of cefadroxil (or inulin) excreted unchanged in urine over 120 min and $AUC_{(0\text{-}120)}$ is the area under the cefadroxil (or inulin) plasma concentration-time curve from 0 to 120 min, as determined by trapezoidal rule.

Renal excretion of cefadroxil is comprised of glomerular filtration, tubular secretion and tubular reabsorption (Bins and Mattie, 1988, Garcia-Carbonell et al.,

1993). Therefore, the renal clearance of cefadroxil can be expressed as (Shen et al., 2007):

$$CL_R = f_u \bullet (GFR + CL_S) \bullet (1 - F_r) \quad (5)$$

where $f_u$ is the unbound fraction of cefadroxil in plasma, $CL_S$ is the secretion clearance mediated by OATs, and $F_r$ is the fraction of reabsorbed drug mediated by PEPT1 and PEPT2. Changes in GFR during inflammation were directly calculated by comparing the inulin clearances of control and LPS-treated groups. In the presence of saturating concentrations of probenecid ($CL_S$ = 0), changes in $F_r$ during inflammation were calculated by comparing the control and LPS-treated groups, since experimental values of $CL_R$, $f_u$ and GFR could be independently obtained in the study. Based on the experimentally estimated values of $CL_R$, $f_u$, GFR and $F_r$, changes in $CL_S$ during inflammation were then able to be determined by comparing the control and LPS-treated groups in the absence of probenecid.

To normalize $CL_R$ for any differences in protein binding ($f_u$) and functional nephron mass (GFR), the excretion ratio of cefadroxil (ER) was expressed as (Ocheltree et al., 2005):

$$ER = CL_R / (f_u \bullet GFR) \quad (6)$$

**Cerebrospinal Fluid Buffer**

The isolated choroid plexus uptake experiments were performed in artificial cerebrospinal fluid (aCSF) buffer. The aCSF buffer consisted of 127 mM NaCl, 20 mM $NaHCO_3$, 2.4 mM KCl, 0.5 mM $KH_2PO_4$, 1.1 mM $CaCl_2$, 0.85 mM $MgCl_2$, 0.5 mM

$Na_2SO_4$, and 5.0 mM glucose (pH 7.4), and was continuously bubbled with 5% $CO_2$ and 95% $O_2$.

**Cefadroxil Uptake**

To induce an acute peripheral inflammation, $PEPT2^{+/+}$ and $PEPT2^{-/-}$ mice (8-10 weeks old) were administered LPS intraperitoneally as a single injection (1, 5, and 10mg/kg) or double injection (5mg/kg twice). Control animals were injected with normal saline. Animals were sacrificed 1, 3, 6, 24, and 48 hours after the LPS or normal saline injection and then the lateral and fourth ventricle choroid plexuses were isolated, as described previously (Keep and Xiang, 1995). Each sample consisted of six pooled plexuses from two animals. The tissues were weighed and then transferred to aCSF buffer, at 37°C, continuously bubbled with 5% $CO_2$ and 95% $O_2$. After a 5 min recovery period, the plexuses were transferred to 0.95 ml of transport buffer with or without inhibitor (5 mM of GlySar or *p*-aminohippurate) for 0.5 min. Uptake was initiated by adding 0.05 ml of buffer with approximately 0.8 uCi of [$^3$H]cefadroxil (1 μM in total) and 0.4 uCi of [$^{14}$C]mannitol. The uptake was terminated at 1 min by transferring the plexuses to ice-cold buffer and filtering under reduced pressure. The filters and choroid plexuses were washed three times with ice-cold buffer and then soaked in 0.33 ml of 1M hyamine hydroxide for 30 min. Ecolite (+) scintillation cocktail (ICN; Irvine, CA) was added to each sample after the tissue were completely dissolved and radioactivity of samples was measured by a dual-channel liquid scintillation counter.

The uptake of radiolabeled cefadroxil into choroid plexus (μl/mg of tissue weight) was calculated, as described previously (Keep and Xiang, 1995):

$$Cefadroxil\ Uptake = \frac{S_t - S_f - (M_t - M_f) \bullet ratio}{S_{media}} \quad (7)$$

where $S_t$ is the total substrate concentration in the plexus plus filter, $S_f$ is the filter binding of substrate, and $S_{media}$ is the concentration of substrate in the external media. The term $(M_t\text{-}M_f)\bullet$ratio is used to correct for the extracellular content of cefadroxil, where $M_t$ is the total mannitol concentration in the plexus plus filter, $M_f$ is the filter binding of mannitol, and ratio represents the ratio of [$^3$H]cefadroxil to [$^{14}$C]mannitol in the external medium. The unidirectional influx rate (V, pmol/mg/min) was calculated by multiplying cefadroxil uptake by $S_{media}$ and dividing by the duration of the experiment.

### Statistics

All the data are reported as mean ± S.E. To determine statistical differences between two different groups, a two-sample t-test was used and $p \leq 0.05$ was considered statistically significant. For multiple comparisons, analysis of variance (ANOVA) was performed followed by pair-wise comparisons using the Tukey test (GraphPad Prism, v4.0; GraphPad Software Inc., San Diego, CA).

## RESULTS

### Plasma Concentration of Pro-Inflammatory Cytokines during LPS-induced Acute Inflammation

Pro-inflammatory cytokine levels in plasma were first measured at 6 hour after LPS treatment to see if acute inflammation was induced. Administration of LPS caused substantial increases in tumor necrosis factor (TNF)-α (15-fold, $p<0.001$),

interleukin(IL)-6 (2,100-fold, $p<0.01$), and IL-1β (610-fold, $p<0.05$), all pro-inflammatory cytokines characterizing the acute immune response (Figure 3.1). The pro-inflammatory cytokines IL-6, IL-1β and TNF-α are known to be involved in numerous complex signaling cascades and trigger the production of acute phase proteins (Gabay and Kushner, 1999). Moreover, it has been reported that these cytokines induce transcription factors which play a role in suppressing expression of the ABC transporters (Ho and Piquette-Miller, 2007, Sukhai et al., 2000), and perhaps other SLC transporters. Therefore, change in the pharmacokinetic profile of cefadroxil was further investigated 6 hour after LPS treatment.

### Changes in Pharmacokinetics of Cefadroxil during Acute Inflammation

The plasma concentration-time profiles and pharmacokinetic parameters of cefadroxil were compared between control and LPS-treated mice. As shown in Figure 3.2, cefadroxil concentrations in plasma were significantly higher for the LPS-treated mice. A summary of pharmacokinetic parameters is reported in Table 3.1. There were no significant differences in maximum plasma concentration (Cmax), volume of the central compartment ($V_1$), and volume of distribution steady state ($Vd_{ss}$), whereas significant reductions were observed in elimination rate constant ($K_{10}$) and total body clearance (CL) of LPS-treated animals (about 3-fold, $p<0.001$). These changes resulted in approximately 3-fold increases in area under the plasma concentration-time curve (AUC), mean residence time (MRT) and terminal half-life ($t_{1/2}$). It seems that LPS-induced acute inflammation mostly affected the elimination kinetics of cefadroxil and not the volume of distribution terms.

## Changes in Tissue Distribution of Cefadroxil during Acute Inflammation

Figure 3.3A shows the changes in cefadroxil concentration for various tissues, CSF and blood during LPS-induced acute inflammation. Significant increases in cefadroxil were observed in CSF (4.8-fold), cerebral cortex (3.4-fold), heart (3.3-fold), lung (3.2-fold), liver (5.0-fold), spleen (3.5-fold) and blood (5.1-fold) during LPS treatment. However, when the data were corrected for differences in blood concentrations between the control and LPS-treated groups, only choroid plexus (5.0-fold decrease) and kidney (2.3-fold decrease) displayed significant changes (Figure 3.3B). When tissue-to-CSF concentration ratios were further investigated in brain, choroid plexus showed a significant decrease (2.5-fold, $p<0.01$), whereas no significant difference was observed for cerebral cortex in LPS-treated mice compared to control animals (Figure 3.3C). Based on these findings, it appears that choroid plexus and kidney are the major tissues in which cefadroxil concentrations are affected by LPS-induced acute inflammation and, therefore, changes in these tissues were further studied.

## Effect of LPS on mRNA Expression of Transporters

The mRNA expression levels of several transporters were evaluated in the kidney and choroid plexuses 6 hour after LPS treatment, a time when there was a significant reduction in tissue-to-blood concentration ratios of cefadroxil. PEPT1/2, OAT1/3, and MRP3/4 are known to be involved in the transport of cefadroxil in epithelial cells (Takeda et al., 2002, de Waart et al., 2011, Ganapathy et al., 1995) and are expressed in kidney and choroid plexus. Figure 3.4A shows that the mRNA

expression of PEPT2, OAT1, OAT3, and MRP4 was somewhat reduced by 19%, 33%, 27%, and 21%, respectively, in kidney of LPS-treated mice compared to that of normal saline-treated animals ($p<0.05$). However, the mRNA expression of PEPT2, OAT3 and MRP4 in choroid plexus was not changed by LPS-induced inflammation, as observed in Figure 3.4B. Therefore, it appears unlikely that the substantial changes in cefadroxil disposition in kidney and choroid plexus are attributable to changes in expression levels of relevant transporters.

### Changes in Renal Clearance of Cefadroxil during Acute Inflammation

We have previously shown that systemic clearance of cefadroxil is reduced 3-fold during LPS-induced acute inflammation. Cefadroxil is mainly excreted by the kidney and the renal clearance of cefadroxil, which approximates systemic clearance, is a combination of glomerular filtration, tubular secretion and tubular reabsorption. To investigate the impact of LPS treatment on each of these elimination processes, a renal clearance study was performed in which probenecid was used to block the OAT-mediated renal secretion pathway.

Figure 3.5 shows the cefadroxil concentration versus time profiles in the absence and presence of probenecid (70 mg/kg and 150 mg/kg). Co-administration of 70 mg/kg of probenecid significantly increased the plasma concentrations of cefadroxil. Even when the dose of co-administered probenecid was increased to 150 mg/kg, there was no further increase in cefadroxil concentration, suggesting that 70 mg/kg dose of probenecid is enough to completely block the renal secretion clearance of cefadroxil. Therefore, 70 mg/kg dose of probenecid was chosen for the subsequent studies.

Plasma concentrations of cefadroxil and inulin were then compared between control and LPS-treated groups, in the absence and presence of probenecid (70 mg/kg), as shown in Figures 3.6 (A-B). Pretreatment of LPS significantly increased the plasma concentrations of both cefadroxil and inulin. Co-administration of probenecid further increased the cefadroxil plasma concentrations in both control and LPS treated groups, whereas the inulin plasma concentrations were not changed by probenecid, suggesting that GFR values were stable in the presence of probenecid (Table 3.2). The plasma protein binding of cefadroxil was not altered by either LPS treatment or probenecid co-administration, with essentially all the drug being unbound in plasma (fu ≥ 0.97). Most of the administered cefadroxil were excreted in urine over 2 hr after an intravenous injection (95% in control group) but the amount of cefadroxil excreted in urine was significantly reduced in the LPS-treated group (65%). The urinary recovery of administered cefadroxil was somewhat lower in the presence of probenecid (i.e., 95 versus 81% in control group and 65 versus 51% in LPS-treated group) because of its saturating effect on renal tubular secretion. The excretion ratio of cefadroxil was essentially unity for both the control and LPS-treated groups, and was significantly reduced in the presence of probenecid (i.e., 1.01 versus 0.60 in control group and 1.06 versus 0.61 in LPS-treated group). The excretion ratio of cefadroxil was not changed by LPS treatment.

The renal clearance of cefadroxil was substantially decreased (about 3-fold) during LPS-induced acute inflammation (i.e., 0.256 versus 0.076 ml/min in absence of probenecid, and 0.127 versus 0.039 ml/min in presence of probenecid). The GFR values were also reduced by about 3-fold in the LPS-treated groups (i.e., 0.254

versus 0.079 ml/min in absence of probenecid, and 0.212 versus 0.067 ml/min in presence of probenecid). The fraction of drug reabsorbed (Fr) was able to be calculated in the presence of probenecid, with a value of about 40% for both the control and LPS-treated groups. Thus, it seems that renal tubular reabsorption was not changed during LPS-induced acute inflammation. Since the renal clearance, GFR and fraction of drug reabsorbed were experimentally determined, the secretion clearance was also able to be calculated for both the control and LPS treated groups. The secretion clearance was determined as 0.177 ml/min for the control group and was substantially reduced (3.6-fold) in the LPS-treated group (0.049 ml/min). However, when the secretion clearance ($CL_S$) was corrected for LPS-induced changes in GFR, no significant difference was observed in $CL_S$/GFR between the control and LPS-treated groups (i.e., 0.70 versus 0.63). Thus, it seems that the reduction in secretion clearance during LPS-mediated acute inflammation was mainly due to changes in GFR and not because of changes in the intrinsic clearance of cefadroxil-mediated transport.

## Time- and Dose-Dependent Changes in Cefadroxil Uptake by LPS-Induced Acute Inflammation

To investigate the underlying mechanism for the inflammation-mediated changes in cefadroxil distribution into choroid plexus, whole tissue uptake studies were performed. In this regard, uptake experiments were initiated with 1 μM cefadroxil and incubated in aCSF buffer over 1 min, a time which represents linear uptake of cefadroxil as based on a previous study (Ocheltree et al., 2004). The time-

dependent changes in cefadroxil uptake, as a function of LPS-induced inflammation, were initially studied. Choroid plexuses were obtained 1, 3, 6, 24, and 48 hours after LPS treatment and the uptake of cefadroxil in this tissue was investigated. As observed in Figure 3.7, cefadroxil uptake was maximally reduced (about 30%) 3 hour after the LPS injection ($p<0.001$), and this reduction was completely reversed 48 hour after the treatment.

To study dose dependency in the LPS-mediated reduction of cefadroxil uptake, different doses of LPS (1, 5, and 10mg/kg, single injection) and double injection of LPS (5mg/kg + 5mg/kg 3 hour after the first dose) were compared. As shown in Figure 3.8, doses greater than 5 mg/kg or double injection of 5 mg/kg LPS did not result in a further reduction of cefadroxil uptake. Therefore, a 3 hour pretreatment of 5mg/kg LPS was chosen as the experimental condition for a subsequent study.

### Effect of Inhibitors on Cefadroxil Uptake during LPS treatment

It was previously shown that 80–85% of cefadroxil uptake in the choroid plexus was mediated by PEPT2, 10–15% by organic anion transporters (OATs), and the remaining 5% by passive diffusion (Ocheltree et al., 2004). Therefore, even though LPS-mediated acute inflammation induced a reduction of cefadroxil uptake into choroid plexus, the mechanism underlying this change was not clear. To examine the effect of LPS-induced acute inflammation on different mechanisms of cefadroxil uptake in choroid plexus, cefadroxil uptake was studied in the presence of potential transport inhibitors and in PEPT2$^{-/-}$ mice. *p*-Aminohippurate (PAH) was selected as an OAT inhibitor and glycylsarcosine (GlySar) as a PEPT2 inhibitor in

this study. As shown in Figure 3.9, PAH treatment reduced cefadroxil uptake by about 15% in both the normal saline and LPS treated groups ($p<0.01$). Moreover, LPS reduced the uptake of cefadroxil by 21% in the PAH treatment group ($p<0.01$). Cefadroxil uptake was substantially reduced by 75% with GlySar ($p<0.001$) and by 77% in PEPT2$^{-/-}$ mice ($p<0.001$), suggesting that PEPT2 plays a major role in cefadroxil uptake in choroid plexus. However, an LPS-mediated reduction of cefadroxil uptake was not observed in the presence of 5 mM GlySar and in PEPT2$^{-/-}$ mice. Thus, it seems that the LPS effects on cefadroxil uptake in choroid plexus primarily reflect a reduction of PEPT2 functional activity, and not changes in passive diffusion or OAT functional activity.

## DISCUSSION

Inflammation is a highly orchestrated process involving a variety of events, which can induce changes in drug pharmacokinetics. In the present study, we showed that elimination and tissue distribution of cefadroxil were substantially changed during LPS-induced acute inflammation. Specifically, it has been demonstrated that: 1) the renal clearance of cefadroxil was reduced 3-fold during inflammatory response; 2) the functional nephrons mass (as reflected by GFR) was significantly decreased during inflammation, resulting in significant reductions in active tubular secretion and renal clearance; 3) cefadroxil distribution into the kidney and choroid plexus was reduced 2.5-fold and 4.6-fold, respectively, by LPS-induced inflammation, and 4) changes in transporter expression played only a minor role in the changes of cefadroxil distribution observed during LPS-mediated acute inflammation.

In our study, GFR was reduced 3-fold during the LPS-induced inflammatory response and it seems that the renal dysfunction, associated with reductions in GFR, was responsible for the substantial increase in cefadroxil plasma concentration-time profiles. Reduced GFR by inflammatory stimuli has been reported in previous studies (Wang et al., 2008a, Wang et al., 2003, Schmidt et al., 2007). In clinical trials, GFR reduction was reported during inflammation especially when blood flow and/or blood pressure were substantially reduced, for example, in hypodynamic septic shock associated with lowered cardiac output, which leads to a significant reduction in clearance of a variety of drugs (Pentel and Benowitz, 1984). In previous studies, 5mg/kg of LPS injection (i.p.), the same dose used in this study, was reported to induce substantial reductions in both renal blood flow and GFR without changes in blood pressure (Wang et al., 2003, Wang et al., 2002).

The reduced renal tubular secretion of cefadroxil observed during LPS-mediated acute inflammation can also be explained by renal dysfunction, as judged by GFR reductions in this study. Renal secretion clearance is dependent upon renal blood flow (Q), unbound fraction of a drug in blood ($f_u$), and intrinsic secretory clearance ($CL_{int,S}$), depending on whether the drug has high extraction ( $f_u \bullet CL_{\text{int},S} >> Q$ and $CL_S = \frac{Q \bullet f_u \bullet CL_{\text{int},S}}{Q + f_u \bullet CL_{\text{int},S}} \approx Q$ ) or low extraction ratio ( $f_u \bullet CL_{\text{int},S} << Q$ and $CL_S = \frac{Q \bullet f_u \bullet CL_{\text{int},S}}{Q + f_u \bullet CL_{\text{int},S}} \approx f_u \bullet CL_{\text{int},S}$). In comparing the secretion clearance of cefadroxil (0.177 ml/min, Table 3.2) to renal blood flow in mouse (1.3 ml/min) (Davies and Morris, 1993), cefadroxil seems to be a low extraction drug. Moreover, protein binding of cefadroxil was negligible (fu≈1, Table 3.2) and the

efficiency of renal secretion per unit nephron (CLs/GFR) was very similar between control and LPS-treated groups (0.70 vs 0.63, Table 3.2) in our study. Therefore, it seems that the reduced renal secretion during LPS-mediated inflammation is mainly driven by a reduction in functional nephron mass, which leads to a reduced intrinsic secretory clearance of cefadroxil. However, even though it appears that a reduced renal blood flow cannot be directly translated into a reduced renal secretion of cefadroxil, we cannot rule out the possibility that hypoxia or a redistribution of renal blood flow during LPS-induced inflammation can change the renal secretion of cefadroxil via altered transporter activity (Rodriguez and Smith, 1992, De Paepe et al., 2002, Hinshaw, 1996). Such changes could also affect the distribution of cefadroxil into kidney, as observed in this study (Figure 3.3B).

In addition to the remarkable changes observed in kidney, cefadroxil distribution into choroid plexus was substantially decreased during acute inflammation (Figure 3.3B). From the RT-PCR study, we confirmed that this reduction was not due to changes in expression of relevant drug transporters (Figure 3.4B). Using primary-cultured epithelial cells of choroid plexus, it was demonstrated that only a nonsaturable component exists for cefadroxil uptake at the basolateral membrane of choroid plexus (Shen et al., 2005). Therefore, the reduced choroid plexus-to-blood concentration ratio of cefadroxil during inflammation may be explained by hypoperfusion of this tissue because of a reduced blood flow (Hinshaw, 1996) or a reduced CSF efflux of cefadroxil into choroid plexus where PEPT2 and OAT play an important role. To evaluate if there are changes in CSF efflux of cefadroxil into brain tissues during LPS-mediated inflammation, tissue-

to-CSF concentration ratios were further investigated for choroid plexus and cerebral cortex (Figure 3.3C). The results indicate that cefadroxil uptake at the apical membrane of choroid plexus was significantly disrupted whereas cefadroxil distribution between CSF and cerebral cortex was not changed by LPS-mediated acute inflammation. It has been reported that PEPT2 is responsible for 80–85% of cefadroxil uptake into choroid plexus and the remaining 15–20% is mediated by OAT and nonsaturable mechanisms. Considering that a major driving force of PEPT2-mediated transport is the proton gradient, it is possible that changes in the cytoplasmic pH environment of tissue during acute inflammation may affect the functional activity of PEPT2 in apical membranes of choroid plexus epithelia (Silver, 1977, Sawyer et al., 1991, Swallow et al., 1992). Future studies should be directed at investigating the underlying mechanism of reduced cefadroxil distribution into choroid plexus during LPS-mediated acute inflammation.

In the present study, drug transporters were less likely to be involved in inflammation-mediated changes of cefadroxil pharmacokinetics. However, it has been increasingly reported that expression of drug transporters are downregulated during inflammation, thereby affecting disposition of drug substrates (Morgan et al., 2008). Little is known about possible changes of PEPT2 expression during inflammation, but one recent study showed that the PEPT2 gene in choroid plexus was significantly upregulated under LPS-induced peripheral inflammation (Marques et al., 2009). However, this study did not specify when the expression started to change after LPS treatments or the extent of change compared to control. Another study reported that both mRNA and protein expression levels of OATs in kidney

were decreased by 30–50% 12 hour after LPS treatment (Hocherl et al., 2009). In our study, mRNA expression levels of PEPT2 and OAT were unchanged in choroid plexus and only midly decreased by 20–30% in kidney (Figure 3.4). One possible reason is that the 6 hour pretreatment of LPS may be too early to induce significant alterations in drug transporter expression. In previous studies, changes in protein expression of drug transporters were usually reported later than when mRNA expression was maximally changed, and the LPS-induced alterations in protein expression were commonly observed at least 12 – 48 hour after the LPS treatment (Piquette-Miller et al., 1998, Hartmann et al., 2001, Hocherl et al., 2009, Hartmann et al., 2002). Therefore, it may be worthwhile to investigate if PEPT2 and OAT protein expression levels are changed 12 – 48 hour after LPS treatment and, if so, how changes in drug transporters induce alterations in cefadroxil pharmacokinetics.

Although distribution of cefadroxil into kidney and choroid plexus was significantly decreased, these changes were not translated into changes in volume of distribution (Table 3.1). In severe inflammation such as septic shock, various endogenous mediators are reported to promote endothelial damage, which results in increased capillary permeability (Bochud and Calandra, 2003, Glauser et al., 1991, Bone, 1991). This capillary leak has large amounts of fluid shifting from intravascular space to the interstitium, called the 'third spacing' phenomenon. For hydrophilic antibiotics with a relatively small volume of distribution such as β-lactams, volume of distribution can be significantly increased by this third spacing phenomenon, leading to significant reductions in plasma and tissue concentrations of drug (Joynt et al., 2001, Lipman et al., 2001). It has been reported that increased

volumes of distribution were observed in the hyperdynamic state of sepsis, whereas these volumes were not changed in hypodynamic state of sepsis (Tang et al., 1999). Even though the volumes of distribution for cefadroxil were not changed by inflammatory stimuli in the present study, changes in volume of distribution during inflammation should still be monitored for hydrophilic anitibiotics such as cefadroxil to be on the safe side of dosing recommendations.

In conclusion, the results of this study demonstrate that cefadroxil elimination and distribution into kidney and choroid plexus were substantially reduced under LPS-mediated acute inflammation, resulting in significant increases in cefadroxil plasma concentration-time profiles. Our findings suggest that dose adjustments would be necessary for those therapeutic agents that are primarily excreted by the kidney and have a narrow therapeutic index. Cephaloridine, another β-lactam antibiotic, is renally excreted and exhibits OAT-mediated tubular secretion. Unlike cefadroxil, cephaloridine can cause severe renal toxicity if serum concentrations exceed the therapeutic limit (Takeda et al., 1999). Aminoglycoside antibiotics, such as vancomycin, are also renally excreted and can induce severe side effects such as nephrotoxicity and ototoxicity. Therefore, for these predominantly renally eliminated drugs, decreased clearances and corresponding increased plasma concentrations during inflammation necessitate that they be carefully monitored to ensure both efficacy and safety concerns during their use.

**Table 3.1.** Pharmacokinetic parameters of 1 nmol/g cefadroxil (intravenous bolus dose) in control and lipopolysaccharide (LPS) - treated mice. Data are expressed as mean ± S.E. (n=5).

| Parameter | Control | LPS |
|---|---|---|
| AUC (min•nmol/ml) | 63.6 ± 4.3 | 203 ± 23*** |
| $t_{1/2}$ (min) | 7.8 ± 0.7 | 24.0 ± 4.7 ** |
| $K_{10}$ ($min^{-1}$) | 0.092 ± 0.008 | 0.034 ± 0.006 *** |
| $C_{max}$ (μM) | 5.9 ± 0.9 | 6.3 ± 0.5 |
| MRT (min) | 26.0 ± 1.1 | 85.7 ± 11.8 ** |
| $Vd_{ss}$ (ml) | 7.1 ± 0.3 | 7.4 ± 0.5 |
| $V_1$ (ml) | 3.1 ± 0.3 | 2.9 ± 0.3 |
| CL (ml/min) | 0.273 ± 0.007 | 0.090 ± 0.007 *** |

** $p<0.01$ and *** $p<0.001$, as compared to control.

**Table 3.2.** Renal pharmacokinetic parameters of 1 nmol/g cefadroxil (intravenous bolus dose) in control and lipopolysaccharide (LPS) - treated mice, in the absence and presence of probenecid (PRO, 70mg/kg). Data are expressed as mean ± S.E. (n=4-5). Different superscript letters denote significant differences between treatment groups (α=0.05).

| Parameter | Control | LPS | Control + PRO | LPS + PRO |
|---|---|---|---|---|
| $CL_R$ (ml/min) | $0.256 \pm 0.013^A$ | $0.076 \pm 0.009^B$ | $0.127 \pm 0.007^C$ | $0.039 \pm 0.004^D$ |
| GFR (ml/min) | $0.254 \pm 0.021^A$ | $0.079 \pm 0.029^B$ | $0.212 \pm 0.014^A$ | $0.067 \pm 0.009^B$ |
| $f_u$ | $0.99 \pm 0.01^A$ | $0.97 \pm 0.01^A$ | $1.00 \pm 0.03^A$ | $1.00 \pm 0.01^A$ |
| $fe_{0\text{-}120}$ | $0.95 \pm 0.03^A$ | $0.65 \pm 0.03^B$ | $0.81 \pm 0.03^C$ | $0.51 \pm 0.05^D$ |
| ER | $1.01 \pm 0.04^A$ | $1.06 \pm 0.20^A$ | $0.60 \pm 0.03^B$ | $0.61 \pm 0.03^B$ |
| $F_r$ | $0.40^A$ | $0.39^A$ | $0.40 \pm 0.03^A$ | $0.39 \pm 0.03^A$ |
| $CL_S$ (ml/min) | 0.177 | 0.049 | 0 | 0 |
| $CL_S$/GFR | 0.70 | 0.63 | 0 | 0 |

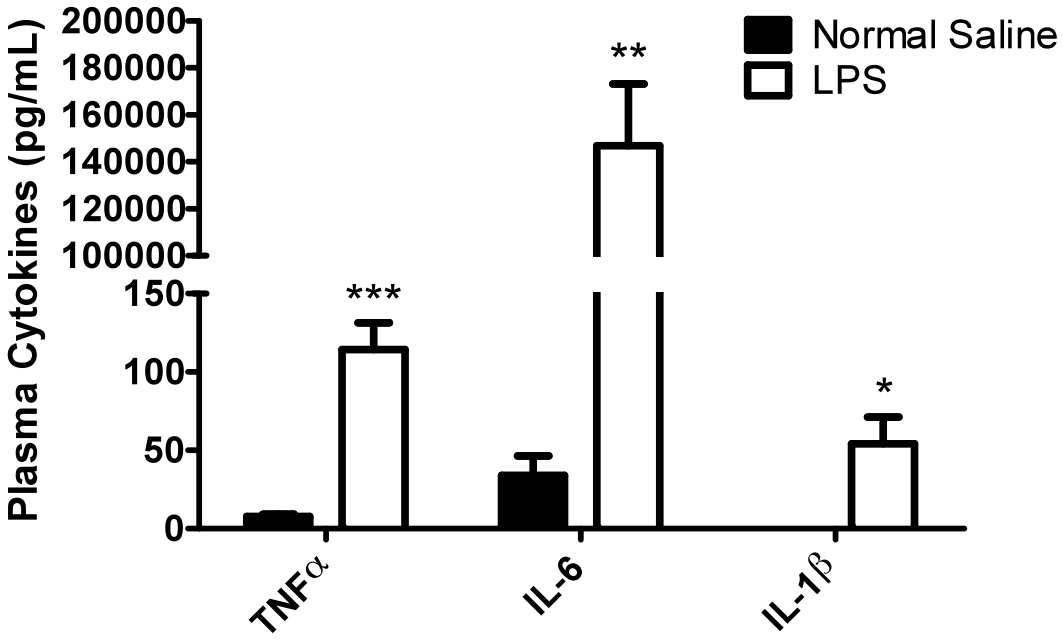


**Figure 3.1.** Pro-inflammatory cytokine levels in the plasma of control (normal saline) and 5mg/kg LPS-treated mice. Plasma was collected 6 hour after the i.p. administration of LPS 5 mg/kg or normal saline. Data are expressed as mean ± S.E. (n=5). * $p<0.05$, ** $p<0.01$ and *** $p<0.001$, as compared to control.

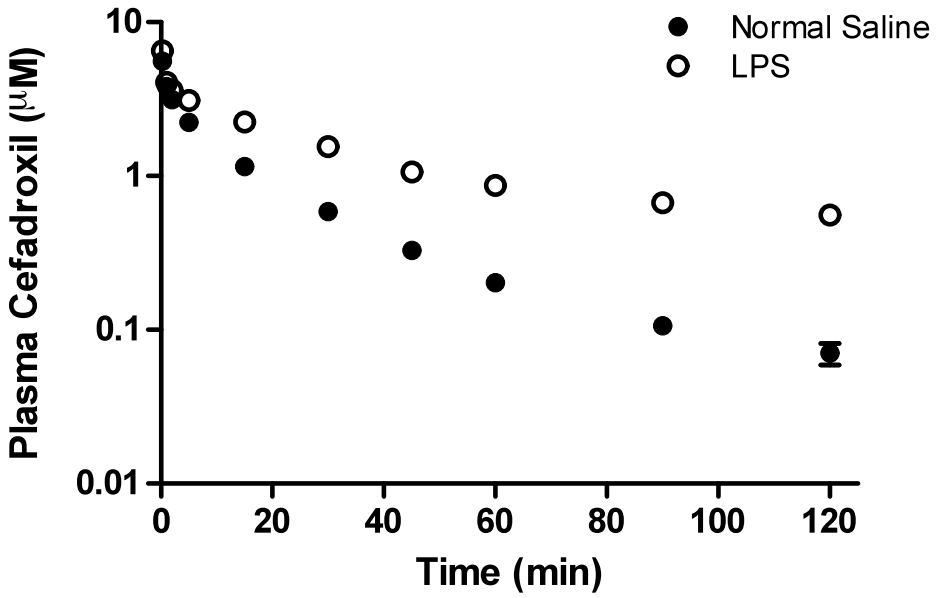


**Figure 3.2.** Effect of 5 mg/kg lipopolysaccharide (LPS) – induced inflammation on the pharmacokinetic profile of cefadroxil (1 nmol/g, i.v. bolus dose), where LPS was administered 6 hour prior to cefadroxil dosing. Data are expressed as mean ± S.E. (n=5).

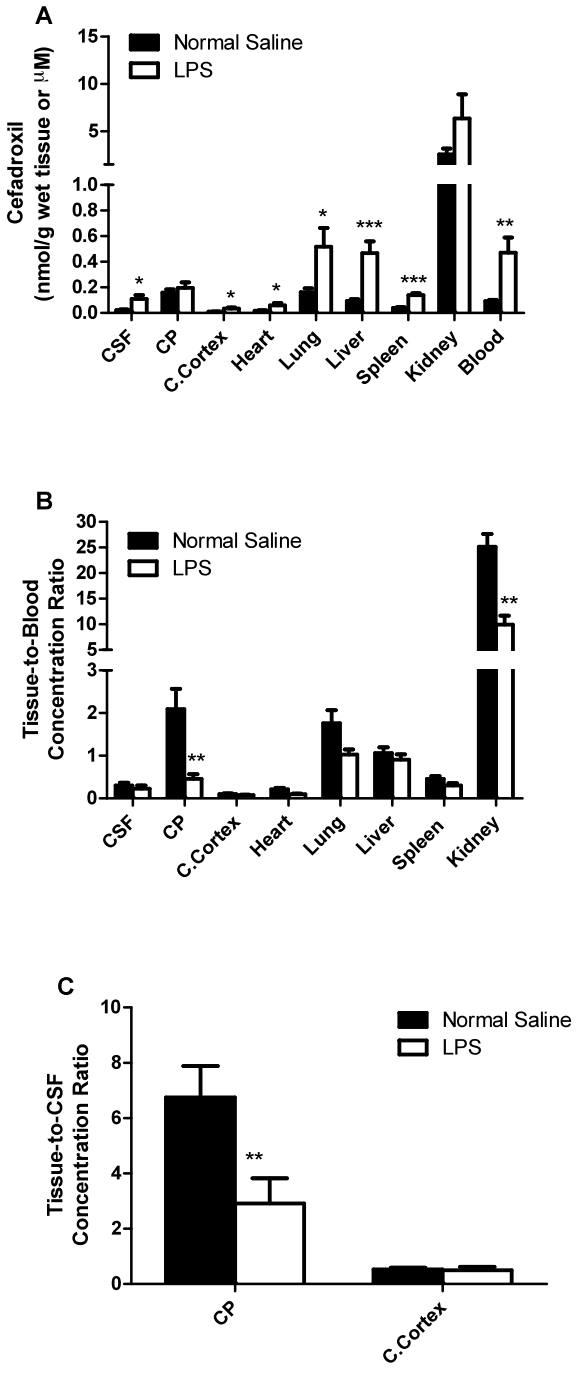


**Figure 3.3.** LPS-induced effects on cefadroxil tissue, CSF and blood concentrations (A), the tissue-to-blood concentration ratio of cefadroxil (B), and the tissue-to-CSF concentration ratio of cefadroxil (C), where 5 mg/kg LPS was administered i.p. 4 hour before an i.v. bolus dose of 1 nmol/g cefadroxil. The tissues, blood and CSF were harvested 2 hour after the cefadroxil dosing (6 hour after LPS dosing). Data are expressed as mean ± SE (n=4-8). * $p < 0.05$, ** $p < 0.01$, and *** $p < 0.001$, as compared to control (normal saline).

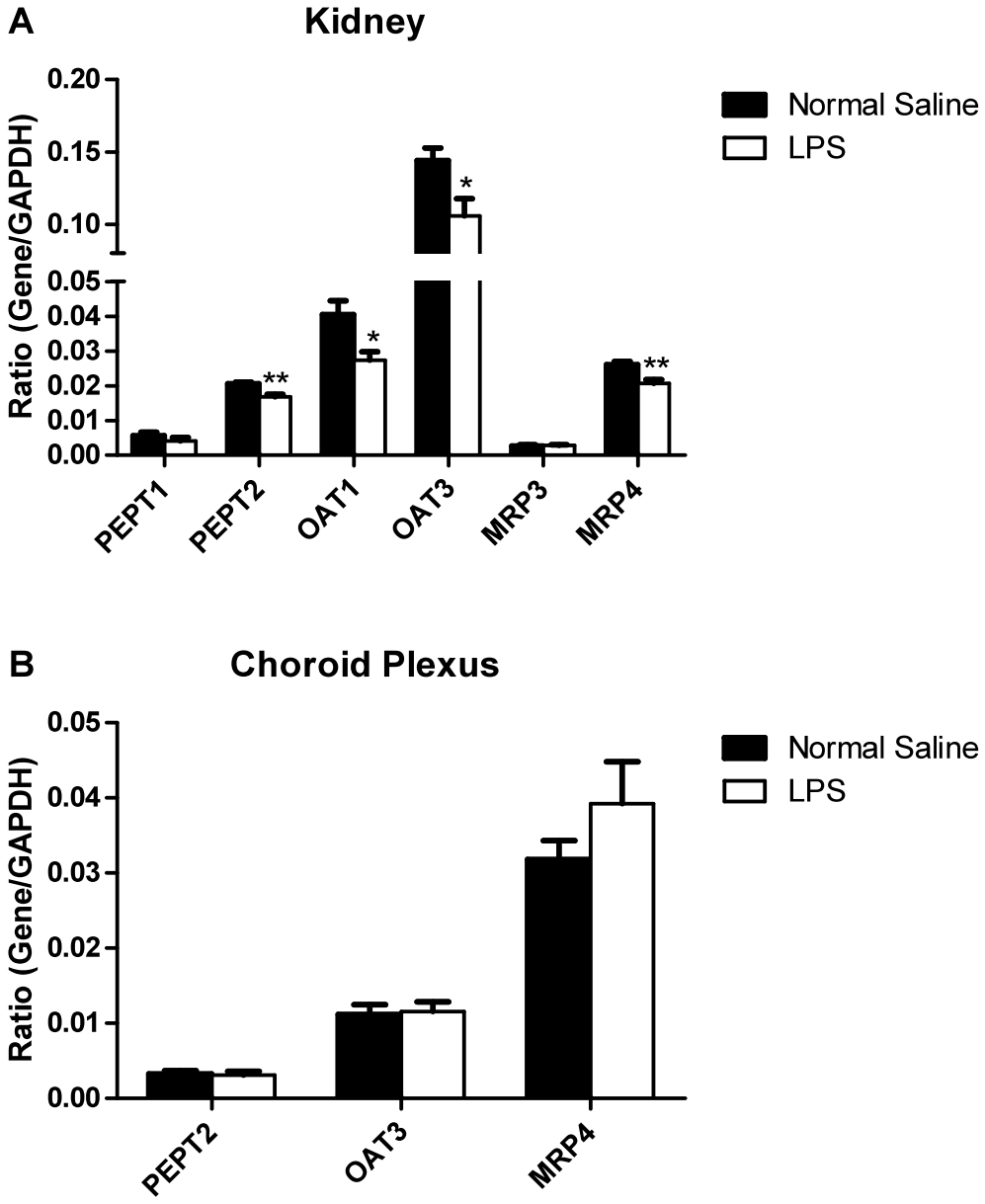


**Figure 3.4.** Effect of 5 mg/kg lipopolysaccharide (LPS) – induced inflammation on mRNA level of transporters 6 hour after i.p. administration. Data are expressed as mean ± S.E. (n=4). * $p < 0.05$ and ** $p < 0.01$, as compared to control (normal saline).

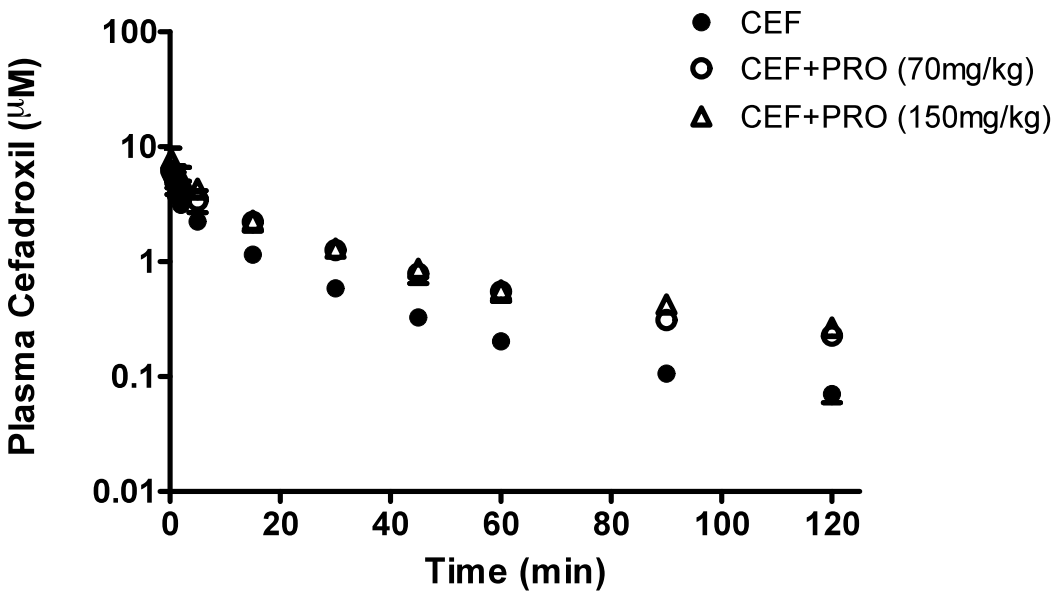


**Figure 3.5.** Plasma concentration versus time profiles of cefadroxil (1 nmol/g, i.v. bolus dose) in the presence and absence of probenecid (70mg/kg or 150 mg/kg). Data are expressed as mean ± S.E. (n=3-5).

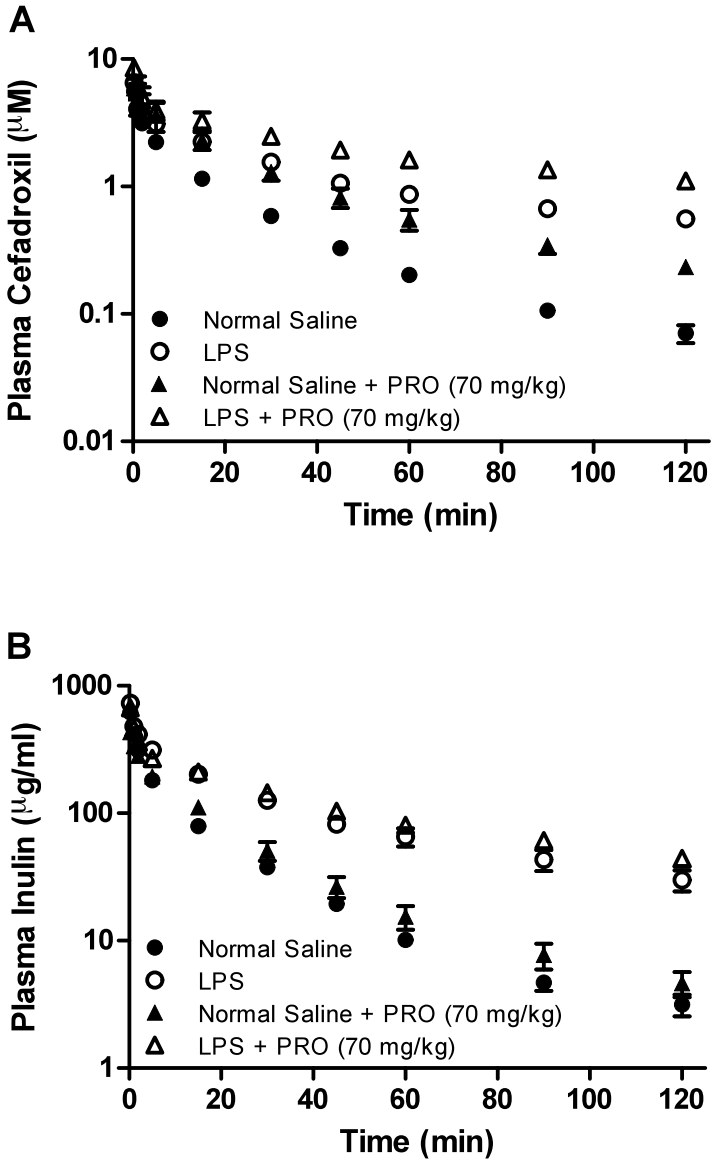


**Figure 3.6.** Effect of 5 mg/kg lipopolysaccharide (LPS) - induced inflammation on the plasma concentration versus time profiles of cefadroxil (1 nmol/g, i.v. bolus dose) and inulin (73.6 mg/kg, i.v. bolus dose) in the presence and absence of probenecid (70mg/kg). Data are expressed as mean ± S.E. (n=4-5).

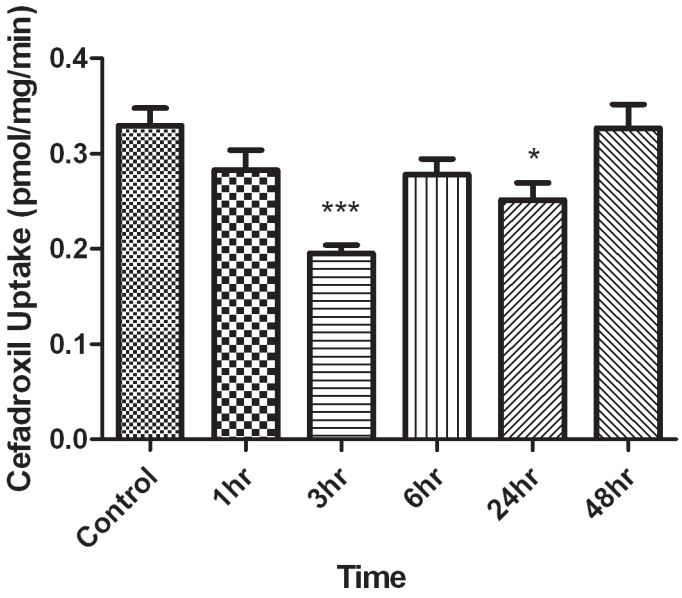


**Figure 3.7.** Effect of 5 mg/kg lipopolysaccharide (LPS) – induced inflammation on 1 μM cefadroxil uptake in isolated choroid plexus over time. Data are expressed as mean ± S.E. (n=3-5). * $p < 0.05$ and *** $p < 0.001$, as compared to control.

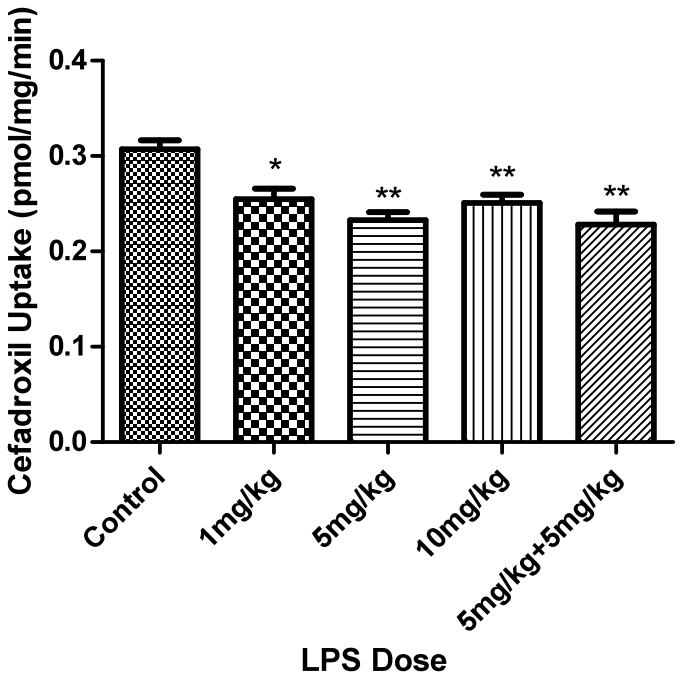


**Figure 3.8.** Effect of LPS dose on 1 μM cefadroxil uptake in isolated choroid plexus. Data are expressed as mean ± S.E. (n=3-5). * $p < 0.05$ and ** $p < 0.01$, as compared to control.

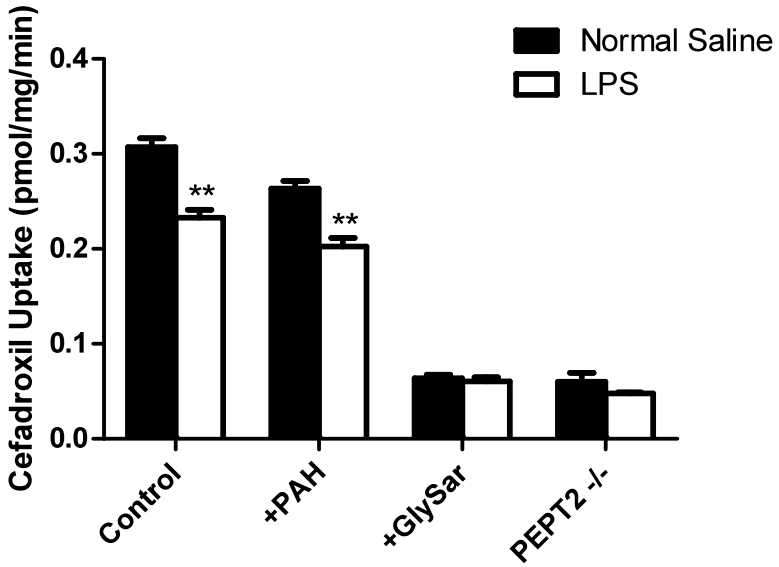


**Figure 3.9.** Effect of 5 mg/kg lipopolysaccharide (LPS) – induced inflammation on 1 μM cefadroxil uptake in isolated choroid plexus in the absence and presence of 5 mM inhibitors. PAH = para-aminohippuric acid (OAT inhibitor); GlySar = glycylsarcosine (PEPT2 inhibitor); PEPT2$^{-/-}$ = CPs from PEPT2 KO mice. Data are expressed as mean ± S.E. (n=3). ** $p < 0.01$, as compared to control.

## REFERENCES


BINS, J. W. & MATTIE, H. (1988) Saturation of the tubular excretion of beta-lactam antibiotics. *Br J Clin Pharmacol,* 25**,** 41-50.

BOCHUD, P. Y. & CALANDRA, T. (2003) Pathogenesis of sepsis: new concepts and implications for future treatment. *BMJ,* 326**,** 262-6.

BONE, R. C. (1991) The pathogenesis of sepsis. *Ann Intern Med,* 115**,** 457-69.

CRESSMAN, A. M., PETROVIC, V. & PIQUETTE-MILLER, M. (2012) Inflammation-mediated changes in drug transporter expression/activity: implications for therapeutic drug response. *Expert Rev Clin Pharmacol,* 5**,** 69-89.

DAVIES, B. & MORRIS, T. (1993) Physiological parameters in laboratory animals and humans. *Pharm Res,* 10**,** 1093-5.

DE PAEPE, P., BELPAIRE, F. M. & BUYLAERT, W. A. (2002) Pharmacokinetic and pharmacodynamic considerations when treating patients with sepsis and septic shock. *Clin Pharmacokinet,* 41**,** 1135-51.

DE WAART, D. R., VAN DE WETERING, K., KUNNE, C., DUIJST, S., PAULUSMA, C. C. & OUDE ELFERINK, R. P. (2011) Oral availability of cefadroxil depends on ABCC3 and ABCC4. *Drug Metab Dispos,* 40**,** 515-21.

DON, B. R. & KAYSEN, G. (2004) Serum albumin: relationship to inflammation and nutrition. *Semin Dial,* 17**,** 432-7.

DUCHIN, K. L. & SCHRIER, R. W. (1978) Interrelationship between renal haemodynamics, drug kinetics and drug action. *Clin Pharmacokinet,* 3**,** 58-71.

GABAY, C. & KUSHNER, I. (1999) Acute-phase proteins and other systemic responses to inflammation. *N Engl J Med,* 340**,** 448-54.

GANAPATHY, M. E., BRANDSCH, M., PRASAD, P. D., GANAPATHY, V. & LEIBACH, F. H. (1995) Differential recognition of beta -lactam antibiotics by intestinal and renal peptide transporters, PEPT 1 and PEPT 2. *J Biol Chem,* 270**,** 25672-7.

GARCIA-CARBONELL, M. C., GRANERO, L., TORRES-MOLINA, F., ARISTORENA, J. C., CHESA-JIMENEZ, J., PLA-DELFINA, J. M. & PERIS-RIBERA, J. E. (1993) Nonlinear pharmacokinetics of cefadroxil in the rat. *Drug Metab Dispos,* 21**,** 215-7.

GLAUSER, M. P., ZANETTI, G., BAUMGARTNER, J. D. & COHEN, J. (1991) Septic shock: pathogenesis. *Lancet,* 338**,** 732-6.

HARTMANN, G., CHEUNG, A. K. & PIQUETTE-MILLER, M. (2002) Inflammatory cytokines, but not bile acids, regulate expression of murine hepatic anion transporters in endotoxemia. *J Pharmacol Exp Ther,* 303**,** 273-81.

HARTMANN, G., KIM, H. & PIQUETTE-MILLER, M. (2001) Regulation of the hepatic multidrug resistance gene expression by endotoxin and inflammatory cytokines in mice. *Int Immunopharmacol,* 1**,** 189-99.

HINSHAW, L. B. (1996) Sepsis/septic shock: participation of the microcirculation: an abbreviated review. *Crit Care Med,* 24**,** 1072-8.

HO, E. A. & PIQUETTE-MILLER, M. (2007) KLF6 and HSF4 transcriptionally regulate multidrug resistance transporters during inflammation. *Biochem Biophys Res Commun,* 353**,** 679-85.

HOCHERL, K., SCHMIDT, C. & BUCHER, M. (2009) COX-2 inhibition attenuates endotoxin-induced downregulation of organic anion transporters in the rat renal cortex. *Kidney Int,* 75**,** 373-80.

JOYNT, G. M., LIPMAN, J., GOMERSALL, C. D., YOUNG, R. J., WONG, E. L. & GIN, T. (2001) The pharmacokinetics of once-daily dosing of ceftriaxone in critically ill patients. *J Antimicrob Chemother,* 47**,** 421-9.

KEEP, R. F., SI, X., SHAKUI, P., ENNIS, S. R. & BETZ, A. L. (1999) Effect of amiloride analogs on DOCA-salt-induced hypertension in rats. *Am J Physiol,* 276**,** H2215-20.

KEEP, R. F. & XIANG, J. (1995) N-system amino acid transport at the blood--CSF barrier. *J Neurochem,* 65**,** 2571-6.

KHAMDANG, S., TAKEDA, M., BABU, E., NOSHIRO, R., ONOZATO, M. L., TOJO, A., ENOMOTO, A., HUANG, X. L., NARIKAWA, S., ANZAI, N., PIYACHATURAWAT, P. & ENDOU, H. (2003) Interaction of human and rat organic anion transporter 2 with various cephalosporin antibiotics. *Eur J Pharmacol,* 465**,** 1-7.

LEROY, A., HUMBERT, G., GODIN, M. & FILLASTRE, J. P. (1982) Pharmacokinetics of cefadroxil in patients with impaired renal function. *J Antimicrob Chemother,* 10 Suppl B**,** 39-46.

LEVY, E. M., VISCOLI, C. M. & HORWITZ, R. I. (1996) The effect of acute renal failure on mortality. A cohort analysis. *JAMA,* 275**,** 1489-94.

LIPMAN, J., WALLIS, S. C., RICKARD, C. M. & FRAENKEL, D. (2001) Low cefpirome levels during twice daily dosing in critically ill septic patients: pharmacokinetic modelling calls for more frequent dosing. *Intensive Care Med,* 27**,** 363-70.

MARQUES, F., SOUSA, J. C., COPPOLA, G., FALCAO, A. M., RODRIGUES, A. J., GESCHWIND, D. H., SOUSA, N., CORREIA-NEVES, M. & PALHA, J. A. (2009) Kinetic profile of the transcriptome changes induced in the choroid plexus by peripheral inflammation. *J Cereb Blood Flow Metab,* 29**,** 921-32.

MORGAN, E. T. (2009) Impact of infectious and inflammatory disease on cytochrome P450-mediated drug metabolism and pharmacokinetics. *Clin Pharmacol Ther,* 85**,** 434-8.

MORGAN, E. T., GORALSKI, K. B., PIQUETTE-MILLER, M., RENTON, K. W., ROBERTSON, G. R., CHALUVADI, M. R., CHARLES, K. A., CLARKE, S. J., KACEVSKA, M., LIDDLE, C., RICHARDSON, T. A., SHARMA, R. & SINAL, C. J. (2008) Regulation of drug-metabolizing enzymes and transporters in infection, inflammation, and cancer. *Drug Metab Dispos,* 36**,** 205-16.

MOSHAGE, H. J., JANSSEN, J. A., FRANSSEN, J. H., HAFKENSCHEID, J. C. & YAP, S. H. (1987) Study of the molecular mechanism of decreased liver synthesis of albumin in inflammation. *J Clin Invest,* 79**,** 1635-41.

NIGHTINGALE, C. (1980) Pharmacokinetics of the oral cephalosporins in adults. *J Int Med Res,* 8**,** 2-8.

OCHELTREE, S. M., SHEN, H., HU, Y., KEEP, R. F. & SMITH, D. E. (2005) Role and relevance of peptide transporter 2 (PEPT2) in the kidney and choroid plexus: in vivo studies with glycylsarcosine in wild-type and PEPT2 knockout mice. *J Pharmacol Exp Ther,* 315**,** 240-7.

OCHELTREE, S. M., SHEN, H., HU, Y., XIANG, J., KEEP, R. F. & SMITH, D. E. (2004) Mechanisms of cefadroxil uptake in the choroid plexus: studies in wild-type and PEPT2 knockout mice. *J Pharmacol Exp Ther,* 308**,** 462-7.

PENTEL, P. & BENOWITZ, N. (1984) Pharmacokinetic and pharmacodynamic considerations in drug therapy of cardiac emergencies. *Clin Pharmacokinet,* 9**,** 273-308.

PIQUETTE-MILLER, M., PAK, A., KIM, H., ANARI, R. & SHAHZAMANI, A. (1998) Decreased expression and activity of P-glycoprotein in rat liver during acute inflammation. *Pharm Res,* 15**,** 706-11.

QUINTILIANI, R. (1982) A review of the penetration of cefadroxil into human tissue. *J Antimicrob Chemother,* 10 Suppl B**,** 33-8.

QUINTILIANI, R. (1986) Efficacy of a twice-daily regimen of cefadroxil in the treatment of respiratory tract infections. *Drugs,* 32 Suppl 3**,** 43-9.

RODRIGUEZ, C. A. & SMITH, D. E. (1992) Influence of angiotensin II-induced alterations in renal flow on excretion of cefonicid in isolated perfused rat kidneys. *Antimicrob Agents Chemother,* 36**,** 616-9.

RUOT, B., BECHEREAU, F., BAYLE, G., BREUILLE, D. & OBLED, C. (2002) The response of liver albumin synthesis to infection in rats varies with the phase of the inflammatory process. *Clin Sci (Lond),* 102**,** 107-14.

SAWYER, R. G., SPENGLER, M. D., ADAMS, R. B. & PRUETT, T. L. (1991) The peritoneal environment during infection. The effect of monomicrobial and polymicrobial bacteria on pO2 and pH. *Ann Surg,* 213**,** 253-60.

SCHMIDT, C., HOCHERL, K., SCHWEDA, F., KURTZ, A. & BUCHER, M. (2007) Regulation of renal sodium transporters during severe inflammation. *J Am Soc Nephrol,* 18**,** 1072-83.

SCHMITTGEN, T. D. & LIVAK, K. J. (2008) Analyzing real-time PCR data by the comparative C(T) method. *Nat Protoc,* 3**,** 1101-8.

SHEN, H., KEEP, R. F., HU, Y. & SMITH, D. E. (2005) PEPT2 (Slc15a2)-mediated unidirectional transport of cefadroxil from cerebrospinal fluid into choroid plexus. *J Pharmacol Exp Ther,* 315**,** 1101-8.

SHEN, H., OCHELTREE, S. M., HU, Y., KEEP, R. F. & SMITH, D. E. (2007) Impact of genetic knockout of PEPT2 on cefadroxil pharmacokinetics, renal tubular reabsorption, and brain penetration in mice. *Drug Metab Dispos,* 35**,** 1209-16.

SILVER, I. A. (1977) Tissue PO2 changes in acute inflammation. *Adv Exp Med Biol,* 94**,** 769-74.

SUKHAI, M., YONG, A., KALITSKY, J. & PIQUETTE-MILLER, M. (2000) Inflammation and interleukin-6 mediate reductions in the hepatic expression and transcription of the mdr1a and mdr1b Genes. *Mol Cell Biol Res Commun,* 4**,** 248-56.

SWALLOW, C. J., GRINSTEIN, S. & ROTSTEIN, O. D. (1992) Lipopolysaccharide impairs macrophage cytoplasmic pH regulation under conditions simulating the inflammatory microenvironment. *J Leukoc Biol,* 52**,** 395-9.

TAKEDA, M., BABU, E., NARIKAWA, S. & ENDOU, H. (2002) Interaction of human organic anion transporters with various cephalosporin antibiotics. *Eur J Pharmacol,* 438**,** 137-42.

TAKEDA, M., TOJO, A., SEKINE, T., HOSOYAMADA, M., KANAI, Y. & ENDOU, H. (1999) Role of organic anion transporter 1 (OAT1) in cephaloridine (CER)-induced nephrotoxicity. *Kidney Int,* 56**,** 2128-36.

TANG, G. J., TANG, J. J., LIN, B. S., KONG, C. W. & LEE, T. Y. (1999) Factors affecting gentamicin pharmacokinetics in septic patients. *Acta Anaesthesiol Scand,* 43**,** 726-30.

TANRISEVER, B. & SANTELLA, P. J. (1986) Cefadroxil. A review of its antibacterial, pharmacokinetic and therapeutic properties in comparison with cephalexin and cephradine. *Drugs,* 32 Suppl 3**,** 1-16.

THADHANI, R., PASCUAL, M. & BONVENTRE, J. V. (1996) Acute renal failure. *N Engl J Med,* 334**,** 1448-60.

WANG, W., FALK, S. A., JITTIKANONT, S., GENGARO, P. E., EDELSTEIN, C. L. & SCHRIER, R. W. (2002) Protective effect of renal denervation on normotensive endotoxemia-induced acute renal failure in mice. *Am J Physiol Renal Physiol,* 283**,** F583-7.

WANG, W., JITTIKANONT, S., FALK, S. A., LI, P., FENG, L., GENGARO, P. E., POOLE, B. D., BOWLER, R. P., DAY, B. J., CRAPO, J. D. & SCHRIER, R. W. (2003) Interaction among nitric oxide, reactive oxygen species, and antioxidants during endotoxemia-related acute renal failure. *Am J Physiol Renal Physiol,* 284**,** F532-7.

WANG, W., LI, C., SUMMER, S. N., FALK, S., LJUBANOVIC, D. & SCHRIER, R. W. (2008a) Role of AQP1 in endotoxemia-induced acute kidney injury. *Am J Physiol Renal Physiol,* 294**,** F1473-80.

WANG, W., ZOLTY, E., FALK, S., SUMMER, S., ZHOU, Z., GENGARO, P., FAUBEL, S., ALP, N., CHANNON, K. & SCHRIER, R. (2008b) Endotoxemia-related acute kidney injury in transgenic mice with endothelial overexpression of GTP cyclohydrolase-1. *Am J Physiol Renal Physiol,* 294**,** F571-6.

# CHAPTER 4 IMPORTANCE OF PEPT2 ON THE CEREBROSPINAL FLUID EFFLUX KINETICS OF GLYCYLSARCOSINE CHARACTERIZED BY NONLINEAR MIXED EFFECTS MODELING


## ABSTRACT

The purpose of this study was to develop a population pharmacokinetic model to quantitate the distribution kinetics of glycylsarcosine (GlySar), a substrate of peptide transporter 2 (PEPT2), in blood, CSF and kidney in wild-type and PEPT2 knockout mice. A stepwise compartment modeling approach was performed to describe the concentration profiles of GlySar in blood, CSF, and kidney simultaneously using nonlinear mixed effects modeling (NONMEM). The final model was selected based on the likelihood ratio test and graphical goodness-of-fit. The profiles of GlySar in blood, CSF, and kidney were best described by a four-compartment model. The estimated systemic elimination clearance, volume of distribution in the central and peripheral compartments were 0.236 vs 0.449 ml/min, 3.79 vs 4.75 ml, and 5.75 vs 9.18 ml for wild-type versus knockout mice. Total CSF efflux clearance was 4.3 fold higher for wild-type compared to knockout mice. NONMEM parameter estimates indicated that 77% of CSF efflux clearance was mediated by PEPT2 and the remaining 23% was mediated by the diffusional and bulk clearances. Due to the availability of PEPT2 knockout mice, we were able to

quantitatively determine the significance of PEPT2 in the efflux kinetics of GlySar at the blood-cerebrospinal fluid barrier.

## INTRODUCTION

The blood-cerebrospinal fluid barrier (BCSFB) is formed by choroid plexus epithelial cells of the ventricles and cells of the arachnoid membrane that cover the surface of the brain. Similar to the blood-brain barrier (BBB), the BCSFB protects the central nervous system (CNS) from unwanted toxic compounds in the blood supply to maintain a constant extracellular environment for normal brain function (Smith et al., 2004, Coisne and Engelhardt, 2011). The BCSFB has several advantages for drug delivery to the brain. First, because of the basolateral infoldings and numerous apical microvilli, choroid plexus epithelial cells have a large surface area for exchange of drug molecules. Second, the tight junctions linking choroid plexus epithelial cells are relatively weak compared to the BBB and, thus, the BCSFB has a relatively high permeability (Thomas and Segal, 1998). Third, the BCSFB allows direct access to the ventricles, ependyma and subependymal tissue, leptomeninges, outerlayers of pial vessels, and perivascular spaces (Ghersi-Egea et al., 1996b, Ghersi-Egea et al., 1996a). Therefore, the BCSFB can be a useful target for drug delivery to the brain in several CNS disease states.

Choroid plexuses possess a variety of transport proteins that act as gate keepers for the inward and outward movement of molecules across the BCSFB. Inwardly directed basolateral transport proteins can facilitate the entry of molecules (e.g., nutrients) into the CSF, whereas outwardly directed apical transport proteins can facilitate the elimination of undesired molecules (e.g., drugs and

CSF-born endogenous metabolites) into the blood. The main drug transporters in choroid plexus belong to two superfamilies, the solute carrier (SLC) family including OAT1-3, OATP3 and PEPT2, and the ATP-binding cassette (ABC) carrier family including P-gp and MRP1. The membrane expression of SLC and ABC transporters are polarized and, thereby, allow for efficient movement of drug substrates across the BCSFB (Ocheltree et al., 2004, Kusuhara and Sugiyama, 2004). Peptide transporter 2 (PEPT2) is abundantly expressed at the apical surface of choroid plexus epithelia and plays an important role in the efflux of substrate molecules from CSF to blood.

PEPT2 belongs to the proton-coupled oligopeptide transporter (POT) family and is responsible for the cellular uptake of di- and tripeptides in the organism via an inwardly directed electrochemical proton gradient. There are four members of the POT family in mammals: PEPT1, PEPT2, PHT1 and PHT2. Compared to PEPT1, which is a low-affinity and high-capacity transporter, PEPT2 is characterized as a high-affinity and low-capacity transporter (Daniel and Rubio-Aliaga, 2003). PEPT2 is predominantly localized in apical membrane of epithelium in the kidney proximal tubule and brain choroid plexus. It also has been detected in the lung, mammary gland and other tissues of brain (astrocytes, sub-ependymal cells, and ependymal cells). It is generally believed that PEPT2 is responsible for the reabsorption of small peptides and peptide-like drugs in kidney (Smith et al., 1998, Takahashi et al., 1998, Shen et al., 1999), as well as neuropeptide homeostasis in choroid plexus (Shu et al., 2002, Teuscher et al., 2004, Shen et al., 2004). Especially in choroid plexus of brain, PEPT2 pumps out peptidomemetic drugs (i.e. cefadroxil) and neuropeptides (i.e. 5-

aminolevulinic acid and L-kyotorphin) from CSF into the blood and thereby restricts the delivery of these substrate molecules to the CNS (Ocheltree et al., 2005, Shen et al., 2007, Hu et al., 2007).

Description of CSF pharmacokinetics is important in predicting and understanding pharmacologic actions of CNS drugs (Shafer et al., 1998). In clinical studies, only limited CSF samples are available per subject because of both medical and ethical reasons, which allows large variation of data in the study. Nonlinear mixed effects modeling (NONMEM) is especially useful in this case to address different sources of variability and to identify major origins of variability. Several studies have developed CSF pharmacokinetic models of drugs using NONMEM data analysis (Shafer et al., 1998, Khatri et al., 2010, Nalda-Molina et al., 2012, Pfister et al., 2003). Since several mechanisms including transport proteins are involved in the influx and efflux of drugs at the brain, quantifying the importance of each distribution mechanism helps us to adjust the dose to meet both the efficacy and safety concerns of CNS drugs. A NONMEM approach can also be a useful tool to parameterize the distribution mechanisms between blood and brain, and to quantatively analyze the importance of different transport proteins as compared to passive processes.

With this in mind, the aim of this study was to develop a population pharmacokinetic model to describe the distribution kinetics of glycylsarcosine (GlySar), a model PEPT2 substrate, at the BCSFB. Our laboratory developed PEPT2-deficient mice, which allows us to study the physiological and pharmacological importance of this transporter in the body (Shen et al., 2003). With the use of PEPT2

knockout mice, we developed a distribution kinetics model that incorporated PEPT2 expression level data and quantitatively analyzed the importance of PEPT2 in the efflux mechanism of GlySar at the BCSFB.

## MATERIALS AND METHODS

The distribution kinetics of the PEPT2 substrate GlySar was assessed at the BCSFB using nonlinear mixed effects modeling (NONMEM) based on data generated previously in our laboratory (Ocheltree et al., 2005). In brief, gender-matched wild-type and PEPT2 knockout mice (6-8 weeks old) were anesthetized with sodium pentobarbital and then administered 100μl of [$^{14}$C]GlySar (5 μCi/mouse for labeled GlySar and a total dose of 0.05 μmol/g body weight for both labeled and unlabeled GlySar) by tail vein injection. Blood samples (5 μl) were obtained at 0.25, 1, 2, 5, 10, 20, 30, 45, and 60 min after the intravenous bolus via tail nicks. A CSF sample (~5 μl) was collected by inserting a 28-gauge needle into the cisterna magna after the end of sampling. The mouse was then decapitated, and choroid plexuses from lateral and fourth ventricles and whole kidney were harvested. To correct the tissue concentrations of GlySar for vascular space, [$^{3}$H]inulin (1 μCi/mouse) was administered intravenously 2 min before harvesting the tissues. Tissue samples were weighed and solubilized in 0.5 ml of 1 M hyamine hydroxide for 24 hour at 37°C. After solubilization, tissue homogenates, CSF, and blood samples were mixed with Ecolite(+) liquid scintillation cocktail (MP Biomedicals) and the level of radioactivity was measured by a dual-channel liquid scintillation counter (Beckman

LS 3801; Beckman Coulter, Fullerton, CA). Corrected tissue concentrations of Glysar ($C_{tissue,\,corr}$, nmol/g wet tissue) were calculated as

$$C_{tiss,corr} = C_{tiss} - V \bullet C_b \quad (1)$$

where $C_{tiss}$ is the uncorrected GlySar tissue concentration (nmol/g), V is the blood volume (ml/g) determined as the inulin space of tissue samples estimated from inulin concentration in the final blood sample (Keep et al., 1999), and $C_b$ is the GlySar blood concentration (nmol/ml).

To investigate time course changes of tissue distributions in choroid plexuses and kidney, the tissue samples were also harvested at preselected time points (2, 5, 15 min) after intravenous administration of [$^{14}$C]GlySar. [$^{3}$H]Inulin (1 μCi/mouse) was administered 2 min before harvesting the tissues to correct for the vascular space and all the tissues were processed as previously described.

**Non-compartment analysis of GlySar pharmacokinetics in blood**

Blood concentration versus time curves of GlySar were initially fit to a non-compartmental model with a weighting factor of unity. Total systemic clearance ($CL_s$), volume of distibution steady state ($V_{ss}$), terminal half-life ($t_{1/2}$), and mean residence time (MRT) were calculated using the standard methods by WinNonlin version 5.0.1 (Pharsignt Inc., Mountain View, CA).

**Population pharmacokinetic modeling of GlySar in blood, CSF and kidney**

Population pharmacokinetic modeling was carried out using a nonlinear mixed effects modeling approach with NONMEM software, version 7 (ICON Development Solutions, MD, USA). A subroutine ADVAN6 TRANS1 and the first-

order conditional estimation were used to build the compartment models throughout the modeling procedure. The best model was determined based on the likelihood ratio test using objective function values (OFV; the lowest value corresponds to the best model) and graphical goodness-of-fit. For nested models, reductions of OFV of at least 3.83 units corresponds to improved fits at $p<0.05$. Graphical and statistical analysis was implemented using S-Plus 6.2 and R version 2.12.2.

***Model building***

A stepwise compartmental model building approach was performed to describe the distribution kinetics of GlySar in the blood, CSF, and kidney. As an initial step, one-, two- and three- compartment models were compared for the Glysar blood concentration-time course after intravenous administration. Nonlinear elimination kinetics have been reported at high doses of PEPT2 substrates possibly associated with a saturation of the reabsorption process in the kidney mediated by PEPT2. Since we only used data in mice following a low dose of GlySar (0.05 mmol/kg), first-order elimination kinetics were assumed in our analysis. Modeling using log-transformed or non-transformed blood concentration data was evaluated and the compartment model with better residual plots was selected.

Once the pharmacokinetic model for blood concentration data was established, the model was extended to include a CSF compartment. It has been shown that PEPT2 is expressed in choroid plexus of the brain and plays a role in transporting drug substrates from CSF to blood (Ocheltree et al., 2004). Since GlySar is a PEPT2 substrate, after it enters the brain, the dipeptide can be removed from

the CSF of brain to blood by passive diffusion, CSF bulk flow, or active clearance mediated by PEPT2. Therefore, distribution kinetics between the blood and CSF compartments can be parameterized by the following equations (Figure 4.1A):

$$\begin{aligned}\frac{dA_{CSF}}{dt} &= K_{in}A_C - K_{out}A_{CSF} \\ &= K_{13\,diff}A_C - (K_{31\,diff} + K_{bulk} + K_{active})A_{CSF} \\ &= \frac{CL_{diff}}{V_C}A_C - \frac{(CL_{diff} + CL_{bulk} + CL_{active})}{V_{CSF}}A_{CSF} \\ &= \frac{CL_{in}}{V_C}A_C - \frac{CL_{CSF\ efflux}}{V_{CSF}}A_{CSF}\end{aligned} \quad (2)$$

where $A_{CSF}$ is the amount of GlySar in CSF, $A_c$ is the amount of GlySar in central blood, $V_c$ is the volume of central compartment, $V_{CSF}$ is the volume of CSF compartment, $K_{in}$ and $K_{out}$ are the inter-compartment rate constants describing GlySar transport between the blood and CSF, $K_{diff,}$ $K_{bulk}$ and $K_{active}$ are distribution rate constants describing GlySar transport between blood and CSF mediated by passive diffusion, CSF bulk flow and PEPT2, respectively, $CL_{diff}$ is the clearance mediated by passive diffusion, $CL_{bulk}$ is the clearance mediated by CSF bulk flow, $CL_{active}$ is the active clearance mediated by PEPT2, $CL_{in}$ and $CL_{CSF\ efflux}$ are the inter-compartment clearances describing GlySar transport between the blood and CSF. $CL_{bulk}$ was set to a physiological value of 0.325 µl/min in mouse (Stroobants et al., 2011). Since PEPT2 is absent in knockout mice, $CL_{diff}$ can be estimated from the knockout animal data. After $CL_{diff}$ was estimated in the model for knockout mice, it was fixed in the model for wild-type mice and the $CL_{active}$ estimated in these animals. Using this stepwise model building process, all parameters for the distribution kinetics between blood and CSF were estimated.

The final step was to incorporate a kidney compartment to the model and establish a full pharmacokinetic model, which describes all the distribution and elimination kinetics of blood, CSF and kidney. The estimated kinetic parameters between blood and CSF in the previous step were fixed in this model building process. Since GlySar is only eliminated by kidney, all tissue distribution reservoirs eventually entered the kidney and were eliminated from the body. The full pharmacokinetic model is presented in Figure 4.1B and the distribution kinetics between the blood and kidney compartment was modeled as follows:

$$\begin{aligned}\frac{dA_{kidney}}{dt} &= K_{14}A_C - K_{41}A_{kidney} - K_{40}A_{kidney} \\ &\approx \frac{CL_S}{V_C}A_C - K_{40}A_{kidney}\end{aligned} \tag{3}$$

where $A_{kidney}$ is the amount of GlySar in kidney, $K_{14}$ is the distribution rate constant describing GlySar transport from blood to kidney, $K_{41}$ is the distribution rate constant describing GlySar transport from kidney to blood, $CL_s$ is the systemic clearance, and $K_{40}$ is the rate constant describing GlySar elimination from the kidney. $K_{41}$ is assumed to be zero in the model, since GlySar is completely renally excreted (Ocheltree et al., 2005).

The inter-animal variability for the PK parameters was described by an exponential variance model using the following equation:

$$P_i = P_{pop}\exp(\eta_i) \tag{4}$$

where $P_i$ is the parameter estimate for the ith animal, $P_{pop}$ is the population estimate of the parameter for a typical animal, and $\eta_i$ is the inter-animal variability representing the inter-animal difference between $P_i$ and $P_{pop}$. The values of $\eta_i$ are

assumed to follow a normal distribution with mean of zero and variance $\omega^2$. All parameters were tested for the necessity of including inter-animal variability. An additive error model was considered for the residual unexplained variability in the log transformed data of GlySar concentration.

***Nonparametric bootstrap analysis***

The stability of the final model was evaluated by nonparametric bootstrap analysis in which 1,000 bootstrap runs were performed using Wings for NONMEM (http://wfn.sourceforge.net/). Each bootstrap sample was generated by sampling with replacement from the original sample and the new data set had the same size as the original data set. These 1,000 individual new data sets were fitted to the final model developed from the original data set and bootstrap parameter estimates were obtained from each bootstrap data set. The median, 5th, and 95th percentile of the parameter estimates were calculated from the successful bootstrap runs to obtain a 90% bootstrap confidence interval.

***Visual predictive check***

The final PK model was also evaluated by visual predictive checks with 1,000 data sets simulated by NONMEM using the parameter estimates of the final model. The median, 5th, and 95th percentiles of the simulated concentrations were calculated at each time point for the blood, CSF and kidney compartments, and visually checked to see if the intervals can cover the observed data points. The visual predictive check plots were generated using R version 2.12.2.

## RESULTS

### Different pharmacokinetic behavior of GlySar between wild-type and PEPT2 knockout mouse

GlySar concentrations were significantly lower in the blood and kidney in knockout mice compared to wild-type animals, whereas the CSF concentrations were significantly higher in knockout mice (Figure 4.2). GlySar pharmacokinetic parameters in blood were estimated by a non-compartmental analysis as summarized in Table 4.1. The volume of distribution ($V_{ss}$) was slightly increased ($p<0.001$) and total systemic clearance ($CL_s$) was increased by almost 2-fold ($p<0.001$) in knockout mice. Meanwhile, the mean residence time (MRT) was significantly decreased in knockout animals ($p<0.05$). Since PEPT2 is absent in knockout animals, these changes in GlySar disposition can be attributable to the deletion of PEPT2 functionality (Ocheltree et al., 2005). Based on these findings, we decided to develop a model, which describes the distribution kinetics of GlySar in blood, CSF and kidney, and to quantify the importance of PEPT2 in the distribution kinetics of GlySar.

### Population pharmacokinetic model building

NONMEM analysis was first performed to fit the blood concentration versus time profile of GlySar using a two-compartment PK model. The expanded model, including CSF, was a three-compartment model as shown in Figure 4.1A and the estimated PK parameters of GlySar are listed in Table 4.2. Since our laboratory maintains both wild-type and PEPT2 knockout mice, we were able to study the

distribution kinetics and estimate the clearance mediated by passive diffusion ($CL_{diff}$), bulk clearance mediated by CSF bulk flow ($CL_{bulk}$), and active clearance mediated by PEPT2 ($CL_{active}$). The total CSF efflux CL ($CL_{CSF\ efflux}$), which equals the sum of $CL_{diff}$, $CL_{bulk}$, and $CL_{active}$, was 4.3-fold higher for wild-type mice compared to PEPT2 knockout mice, demonstrating that PEPT2 plays an important role as an efflux pump in brain. Based on the estimates, it seems that 77% of $CL_{CSF\ efflux}$ is mediated by $CL_{active}$ (i.e., by PEPT2) and the remaining 23% is mediated by $CL_{diff}$ and $CL_{bulk}$. In addition, the estimated $CL_s$ values of GlySar for wild-type and PEPT2 knockout mouse were 0.239 and 0.447 ml/min, respectively, which are similar to the results from non-compartmental analysis (Table 4.1). The $V_{ss}$ values for wild-type (9.52 ml) and PEPT2 knockout mouse (14.2 ml) were also similar to the ones observed from non-compartmental analysis. Therefore, it seems that both the WinNonlin and NONMEM analyses agree on the estimation of pharmacokinetic parameters. The three-compartment model also includes inter-subject variability (% CV) on volume of central compartment ($V_c$, 5.9%), $CL_{diff}$ (36.9%) and $CL_s$ (1.4%) for PEPT2 knockout mice, and $V_c$ (3.8%) and $CL_s$ (2.1%) for wild-type mice.

A four-compartment model was subsequently developed by adding kidney as a separate compartment (Figure 4.1B and Table 4.3). The values of $CL_{diff}$ and $CL_{bulk}$ were fixed in the four-compartment model based on the parameter estimates from the previous three-compartment model. Since GlySar is completely eliminated by the kidney, this organ was regarded as the sole eliminating compartment in the four-compartment model. $CL_S$ was almost 2-fold higher for PEPT2 knockout mice compared to wild-type animals, and this is consistent with the results from the

three-compartment model. The other estimated parameters of $V_c$, $V_p$, $V_{CSF}$, $CL_{active}$, and Q are very similar between the three-compartment (Table 4.2) and four-compartment (Table 4.3) models, which demonstrates the robustness of our model. The rate constant K14 was calculated as $K_{14} = \frac{CLs}{V_c}$ and the values were 0.0623 $min^{-1}$ for wild-type mouse and 0.0945 $min^{-1}$ for knockout mouse.

**Final model validation**

Basic goodness-of-fit plots for the final four-compartment model are displayed in Figure 4.3. Predicted concentrations of GlySar were highly correlated with observed concentrations in all the blood, CSF and kidney compartments. There were no obvious patterns in the residual plots and the residuals were randomly distributed along the zero line.

The final model was further evaluated using a nonparametric bootstrap analysis. Among 1,000 independent runs, 929 and 968 runs were successfully minimized for wild-type and knockout mice respectively. Median estimates and 90% bootstrap confidence intervals of the final model parameters are shown in Table 4.4. NONMEM estimates were very similar to median values of the bootstrap estimates and were inside of bootstrap confidence intervals (Table 4.3 vs Table 4.4), indicating there was no significant bias in the NONMEM parameter estimates. Based on the confidence intervals, $V_p$ and $CL_S$ were significantly different between wild-type and knockout mice, as was $CL_{CSF\ efflux}$, since the confidence interval for $CL_{active}$ does not include zero for wild-type mice.

Visual predictive check plots are shown in Figure 4.4 as an additional validation method. It seems that the final model well describes the GlySar concentration-time profiles in the blood, CSF and kidney compartments. Moreover, the 5th and 95th percentiles of simulated results were able to cover almost all the observed data.

## DISCUSSION

In the present study, a four-compartment PK model was successfully developed to define the distribution and elimination kinetics of a PEPT2 substrate, GlySar, at the BCSFB. Due to the availability of PEPT2 knockout mice, we were able to quantitatively predict, for the first time, the significance of PEPT2 in the efflux kinetics of a PEPT2 substrate at the blood-CSF interface. In this study, we demonstrated that: 1) the distribution of GlySar in blood, CSF and kidney using nonlinear mixed effects modeling approach is best described by a four compartment model; 2) PEPT2 is responsible for 77% of the total CSF efflux of GlySar at the BCSFB with the remaining 23% being mediated by passive diffusion and CSF bulk flow; and 3) the elimination of GlySar was increased by almost 2-fold in the absence of PEPT2 in knockout mice.

CSF is used to predict the extent of CNS penetration of drug molecules since it is easier to collect and analyze compared to other tissues of the brain, and because of ethical constraints in human studies. Drug concentrations in CSF are especially important when the drug target is close to the ventricles, ependyma and leptomeninges, such as in meningitis (de Lange and Danhof, 2002). The CSF is primarily formed in the choroid plexuses and secreted out of the ventricles into the

subarachnoid space. Due to the nature of CSF production and bulk flow, the concentration of compounds that are either produced endogenously in brain or passively diffused from blood to brain are low in CSF (Ocheltree et al., 2004). There are also other regulatory mechanisms that can influence drug exchange across the BCSFB such as the tight junctions of choroid plexus, metabolism of drugs at the BCSFB, and the inwardly- or outwardly-directed movement of drug molecules by transport proteins (Ocheltree et al., 2004). It has been shown that the morphology of choroid plexus was not changed in PEPT2 knockout mice (Shen et al., 2003). Therefore, we were able to assume that $CL_{diff}$ is the same for both wild-type mice and PEPT2 knockout animals. In addition, GlySar is resistant to hydrolysis and excreted from the body in intact form (Krzysik and Adibi, 1979). Thus, metabolic clearance at the BCSFB was assumed to be zero for GlySar. Based on these assumptions, we were able to construct a model that quantitatively separates the three components contributing to the efflux of GlySar at the BCSFB (i.e., $CL_{diff}$, $CL_{bulk}$, and $CL_{active}$).

To our knowledge, there are no other transporters involved in GlySar uptake into choroid plexus except PEPT2. GlySar may also be transported by PEPT1, PHT1 and PHT2, but there is no molecular or functional evidence to support these transporters having a role in peptide transport systems at the BCSFB (9). In an isolated choroid plexus study, GlySar uptake was very low in PEPT2 knockout mice (almost 10-fold lower compared to wild-type animals), which demonstrates that no other transporters were significantly involved in GlySar uptake into choroid plexus (13). When uptake study was performed using choroid plexus epithelial cells in

primary culture, GlySar uptake was significantly inhibited by dipeptides and not L-histidine, ruling out the possibility of other transporters participating in GlySar uptake at the apical membrane (14). At the basolateral membrane, on the other hand, a low affinity uptake process was observed, but the molecular properties of this transporter have not yet been elucidated. Compared to the apical-to-basal transport of GlySar, the reverse transport was very small. Based on this information about di/tripeptide transport mechanisms at the BCSFB, $CL_{in}$ was approximated as $CL_{diff}$, $CL_{CSF\ efflux}$ was simplified as the combination of $CL_{diff}$, $CL_{bulk}$ and $CL_{active}$, and $CL_{active}$ was regarded as only being mediated by PEPT2 in our model.

The quantitative analysis of efflux mechanisms in the brain is meaningful in that the dose of CNS drugs can be adjusted based on expression levels of relevant transporters. The PEPT2 gene is known to be polymorphically expressed in humans with single nucleotide polymorphisms. For example, the genetic variant R57H of PEPT2 shows a complete loss of transport activity (Pinsonneault et al., 2004, Terada et al., 2004). Based on our estimation that PEPT2 mediates 77% of CSF efflux kinetics for GlySar, we expect the concentrations of this dipeptide to be 4.3-fold greater in CSF during gene deletion. In a previous study, it was shown that CSF-to-blood concentration ratios of GlySar were 4.5-fold higher for PEPT2 null mice compared to wild-type animals (Ocheltree et al., 2005). Other studies in our laboratory demonstrated that PEPT2 null mice exhibited 6- and 8-fold greater CSF-to-blood concentration ratios for the PEPT2 substrate, cefadroxil and carnosine, respectively (Shen et al., 2007, Kamal Ma Fau - Jiang et al., 2009). Additionally, when dose-response studies were performed for L-kyotorphin (L-KTP), an endogenous

analgesic neuropeptide and PEPT2 substrate, the ED50 of L-KTP in PEPT2 null mice was five times smaller than in wild-type mice (Jiang et al., 2009). These findings are in agreement with our present results and suggest that dose adjustments for PEPT2 substrate drugs would be needed for brain drug delivery in patients whose PEPT2 function is disrupted.

It would be valuable if we could extrapolate these findings in mouse to human. PEPT2 is expressed in mouse astrocytes, ependymal cells and choroid plexus epithelial cells of brain (9), which forms BCSFB, whereas no evidence of PEPT2 expression at the BBB has been reported. Compared to BBB, little is known about the expression levels of transporters at the BCSFB in human, especially for PEPT2. However, peptide transporters including PEPT2 are known to have high homology (about 80%) and similarities in driving forces, substrate specificity and affinity between mouse and human (3, 10-12). If it is further elucidated that both species exhibit similar proton gradients across the membrane and similar expression levels of PEPT2 at the BCSFB, then inter-individual differences in CSF pharmacokinetics of peptide-like drugs, due to PEPT2, could also be simulated in humans.

It has been reported that drug transport systems at the BCSFB are altered in CNS diseases, and these alterations may be associated with morphological and/or functional changes of transport proteins. With respect to morphological changes, alterations of choroid plexus microvilli, severe vacuolization, mitochondria alterations and disruption of tight junction complexes have been reported during CNS inflammatory diseases (Endo et al., 1998, Johanson et al., 2000, Engelhardt et

al., 2001, Coisne and Engelhardt, 2011). With respect to functional changes, several reports have shown that the altered function of transport proteins during CNS diseases contributes to changes in the pharmacokinetics of drugs in brain. For example, the active clearance of organic anions in the choroid plexus was strongly impaired by exposure to inflammatory stimuli (Strazielle et al., 2003). It has also been reported that the uptake of benzylpenicillin in choroid plexus was reduced and CSF levels was increased in an experimental meningitis model (Spector and Lorenzo, 1974, Han et al., 2002, Strazielle et al., 2003). These changes can disrupt both the diffusion clearance and active clearance of drugs at BCSFB in our model. Therefore, future studies should be directed at investigating quantitatively any changes in efflux mechanisms during CNS inflammatory diseases.

In addition to CSF, there were differences of GlySar concentrations in the kidney of wild-type and PEPT2 knockout mice, which we successfully incorporated into a four-compartment model. PEPT2 is highly expressed in the apical membrane of renal proximal tubular epithelium and plays an important role in the reabsorption of small peptides and peptide-like drugs (Shen et al., 1999, Smith et al., 1998, Takahashi et al., 1998). GlySar is only renally excreted and PEPT2 is involved in the renal elimination of Glysar. PEPT1 is also known to be involved in the elimination, especially in the reabsorption of peptide-like drugs, but its contribution is relatively minor compared to PEPT2. It has been previously reported that PEPT2 is responsible for 86% of the reabsorption of GlySar and PEPT1 is responsible for only 14% of the reabsorption (Ocheltree et al., 2005). The model with bootstrap dataset estimated $CL_S$ values of 0.237 and 0.453 in wild-type and PEPT2 knockout

mice, respectively (Table 4.4), showing a statistically significant (1.9 fold) difference between the genotypes ($p < 0.05$). $CL_S$ describes clearance of drug from the blood compartment and, therefore, it reflects the systemic clearance. The predicted value of $CL_S$ in four-compartment model (Table 4.3) was very similar to those value estimated from the non-compartment (Table 4.1) and the three-compartment model (Table 4.2). Gene deletion of PEPT2 in knockout mouse disrupts reabsorption of GlySar at the apical membrane of renal epithelium, which eventually results in low concentration of GlySar in blood. It seems that the low blood concentration was then reflected as high value of $CL_S$ in knockout mouse. Since GlySar is not actively secreted, has negligible protein binding and golumerular filtration rate is the same for both wild-type and PEPT2 knockout mice (Ocheltree et al., 2005, Shen et al., 2007), the difference in $CL_S$ between wild-type and knockout animal may not be attributable to filtration and secretion at the basolateral membrane of renal epithelium.

Peripheral volume ($V_p$) also shows a 1.6-fold difference in wild-type versus PEPT2 knockout animals in the final model (Table 4.3 and 4.4). From the model, peripheral volume is the sum of apparent tissue volumes, which can be expressed as $V_p = \Sigma V_t \frac{f_u}{f_{u,t}}$, where $V_t$ is the apparent tissue volume, $f_u$ is the fraction unbound in blood and $f_{u,t}$ is the fraction unbound in tissue. GlySar has negligible protein binding in plasma (Ocheltree et al., 2005) and, therefore, differences in peripheral volume between wild-type and PEPT2 knockout mice may be mediated by changes in $f_{u,t}$. PEPT2 is not only expressed in CP and kidney, but it is also expressed in other

tissues such as lung and mammary gland (Berger and Hediger, 1999, Meredith and Boyd, 2000, Groneberg et al., 2004). Therefore, PEPT2 gene deletion in other tissues may affect the increased peripheral volume of GlySar in PEPT2 knockout mice.

In conclusion, a population pharmacokinetic model was successfully developed to describe the distribution and elimination kinetics of GlySar, a model PEPT2 substrate, in the blood, CSF and kidney using a nonlinear mixed effects modeling approach. Due to the availability of mice in which the PEPT2 gene is deleted, we were able to quantify the contribution of PEPT2 in the efflux kinetics of GlySar at the BCSFB. In particular, we demonstrated that 77% of the CSF efflux of Glysar was mediated by PEPT2 resulting in 4.3-fold higher CSF concentrations in the PEPT2 knockout mice. Our findings suggest that, given relevant transporter expression levels in tissue, it may be feasible to quantitatively predict the distribution of CNS drugs at the BCSFB and to use this information accordingly for dose adjustments in clinical therapy. Future studies should investigate changes in the distribution kinetics of peptides/mimetics at the BCSFB in disease states such as meningitis, and the possibility of quantifying the impact of such changes on the CSF efflux of peptide-like drugs using a modeling approach.

**Table 4.1.** Non-compartmental analysis of GlySar blood concentrations in wild-type and PEPT2 knockout mice

| Parameter | Wild-type mice | Knockout mice |
|---|---|---|
| Vss (ml) | 10.7 ± 2.3 | 15.6 ± 2.6*** |
| $CL_s$ (ml/min) | 0.235 ± 0.034 | 0.438 ± 0.074*** |
| $t_{1/2}$ (min) | 36.1 ± 9.5 | 30.8 ± 5.7 |
| MRT (min) | 45.8 ± 11.3 | 36.1 ± 5.7* |
| $AUC_{blood,\ 0\text{-}tlast}$ (min•nmol/ml) | 3149 ± 500 | 1848 ± 285*** |
| $AUC_{CSF,\ 0\text{-}tlast}$ (min•nmol/ml)[a] | 482 | 880 |
| $AUC_{CSF,\ 0\text{-}tlast}/AUC_{blood,\ 0\text{-}tlast}$ | 0.153 | 0.476 |

* $p<0.05$

*** $p<0.001$

[a] AUC in the CSF compartment was estimated using mean data since every sample was collected from a different animal.

**Table 4.2.** Parameter estimates for the three-compartment model of Glysar in wild-type and PEPT2 knockout mice.

| | Wild-type mice | | Knockout mice | |
|---|---|---|---|---|
| Parameters | Estimate | RSE (%) | Estimate | RSE (%) |
| Distribution parameters | | | | |
| $V_c$ (ml) | 3.83 | 10.1 | 4.93 | 7.40 |
| $V_p$ (ml) | 5.67 | 9.07 | 9.27 | 4.79 |
| $V_{CSF}$ (ml) | 0.0230 | 14.9 | 0.0112 | 11.4 |
| $V_{ss}$ (ml)[a] | 9.52 | - | 14.2 | - |
| Q (ml/min)[b] | 1.36 | 23.2 | 1.66 | 14.8 |
| $CL_{diff}$ (µl/min) | 0.509 | - | 0.509 | 19.3 |
| $CL_{bulk}$ (µl/min)[c] | 0.325 | - | 0.325 | - |
| $CL_{active}$ (µl/min) | 2.73 | 22.7 | - | - |
| $CL_{CSF\ efflux}$ (µl/min) | 3.564 | - | 0.834 | - |
| $CL_s$ (ml/min)[d] | 0.239 | 4.35 | 0.447 | 3.67 |
| $t_{1/2}$ (min)[e] | 27.6 | - | 22.0 | - |
| Inter-subject variability[f] (CV%) | | | | |
| $V_c$ | 3.82 | 16.9 | 5.94 | 42.8 |
| $CL_{diffusion}$ | - | - | 36.9 | 44.2 |
| $CL_s$ | 2.12 | 40.0 | 1.39 | 42.4 |
| Residual variability[f] (CV%) | | | | |
| Plasma | 20.3 | 8.38 | 42.3 | 8.79 |
| CSF | 39.4 | 14.7 | 23.1 | 54.1 |

[a] $V_{ss}$ was calculated as sum of $V_c$, $V_p$, and $V_{CSF}$

[b] $Q=K_{12}V_c=K_{21}V_p$

[c] $CL_{bulk}$ was fixed based on the literature value (22)

[d] $CL_s=K_{10}V_c$

[e] $t_{1/2}$ was calculated as $t_{1/2} = \ln 2 \times \frac{V_{ss}}{CL_s}$

[f] Inter-subject and residual variabilities were expressed as coefficient of variation (CV%)

**Table 4.3.** Parameter estimates for the four-compartment model of Glysar in wild-type and PEPT2 knockout mice.

| | Wild-type mice | | Knockout mice | |
|---|---|---|---|---|
| Parameters | Estimate | RSE (%) | Estimate | RSE (%) |
| Distribution parameters | | | | |
| $V_c$ (ml) | 3.79 | 9.71 | 4.75 | 7.40 |
| $V_p$ (ml) | 5.75 | 8.87 | 9.18 | 4.78 |
| $V_{CSF}$ (ml) | 0.0229 | 18.3 | 0.0112 | 19.9 |
| $V_{kidney}$ (ml) | 0.199 | 35.1 | 0.408 | 26.0 |
| $V_{ss}$ (ml)[a] | 9.76 | - | 14.3 | - |
| Q (ml/min)[b] | 1.39 | 22.1 | 1.78 | 42.2 |
| $CL_{diff}$ (µl/min) | 0.509 | - | 0.509 | - |
| $CL_{bulk}$ (µl/min)[c] | 0.325 | - | 0.325 | - |
| $CL_{active}$ (µl/min) | 2.76 | 29.2 | - | - |
| $CL_{CSF\ efflux}$ (µl/min) | 3.594 | - | 0.834 | - |
| $CL_S$(ml/min)[d] | 0.236 | 6.06 | 0.449 | 3.79 |
| $K_{40}$($min^{-1}$) | 0.220 | 43.6 | 0.405 | 32.3 |
| $t_{1/2}$ (min)[e] | 28.7 | - | 22.1 | - |
| Inter-subject variability[f] (CV%) | | | | |
| $V_c$ | 2.36 | 32.4 | 1.35 | 43.2 |
| $CL_S$ | 2.66 | 40.3 | 5.54 | 44.9 |
| Residual variability[f] (CV%) | | | | |
| Plasma | 20.2 | 8.04 | 17.9 | 8.85 |
| CSF | 36.2 | 17.4 | 31.5 | 16.5 |
| Kidney | 39.1 | 15.0 | 55.0 | 19.5 |

[a] $V_{ss}$ was calculated as sum of $V_c$, $V_p$, $V_{CSF}$ and $V_{kidney}$

[b] $Q=K_{12}V_c=K_{21}V_p$

[c] $CL_{bulk}$ was fixed based on the literature value (22)

[d] $CL_s=K_{14}V_c$

[e] $t_{1/2}$ was calculated as $t_{1/2} = \ln 2 \times \frac{V_{ss}}{CL_{14}}$

[f] Inter-subject and residual variabilities were expressed as coefficient of variation (CV%)

**Table 4.4.** Parameter confidence intervals (CI) for the finalized four-compartment model, estimated by bootstrap method.

| | Wild-type mice | | Knockout mice | |
|---|---|---|---|---|
| Parameters | Median | 90% CI | Median | 90% CI |
| $V_c$ (ml) | 3.86 | 3.16 – 4.69 | 4.94 | 4.23 – 6.21 |
| $V_p$ (ml) | 5.87 | 4.98 – 7.24 | 9.35 | 8.49 – 11.6 |
| $V_{CSF}$ (ml) | 0.0226 | 0.016 – 0.0312 | 0.0111 | 0.00676 – 0.0163 |
| $V_{kidney}$ (ml) | 0.201 | 0.0725 – 0.301 | 0.378 | 0.166 – 0.653 |
| Q (ml/min) | 1.33 | 0.485 – 1.84 | 1.76 | 0.771 – 2.27 |
| $CL_{diff}$ (µl/min) | 0.509 | - | 0.509 | - |
| $CL_{bulk}$ (µl/min)[a] | 0.325 | - | 0.325 | - |
| $CL_{active}$ (µl/min) | 2.82 | 1.84 – 4.11 | - | - |
| $CL_{CSF\ efflux}$ (µl/min) | 3.654 | - | 0.834 | - |
| $CL_S$(ml/min) | 0.237 | 0.205 – 0.255 | 0.453 | 0.419 – 0.492 |
| $K_{40}$($min^{-1}$) | 0.216 | 0.123 – 0.446 | 0.458 | 0.244 – 0.993 |

[a] $CL_{bulk}$ was fixed based on the literature value (22)

**A**

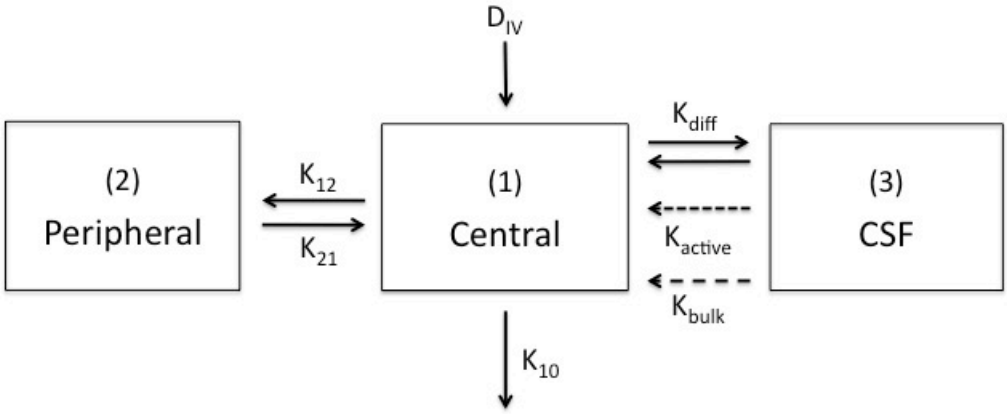


**B**

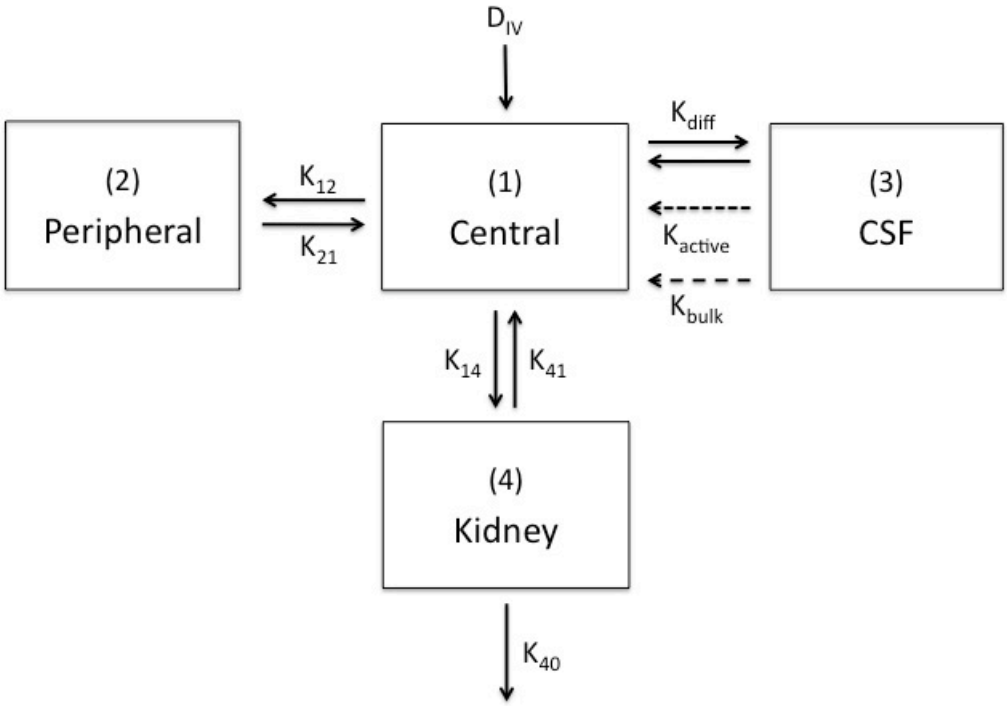


**Figure 4.1.** Schematic representation of (A) three- and (B) four-compartment models to simultaneously describe the blood, CSF, and kidney data. Drug molecules are eliminated by the kidney. $K_{diff,}$ $K_{bulk}$ and $K_{active}$ are distribution rate constants describing GlySar transport between blood and CSF mediated by passive diffusion, CSF bulk flow and PEPT2, respectively.

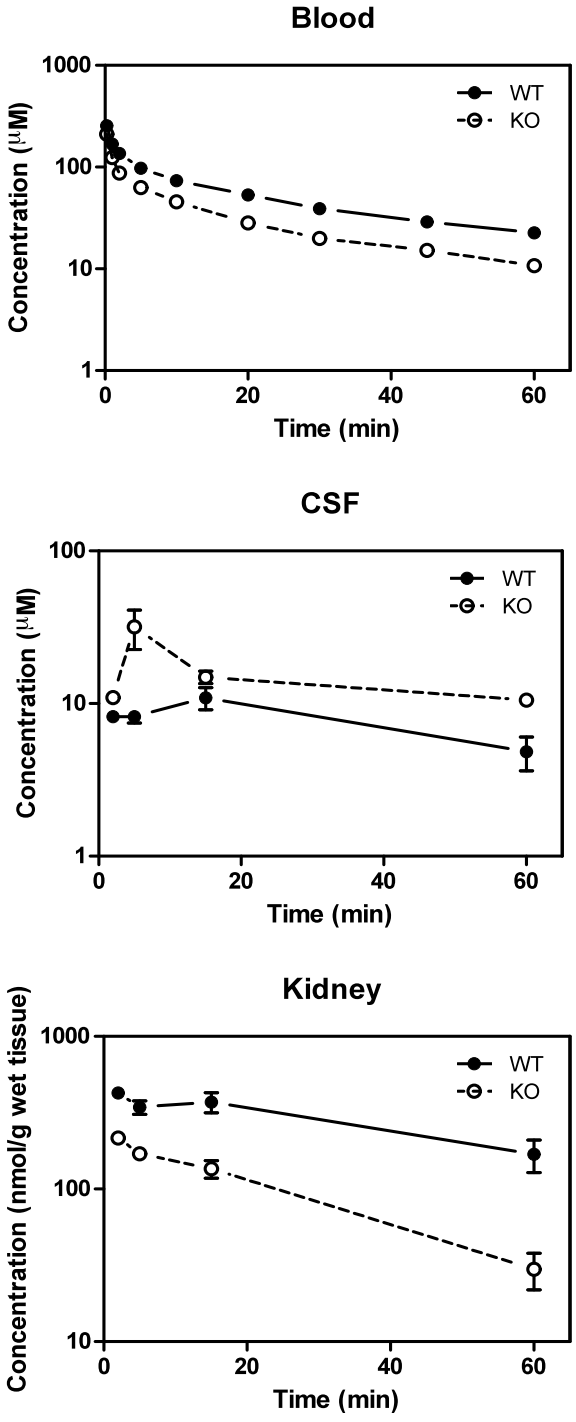


**Figure 4.2.** GlySar concentration versus time plots for the blood, CSF and kidney compartments. Closed circles represent the data from wild-type mice (WT) and open circles represent the data from PEPT2 knockout mice (KO). The figures were adapted from a previous publication (Ocheltree et al.).

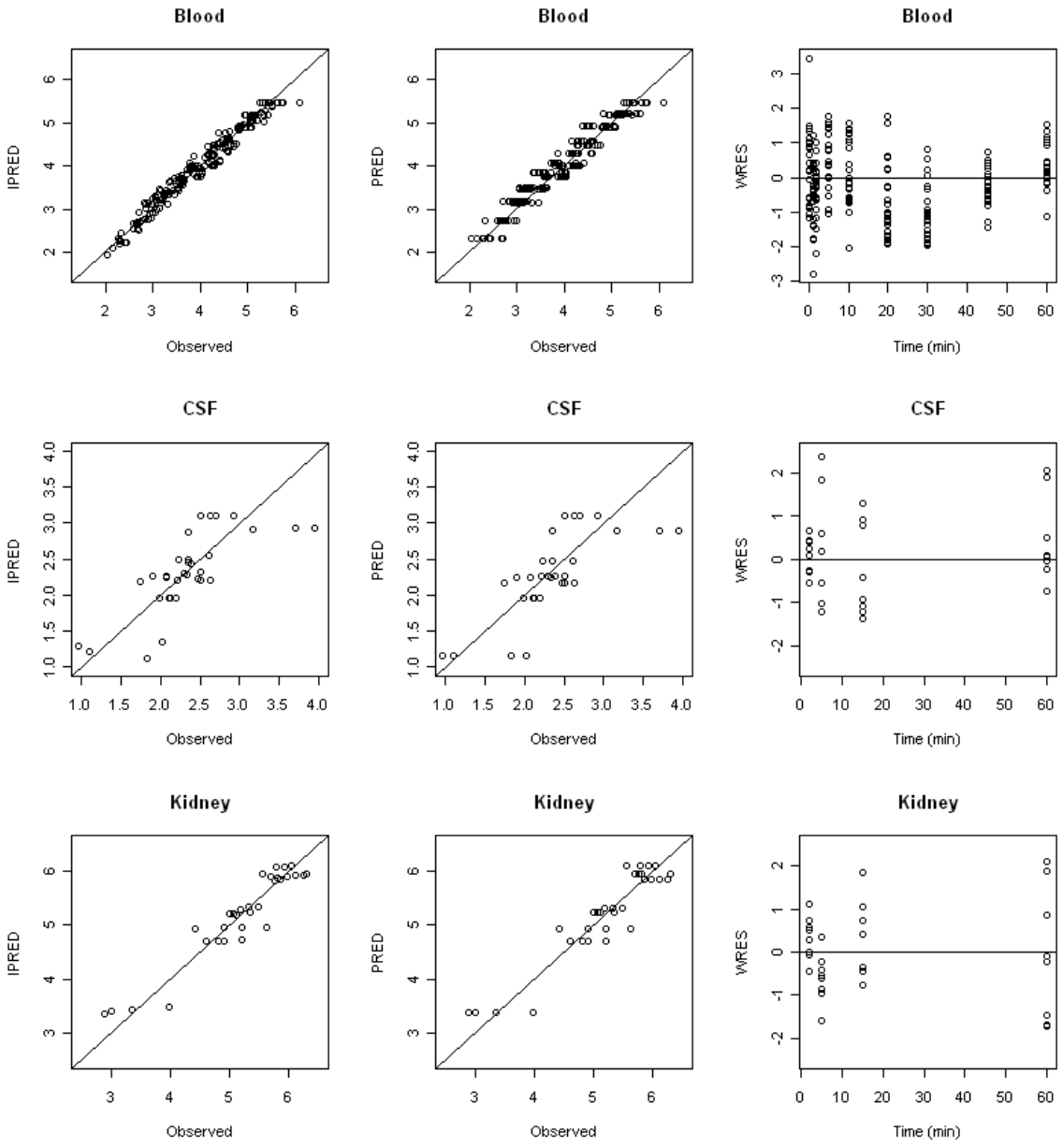


**Figure 4.3.** Goodness-of-fit plots for the final pharmacokinetic model. Wild-type and knockout animal data were combined. Solid lines represent the identity line. PRED, population model predictions; IPRED, individual model predictions; WRES, weighted residuals.

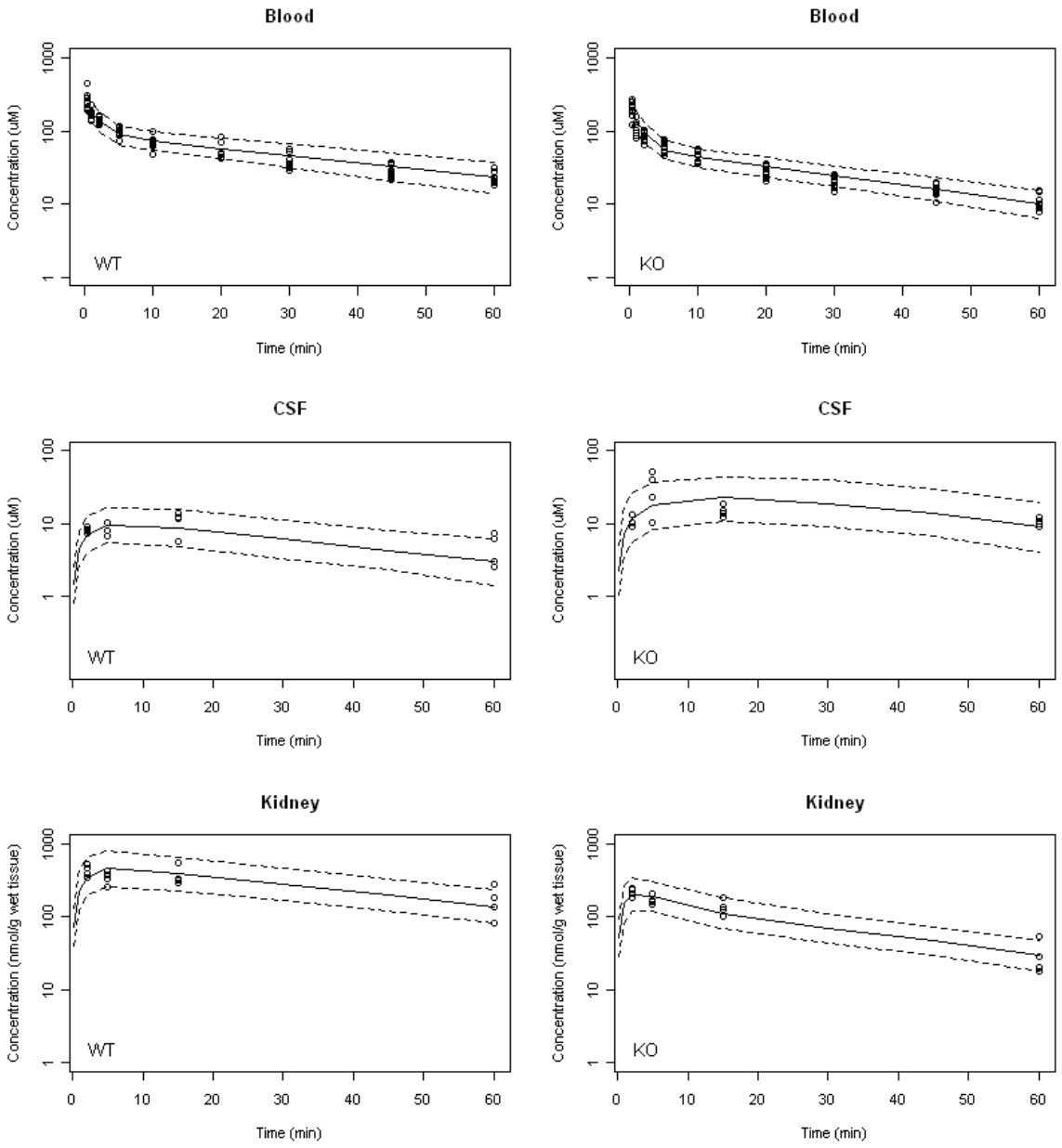


**Figure 4.4.** Simulated concentration-time profiles of 1000 subjects in the blood, CSF and kidney compartments of wild-type (WT) and knockout (KO) mice. Simulations are based on the final model. The circles represent the observed data in mice. Dashed lines depict the 5$^{th}$ and 95$^{th}$ percentiles and solid lines depict the median values of simulated data sets.

## REFERENCE


BERGER, U. V. & HEDIGER, M. A. (1999) Distribution of peptide transporter PEPT2 mRNA in the rat nervous system. *Anat Embryol (Berl),* 199**,** 439-49.

COISNE, C. & ENGELHARDT, B. (2011) Tight junctions in brain barriers during central nervous system inflammation. *Antioxid Redox Signal,* 15**,** 1285-303.

DANIEL, H. & RUBIO-ALIAGA, I. (2003) An update on renal peptide transporters. *Am J Physiol Renal Physiol,* 284**,** F885-92.

DE LANGE, E. C. & DANHOF, M. (2002) Considerations in the use of cerebrospinal fluid pharmacokinetics to predict brain target concentrations in the clinical setting: implications of the barriers between blood and brain. *Clin Pharmacokinet,* 41**,** 691-703.

ENDO, H., SASAKI, K., TONOSAKI, A. & KAYAMA, T. (1998) Three-dimensional and ultrastructural ICAM-1 distribution in the choroid plexus, arachnoid membrane and dural sinus of inflammatory rats induced by LPS injection in the lateral ventricles. *Brain Res,* 793**,** 297-301.

ENGELHARDT, B., WOLBURG-BUCHHOLZ, K. & WOLBURG, H. (2001) Involvement of the choroid plexus in central nervous system inflammation. *Microsc Res Tech,* 52**,** 112-29.

GHERSI-EGEA, J. F., FINNEGAN, W., CHEN, J. L. & FENSTERMACHER, J. D. (1996a) Rapid distribution of intraventricularly administered sucrose into cerebrospinal fluid cisterns via subarachnoid velae in rat. *Neuroscience,* 75**,** 1271-88.

GHERSI-EGEA, J. F., GOREVIC, P. D., GHISO, J., FRANGIONE, B., PATLAK, C. S. & FENSTERMACHER, J. D. (1996b) Fate of cerebrospinal fluid-borne amyloid beta-peptide: rapid clearance into blood and appreciable accumulation by cerebral arteries. *J Neurochem,* 67**,** 880-3.

GRONEBERG, D. A., FISCHER, A., CHUNG, K. F. & DANIEL, H. (2004) Molecular mechanisms of pulmonary peptidomimetic drug and peptide transport. *Am J Respir Cell Mol Biol,* 30**,** 251-60.

HAN, H., KIM, S. G., LEE, M. G., SHIM, C. K. & CHUNG, S. J. (2002) Mechanism of the reduced elimination clearance of benzylpenicillin from cerebrospinal fluid in rats with intracisternal administration of lipopolysaccharide. *Drug Metab Dispos,* 30**,** 1214-20.

HU, Y., SHEN, H., KEEP, R. F. & SMITH, D. E. (2007) Peptide transporter 2 (PEPT2) expression in brain protects against 5-aminolevulinic acid neurotoxicity. *J Neurochem,* 103**,** 2058-65.

JIANG, H., HU, Y., KEEP, R. F. & SMITH, D. E. (2009) Enhanced antinociceptive response to intracerebroventricular kyotorphin in Pept2 null mice. *J Neurochem,* 109**,** 1536-43.

JOHANSON, C. E., PALM, D. E., PRIMIANO, M. J., MCMILLAN, P. N., CHAN, P., KNUCKEY, N. W. & STOPA, E. G. (2000) Choroid plexus recovery after transient forebrain ischemia: role of growth factors and other repair mechanisms. *Cell Mol Neurobiol,* 20**,** 197-216.

KAMAL MA FAU - JIANG, H., JIANG H FAU - HU, Y., HU Y FAU - KEEP, R. F., KEEP RF FAU - SMITH, D. E. & SMITH, D. E. (2009) Influence of genetic knockout of Pept2 on the in vivo disposition of endogenous and exogenous carnosine in wild-type and Pept2 null mice. *Am J Physiol Regul Integr Comp Physiol,* 296**,** R986-91.

KEEP, R. F., SI, X., SHAKUI, P., ENNIS, S. R. & BETZ, A. L. (1999) Effect of amiloride analogs on DOCA-salt-induced hypertension in rats. *Am J Physiol,* 276**,** H2215-20.

KHATRI, A., GABER, M. W., BRUNDAGE, R. C., NAIMARK, M. D., HANNA, S. K., STEWART, C. F. & KIRSTEIN, M. N. (2010) Effect of radiation on the penetration of irinotecan in rat cerebrospinal fluid. *Cancer Chemother Pharmacol,* 68**,** 721-31.

KRZYSIK, B. A. & ADIBI, S. A. (1979) Comparison of metabolism of glycine injected intravenously in free and dipeptide forms. *Metabolism,* 28**,** 1211-7.

KUSUHARA, H. & SUGIYAMA, Y. (2004) Efflux transport systems for organic anions and cations at the blood-CSF barrier. *Adv Drug Deliv Rev,* 56**,** 1741-63.

MEREDITH, D. & BOYD, C. A. (2000) Structure and function of eukaryotic peptide transporters. *Cell Mol Life Sci,* 57**,** 754-78.

NALDA-MOLINA, R., DOKOUMETZIDIS, A., CHARKOFTAKI, G., DIMARAKI, E., MARGETIS, K., ARCHONTAKI, H., MARKANTONIS, S., BOUTOS, N., SAKAS, D., VRYONIS, E., SKOUTELIS, A. & VALSAMI, G. (2012) Pharmacokinetics of doripenem in CSF of patients with non-inflamed meninges. *J Antimicrob Chemother*.

OCHELTREE, S. M., SHEN, H., HU, Y., KEEP, R. F. & SMITH, D. E. (2005) Role and relevance of peptide transporter 2 (PEPT2) in the kidney and choroid plexus: in vivo studies with glycylsarcosine in wild-type and PEPT2 knockout mice. *J Pharmacol Exp Ther,* 315**,** 240-7.

OCHELTREE, S. M., SHEN, H., HU, Y., XIANG, J., KEEP, R. F. & SMITH, D. E. (2004) Mechanisms of cefadroxil uptake in the choroid plexus: studies in wild-type and PEPT2 knockout mice. *J Pharmacol Exp Ther,* 308**,** 462-7.

PFISTER, M., ZHANG, L., HAMMARLUND-UDENAES, M., SHEINER, L. B., GERBER, C. M., TAUBER, M. G. & COTTAGNOUD, P. (2003) Modeling of transfer kinetics at the serum-cerebrospinal fluid barrier in rabbits with experimental meningitis: application to grepafloxacin. *Antimicrob Agents Chemother,* 47**,** 138-43.

PINSONNEAULT, J., NIELSEN, C. U. & SADEE, W. (2004) Genetic variants of the human H+/dipeptide transporter PEPT2: analysis of haplotype functions. *J Pharmacol Exp Ther,* 311**,** 1088-96.

SHAFER, S. L., EISENACH, J. C., HOOD, D. D. & TONG, C. (1998) Cerebrospinal fluid pharmacokinetics and pharmacodynamics of intrathecal neostigmine methylsulfate in humans. *Anesthesiology,* 89**,** 1074-88.

SHEN, H., OCHELTREE, S. M., HU, Y., KEEP, R. F. & SMITH, D. E. (2007) Impact of genetic knockout of PEPT2 on cefadroxil pharmacokinetics, renal tubular reabsorption, and brain penetration in mice. *Drug Metab Dispos,* 35**,** 1209-16.

SHEN, H., SMITH, D. E., KEEP, R. F. & BROSIUS, F. C., 3RD (2004) Immunolocalization of the proton-coupled oligopeptide transporter PEPT2 in developing rat brain. *Mol Pharm,* 1**,** 248-56.

SHEN, H., SMITH, D. E., KEEP, R. F., XIANG, J. & BROSIUS, F. C., 3RD (2003) Targeted disruption of the PEPT2 gene markedly reduces dipeptide uptake in choroid plexus. *J Biol Chem,* 278**,** 4786-91.

SHEN, H., SMITH, D. E., YANG, T., HUANG, Y. G., SCHNERMANN, J. B. & BROSIUS, F. C., 3RD (1999) Localization of PEPT1 and PEPT2 proton-coupled oligopeptide transporter mRNA and protein in rat kidney. *Am J Physiol,* 276**,** F658-65.

SHU, C., SHEN, H., TEUSCHER, N. S., LORENZI, P. J., KEEP, R. F. & SMITH, D. E. (2002) Role of PEPT2 in peptide/mimetic trafficking at the blood-cerebrospinal fluid barrier: studies in rat choroid plexus epithelial cells in primary culture. *J Pharmacol Exp Ther,* 301**,** 820-9.

SMITH, D. E., JOHANSON, C. E. & KEEP, R. F. (2004) Peptide and peptide analog transport systems at the blood-CSF barrier. *Adv Drug Deliv Rev,* 56**,** 1765-91.

SMITH, D. E., PAVLOVA, A., BERGER, U. V., HEDIGER, M. A., YANG, T., HUANG, Y. G. & SCHNERMANN, J. B. (1998) Tubular localization and tissue distribution of peptide transporters in rat kidney. *Pharm Res,* 15**,** 1244-9.

SPECTOR, R. & LORENZO, A. V. (1974) Inhibition of penicillin transport from the cerebrospinal fluid after intracisternal inoculation of bacteria. *J Clin Invest,* 54**,** 316-25.

STRAZIELLE, N., KHUTH, S. T., MURAT, A., CHALON, A., GIRAUDON, P., BELIN, M. F. & GHERSI-EGEA, J. F. (2003) Pro-inflammatory cytokines modulate matrix metalloproteinase secretion and organic anion transport at the blood-cerebrospinal fluid barrier. *J Neuropathol Exp Neurol,* 62**,** 1254-64.

STROOBANTS, S., GERLACH, D., MATTHES, F., HARTMANN, D., FOGH, J., GIESELMANN, V., D'HOOGE, R. & MATZNER, U. (2011) Intracerebroventricular enzyme infusion corrects central nervous system pathology and dysfunction in a mouse model of metachromatic leukodystrophy. *Hum Mol Genet,* 20**,** 2760-9.

TAKAHASHI, K., NAKAMURA, N., TERADA, T., OKANO, T., FUTAMI, T., SAITO, H. & INUI, K. I. (1998) Interaction of beta-lactam antibiotics with H+/peptide cotransporters in rat renal brush-border membranes. *J Pharmacol Exp Ther,* 286**,** 1037-42.

TERADA, T., IRIE, M., OKUDA, M. & INUI, K. (2004) Genetic variant Arg57His in human H+/peptide cotransporter 2 causes a complete loss of transport function. *Biochem Biophys Res Commun,* 316**,** 416-20.

TEUSCHER, N. S., SHEN, H., SHU, C., XIANG, J., KEEP, R. F. & SMITH, D. E. (2004) Carnosine uptake in rat choroid plexus primary cell cultures and choroid plexus whole tissue from PEPT2 null mice. *J Neurochem,* 89**,** 375-82.

THOMAS, S. A. & SEGAL, M. B. (1998) The transport of the anti-HIV drug, 2',3'-didehydro-3'-deoxythymidine (D4T), across the blood-brain and blood-cerebrospinal fluid barriers. *Br J Pharmacol,* 125**,** 49-54.

# CHAPTER 5 PERSPECTIVE

The first objective of this dissertation demonstrated that cefadroxil elimination and distribution into kidney and choroid plexus were substantially reduced under LPS-mediated acute inflammation, resulting in significant increases in cefadroxil plasma concentration-time profiles. It appears that changes in transporter expression played a minor role during 6 hour pretreatment of LPS and that renal dysfunction, associated with reductions in GFR, was responsible for the substantial increase in cefadroxil plasma concentrations. However, the present study only focused on the early phase of inflammatory response and it has been increasingly reported that expression of drug transporters is downregulated during 24–48 hour LPS treatment, thereby affecting disposition of drug substrates. Inflammation-induced changes are time-dependent and, therefore, it would be worthwhile to investigate if PEPT2 and OAT protein expression levels are altered over 48 hour (or longer) after LPS pretreatment and if these changes influence the pharmacokinetics of cefadroxil. Moreover, potential alterations in hemodynamics should be investigated to fully understand the late phase of inflammatory response. In this way, the full spectrum of inflammation-associated changes could be evaluated, and its effect on drug disposition.

In the second objective of this dissertation, a population pharmacokinetic model was successfully developed to describe the distribution and elimination

kinetics of GlySar, a model PEPT2 substrate, using a nonlinear mixed effects modeling approach. Using PEPT2 knockout mice, the efflux mechanisms of GlySar at the BCSFB were separated into passive diffusion, CSF bulk flow, and active clearance mediated by PEPT2, while accounted for 77% of GlySar's total efflux pathways. However, drug transport systems at the BCSFB are changed during CNS inflammatory diseases, and these alterations appear to be associated with morphological changes of choroid plexus affecting passive diffusion and changes in transporter activity affecting the active clearance at the BCSFB. Considering our current findings that the efflux mechanisms of PEPT2 drug substrates at the BCSFB can be quantitatively separated, changes in each of those efflux mechanisms should be studied during CNS inflammatory diseases. In doing so, significant insight would be gained to further guide optimized dosing regimens of PEPT2 drug substrates, such as α-amino-β-lactam antibiotics, for treating CNS inflammatory diseases.

# APPENDIX A INTERSPECIES SCALING AND PREDICTION OF HUMAN CLEARANCE: COMPARISON OF SMALL- AND MACRO-MOLECULE DRUGS


## ABSTRACT

Human clearance prediction for small- and macro-molecule drugs was evaluated and compared using various scaling methods and statistical analysis. Human clearance is generally well predicted using single or multiple species simple allometry for macro- and small-molecule drugs excreted renally. The prediction error is higher for hepatically eliminated small-molecules using single or multiple species simple allometry scaling, and it appears that the prediction error is mainly associated with drugs with low hepatic extraction ratio (Eh). The error in human clearance prediction for hepatically eliminated small-molecules was reduced using scaling methods with a correction of maximum life span (MLP) or brain weight (BRW). Human clearance of both small- and macro-molecule drugs is well predicted using the monkey liver blood flow method. Predictions using liver blood flow from other species did not work as well, especially for the small-molecule drugs.


## INTRODUCTION

Allometric scaling is an empirical approach developed based on cross species similarities in anatomy, physiology, and biochemistry with a power function correlating physiological parameters with body size ($Y = aW^b$, where Y is the

parameter of interest, W is the body weight, and a and b are the coefficient and exponent of the allometric equation, respectively). This method has been applied to the projection of human pharmacokinetics for small-molecule drugs as well as therapeutic proteins and is widely used in the pharmaceutical industry for early decision making at several stages in drug discovery and development (e.g., lead compound selection and optimization, first dose in human, etc).

It is known that allometric projections generally work well for drugs mainly renally eliminated. However, for some small-molecule drugs with high cross-species variability in hepatic metabolism, this method may not work well in the extrapolation of hepatic metabolic CL from laboratory animals to humans. To improve the predictability of metabolic CL in humans, several modified scaling methods have been suggested and examined. Because longevity is frequently inversely correlated with hepatic cytochrome P450 drug oxidation rates, maximum life-span potential (MLP) and brain weight (BRW) were proposed as correction factors in allometric scaling by Boxenbaum (Boxenbaum, 1982). His work was later supported by other scientists, and their work also demonstrated that MLP and BRW corrections improved the accuracy of human CL prediction when the allometry power exponent b was higher than 0.80 – 0.90 (Feng et al., 2000, Mahmood and Balian, 1996). Recently, Nagilla and Ward suggested using liver blood flow (LBF) as a correction factor for the scaling of small-molecule drugs (Nagilla and Ward, 2004). Based on their analysis of 103 compounds comparing simple allometry with LBF or MLP/BRW correction, they concluded that scaling with monkey liver blood flow was

the best approach among the methods tested (68% success rate). These modified approaches have improved the accuracy of prediction to some extent.

While many studies have demonstrated the use of allometric scaling in the prediction of human CL for small-molecule drugs, only a few articles reported the application of this method to macro-molecule drugs. Currently, the market of biotherapeutics, including peptide, protein and oligonucleotide drugs have been growing rapidly. The annual growth rate of biotherapeutics sales was approximately 20% from 2001 and 2006, which is much higher compared to a growth rate of only 6 - 8% for small-molecule drugs (Aggarwal, 2007). Although the general principles of pharmacokinetics and pharmacodynamics are applicable to biotherapeutics, their disposition in the body is known to be unique and different from conventional small-molecules (Tang et al., 2004, Lin, 2009). The binding process of biotherapeutics with receptors or other targets in the body may be species-specific and saturable exhibiting non-linear kinetics. In addition, protein drugs derived from human sources may be recognized as a foreign compound in animal species and thereby induce immune system mediated reaction, known as immunogenicity. Therefore, differences are expected in interspecies scaling from animals to humans when comparing small- versus macro-molecule drugs. Since clearance is an important pharmacokinetic parameter critical for the design of first-time-in-human study and the selection of dose regimen, it is important to understand differences and the mechanism associated with the human clearance prediction between small and macro-molecule drugs.

Positive results from human clearance prediction of macro-molecule drugs using allometric scaling have already been reported by several groups (Mordenti et al., 1991, Mahmood, 2004, Mahmood, 2009b, Ling et al., 2009, Wang and Prueksaritanont, 2010). Mordenti et al demonstrated reasonable accuracy in predicting human clearance and volume of distribution using interspecies scaling for five protein drugs with molecular weights ranging from 6 to 98 kDa (Mordenti et al., 1991). Mahmood expanded the data set to 15 therapeutic proteins and reported a low prediction error of human clearance (Mahmood, 2004, Mahmood, 2009b). He also suggested the use of at least three animal species for interspecies scaling. However, acceptable prediction of human clearance using single animal species for macro-molecule drugs has also been reported later by Ling and Wang (Ling et al., 2009, Wang and Prueksaritanont, 2010). Ling et al suggested using a fixed exponent of '0.85' or '0.90' for human CL prediction of monoclonal antibody drugs, and '0.80' was suggested by Wang and Prueksaritanont not only for monoclonal antibodies, but also for other protein drugs.

In this study, literature data for small- and macro-molecule drugs were collected and analyzed by various allometry methods using single or multiple species scaling, and the accuracy of human clearance prediction was compared. For macro-molecule drugs, almost all the peptide and protein drugs previously reported in the literature with molecular weights ranging from 1 to 340 kDa were included in our data set, along with several oligonucleotide drugs. As a result, this study provides very useful information of the potential application of allometric scaling in human clearance prediction for both small- and macro-molecule drugs.

## METHODS

### Data collection

Clearance data of 675 small-molecule drugs and 80 macro-molecule drugs following intravenous administration were obtained from the literature. The criteria that divide the drugs into small versus macro-molecule is 1000 Da. Drugs having molecular weights greater than 1000 Da are regarded as macro-molecule and the others as small-molecule. Based on these criteria, all biotherapeutics including protein, peptide and oligonucleotide drugs were classified as macro-molecule drugs. The clearance of 81 of the small-molecule drugs in animals and humans were collected and used for the analysis of interspecies scaling and compared with 53 of macro-molecule drugs in human clearance prediction (Tables A.1 – A.2).

### Allometric scaling using single species

Human clearance was predicted using single species with the allometry exponent fixed at 0.60, 0.65, 0.70, 0.75, 0.80, 0.85, or 0.90. The following equation was used to calculate human clearance:

$$Clearance_{human} = Clearance_{animal} \times (BW_{human} / BW_{animal})^{b} \quad (1)$$

where BW is the body weight and b is the allometry exponent. Based on the availability of literature data, 36, 78, 78, and 63 small-, and 25, 40, 19, and 43 macro-molecule drugs were used in single species scaling for mouse, rat, dog, and monkey, respectively.

## Single species scaling using liver blood flow

Human clearance was estimated using liver blood flow (LBF) with the following equation as proposed by Ward and Smith (Ward and Smith, 2004):

$$Clearance_{human} = Clearance_{animal} \times (LBF_{human} / LBF_{animal}) \quad (2)$$

LBF values used for mouse, rat, dog, monkey and human were 90.0, 55.2, 30.9, 43.6 and 20.7 mL/min/kg, respectively (Davies and Morris, 1993). To be used in this equation, each LBF value was multiplied by the corresponding body weight. For example, for a mouse weighting 0.02 kg, the $LBF_{mouse}$ became 1.8 mL/min.

## Allometric scaling using multiple species

Several methods (i.e. simple allometry, exponent rule-corrected allometry, multiexponential allometry and exponent rule-corrected multiexponential allometry) were evaluated. At least three animal species were used for the scaling and the prediction of human clearance for each compound. Based on the availability of literature data, 81 small- and 36 macro-molecule drugs were used in multiple species scaling. Small-molecule drugs were divided by 3 groups based on elimination mechanism: (1) “hepatic” - if the drugs are mainly eliminated via metabolism or biliary excretion (n=50), (2) “renal” - if most of drug molecules are eliminated renally as unchanged (n = 19), (3) “mixed” – if both renal and hepatic routes contribute to the elimination (n=12).

### *Simple allometry (SA)*

Human clearance was predicted with the following allometric equation as previously described (Boxenbaum and DiLea, 1995):

$$Clearance = a(BW)^b \quad (3)$$

where a is the coefficient and b is the allometry exponent.

***Exponent rule-corrected allometry (ROE)***

As mentioned previously, Boxenbaum (1982) proposed using maximum life-span potential (MLP) and brain weight (BRW) as correction factors in allometric scaling since longevity is frequently inversely correlated with hepatic cytochrome P450 drug oxidation rates. The application of MLP and BRW were also assessed and supported by other scientists including Feng (Feng et al., 2000), and Mahmood and Balian (Mahmood and Balian, 1996). In this study, the exponent rule-corrected method previously suggested by Mahmood and Balian was adopted: If $b < 0.71$ in simple allometry, no correction factor was applied; if $0.71 \leq b < 1$, MLP was used as a correction factor; if $1 \leq b$, BRW was used as an correction factor. Human clearance was predicted using the following equations:

$$Clearance \times MLP = a(BW)^b \quad (4)$$

$$Clearance \times BRW = a(BW)^b \quad (5)$$

BRW values were 1.65, 0.57, 0.78, 1.56, and 2% of body weight, and the MLP values 2.7, 4.7, 22.0, 20.0, and 93.4 for mouse, rat, dog, monkey, and human respectively (Brown et al., 1997, Sacher, 2008).

***Multiexponential allometry (MA)***

Multiexponential allometry method was used to predict human clearance as suggested by Goteti et al using the following equation (Goteti et al., 2008):

$$CL = aBW^{b} + \left[\frac{(1-\frac{3}{2}b)}{(1-\frac{1}{2}b)}\right] aBW^{0.9} \quad (6)$$

where a and b are the coefficient and the allometry exponent determined from the simple allometry analysis.

***Exponent rule-corrected multiexponential allometry (SA+MA)***

Human clearance was predicted using simple allometry method if the exponent b is < 0.71 with no correction factor applied. If the exponent b is ≥ 0.71, the multiexponential allometry equation listed above was used for human clearance prediction.

## Relationship between CL and molecular size

Literature data of 675 small- and 80 macro-molecule drugs were collected and the correlation between total clearance and molecular weight (MW) was assessed.

## Statistical Analysis

Average-fold error (AFE) for human CL prediction was calculated based on equation 7 (Bolton, 1997) and used to compare the various prediction methods,

$$AFE = 10^{\Sigma|\log(predicted/actual)|/N} \quad (7)$$

By using this equation, under-estimations can have the same magnitude of error as over-estimations. For example, a 2-fold over-prediction and under-prediction would have the same value of 2 for AFE.

Students *t*-test was used to determine the statistical differences in AFE values between two groups and $p < 0.05$ was considered statistically significant. For multiple-group comparison in AFE values, analysis of variance (ANOVA) was performed followed by Tukey or Students *t*-test.

## RESULTS

### Scaling using single species

The results from single species scaling with a fixed allometry exponent are summarized in Figure A.1 – A.3. For macro-molecule drugs, human clearance is generally well predicted with average-fold error < 2 using a fixed allometry exponent of 0.75 – 0.80. Increase or decrease of the exponent "b" only results in a small fluctuation of the AFE (Figure A.1(a)). It appears that human clearance of macro-molecules is best predicted using monkey as a single species with the AFE value of 1.45, which is statistically lower ($p < 0.05$) than the AFEs of 1.89, 1.94, 1.72 using mouse, rat or dog for single species scaling with optimal allometry exponent fixed at 0.80 (Figure A.3). For the small-molecule drugs, human clearance is best predicted using a fixed allometry exponent of 0.65 - 0.70. The AFEs for small-molecule drugs increased significantly when the exponent "b" value was higher than 0.80 (Figure A.1(a)). The AFEs are 2.67, 2.31, 2.50, and 2.00, respectively, using mouse, rat, dog, or monkey as a single species with an optimal allometry exponent fixed at 0.65. Those AFE values are not statistically different across the species, although human clearance appears better predicted using monkey data. As shown in Figure A.1(c), when the small-molecule drugs are divided by 3 groups based on

elimination mechanism: “hepatic”, “renal” and “mixed”, similar trend is observed with human clearance best predicted using a fixed allometry exponent of 0.65 - 0.70 and the AFEs increased significantly when the exponent “b” value was higher than 0.80. The correlation between the prediction accuracy [ratio of predicted/observed (Pred/Obs)] and the actual value of human clearance for small-molecule drugs using single species allometric scaling with fixed exponent of 0.65 is presented in Figure A.2 and the plots suggest the prediction error is mainly associated with drugs with low extraction ratio.

Prediction of human clearance using single species liver blood flow is also examined in this study for macro- and hepatically eliminated small-molecule drugs, and the results suggest that human clearance is well predicted with AFE ≤ 2.0 for all drugs using monkey liver blood flow (Table A.3). However, the liver blood flow method did not work as well using other species especially for the small-molecule drugs with high AFE values of 4.04, 3.47, and 2.83 in mouse, rat, and dog, respectively.

**Scaling using multiple species**

The multiple species scaling methods, SA, ROE, MA and exponent rule-corrected MA (SA+MA), are evaluated in this study. Although several studies have reported the scaling of 2 animal species for the prediction of human clearance, we used three or more species in our analysis and the results are summarized in Tables A.4 and A.5. The results indicated that the SA method delivered a high accuracy in human clearance prediction for macro-molecule drugs with an AFE of 1.67, and no additional correction using MLP or BRW seems needed. This may be explained by

their elimination mechanism. The therapeutic proteins are mainly eliminated by non-specific proteolysis that is very different compared to the complicated oxidative metabolic pathways for small-molecule drugs. Therefore, the use of ROE, MA, and SA+MA did not improve the prediction of human clearance for macromolecule drugs and resulted in a higher AFE of 2.06, 1.87, and 1.95, respectively. As mentioned previously, the small-molecule drugs were grouped by mechanism of elimination to assess if the elimination mechanism may affect the prediction accuracy of human clearance. As listed in Table A.4, for drugs in the "renal" group, the human clearance is generally well predicted using simple allometry with AFE of 1.84 and it appears that no MLP or BRW correction is needed for those drugs. The AFEs from ROE, MA, and SA+MA methods are 1.95, 1.73, 1.66, respectively and not statistically different from the AFE of the SA method. The AFE of human clearance prediction is 3.14 using the SA method for drugs in the "hepatic" group, which is statistically significantly higher than the values in other groups ($p < 0.05$). Results from additional analysis presented in Table A.5 indicated that the prediction error for hepatically eliminated small-molecules is mainly associated with drugs with low hepatic extraction ratio (Eh) with AFE of 4.51. The AFE is 2.46 and 1.35 for drugs with medium and high Eh, respectively, and the AFE in the high Eh group is significantly lower ($p < 0.05$) than the corresponding values in the other two groups, which is consistent with the outcome from single species scaling (Figure A.2) and the literature information as the elimination process of drugs with high Eh is mainly controlled by liver blood flow, a physiological parameter extrapolated very well from animals to humans (Feng et al 1998a and 1998b). Correction with MLP or BRW did help to reduce the

prediction error for hepatically eliminated drugs with low and medium Eh. The AFE is 2.25 for small-molecule drugs in the mixed group and the correction with MLP or BRW also reduced the error of prediction (Table A.4).

### Relationship between CL and molecular size

The relationship between human clearance and molecular weight is presented in Figure A.4. The small-molecule drugs were divided into 3 groups with MW < 300Da in group 1 (n = 233), 300 ≤ MW < 400Da in group 2 (n = 221); and 400 ≤ MW < 500Da in group 3 (n = 221). Based on one-way ANOVA analysis, the clearance values in the 3 groups are not statistically different ($p > 0.05$). The macro-molecule drugs were also divided into 2 groups with MW < 69kDa in group 1 (n = 49) and MW ≥ 69kDa in group 2 (n = 29). The clearance values in group 2 are significantly lower and statistically different compared to those in group 1 based on *t*-test ($p < 0.01$).

## DISCUSSION

### Scaling using single species

Single species scaling with a fixed allometry exponent or using LBF was evaluated in the current study. Although there are different opinions regarding the use of single species scaling (Mahmood, 2009a, Mahmood, 2005), the method does have advantages in the respect of cost-effectiveness. Finding an optimal value for the allometry exponent in single species scaling is always a challenge. Although previous studies have suggested there could be a universal exponent value across animal species, the reported results are still controversial (Hu and Chiu, 2009, Hu

and Hayton, 2001). In our study, optimal allometry exponent values of '0.65 - 0.70' with AFE of 2.40 – 2.49 were identified that generally worked best for human clearance predictions for small-molecules, while for the macro-molecules, optimal exponent value of '0.75 - 0.80' with AFE of 1.75 – 1.77 were selected. These values are close to the historically recommended standard exponent value of '0.75' in interspecies scaling derived from the observation that basal metabolic rates across species could be scaled by body weight with an exponent of '0.75' (Kleiber, 1947, Feldman and McMahon, 1983). For the macro-molecules, the prediction error from single species scaling is generally within 2-fold for majority of the drugs in our analysis (Figure A.3), which is consistent with other results in the literature (Ling et al., 2009, Wang and Prueksaritanont, 2010). Most macro-molecule drugs are peptides or proteins that are eliminated from the body via non-specific proteolysis, a process very different from the complicated oxidative metabolic pathways for small-molecule drugs. It is known that ubiquitously expressed proteolytic enzymes responsible for the elimination of macro-molecules are universal across animal species, which could help to explain the successful extrapolation from animals to humans for macro-molecule drugs. As mentioned previously, several antisense oligonucleotide drugs (e.g., ISIS compounds) were included in the macro-molecule category. Oligonucleotide drugs are mainly eliminated from the body by metabolic pathways via nucleases (Levin, 1999, Levin et al., 2001). Nucleases are also ubiquitously expressed throughout the body and could be scaled across animal species. Interestingly, it has been shown that the plasma clearance values of ISIS compounds are quite similar in rat, rabbit, dog and monkey ranging from 1 to 3

mL/min/kg (Geary et al., 2001). Several outliers (infliximab, IFNβ and EGFr3) with relatively high prediction errors (6- or 7-fold) were, however, observed in our analysis of macro-molecules (Figure A.3), which may be the result of species-specific differences in binding activity and non-linear pharmacokinetics. While human IFNs bind to receptors in monkey, they lack binding activity in rodents (Kagan et al., 2010). This may help to explain why the prediction error of IFNβ was high when mouse or rat was used in single species scaling. Non-linear pharmacokinetics can be a potential explanation for the high prediction error of EGFr3 in dog, since a relatively low dose was used for the pharmacokinetic study of EGFr3 in dogs compared to other preclinical studies as previous study has shown (Wang and Prueksaritanont, 2010). For small-molecule drugs, the plots in Figure A.1 and A.2 suggest that human clearance is better predicted using monkey data although the cross-species comparison of AFEs does not indicate statistical differences.

The LBF method appears useful in human clearance prediction for both small and macro-molecule drugs when monkey data are available. If data from other animal species were used, the prediction accuracy may be acceptable for most of the macro-molecule drugs (within 2-fold), but the error appears high for small-molecule drugs.

### Scaling using multiple species

Interspecies scaling using 3 or more animal species was also evaluated in this study. The results suggest that the SA method delivered a high accuracy prediction of human clearance for macro-molecule drugs (AFE = 1.67, Table A.4),

which is consistent with the phenomena that the clearance mechanism of macro-molecule drugs is evolutionally well conserved compared to the species-specific metabolism of small-molecule drugs. Only EGFr3 is a notable outlier in the SA method and it may be associated with nonlinear pharmacokinetics as previously discussed.

In general, the SA method also worked well with AFEs < 2.0 for small-molecule drugs excreted renally (Table A.4). The AFE from the SA method is higher for drugs mainly eliminated hepatically, and a correction with MLP or BRW (using the ROE, MA, or SA+MA methods) helped to reduce the prediction error for those drugs (Table A.4 and A.5). The correction with MLP was proposed in 1982 by Boxenbaum based on the observation that longevity was frequently inversely correlated with hepatic cytochrome P450 drug oxidation rates (Boxenbaum, 1982, Boxenbaum and Ronfeld, 1983). The MLP•Clearance product represents the volume from which drug would be cleared per person's maximum life-span potential assuming constant drug exposure. Using antipyrine as an example, Boxenbaum demonstrated that the regression of volume cleared per MLP is approximately proportional to body weight. With respect to humans, it would appear that the relatively low intrinsic unbound clearance (with respect to liver weight) is synchronized to his (or hers) longevity; i.e. the low activity is conserved over the relatively longer chronological MLP. Boxenbaum also explored the possibility of using brain weight (BRW) as a correction factor since MLP is closely correlated to BRW ($MLP = 185.4(BRW)^{0.636}(W)^{-0.225}$). Boxenbaum's work was later supported by the results of other scientists. Results from our previous work also demonstrated

that the MLP and BRW correction improved the accuracy of human clearance predictions when the allometry power exponent b was higher than 0.80 – 0.90 (Feng et al., 1998a, Feng et al., 1998b, Feng et al., 2000, Mahmood and Balian, 1996). The results from our current study indicated that multiple species scaling generally worked better than single species allometry for small-molecule drugs, and the ROE, MA and SA+MA methods using a correction with MLP or BRW could help to increase the accuracy of prediction for small-molecule drugs mainly hepatically eliminated. However, there were a few notable outliers with high prediction error even after using MLP or BRW as a correction factor. All these drugs are mainly hepatically eliminated either by metabolism or by biliary excretion and have relatively low clearance.

**Relationship between CL and molecular size**

The results of this study also indicated that the pharmacokinetic properties of small- and macro-molecule drugs are quite different when the relationship between clearance and molecular weight was examined. A trend for macro-molecules is observed (Figure A.4), in which the CL values of those drugs in group 2 (MW ≥ 69 kDa) are significantly lower than those in group 1 (MW < 69 kDa). It is generally known that a molecule with MW < 10 kDa is readily excreted by glomerular filtration in the kidney, while a molecule with MW ≥ 69 kDa (MW of albumin ≈ 69 kDa) is highly restricted at the glomerulus (Braeckman, 2000, Lin, 2009). Therefore, glomerular filtration could limit the renal excretion of group 2 drugs, and this may help us to understand the differences in clearance between group 1 and 2. However, one needs to be cautious in directly relating clearance with

molecular weight, since MW does not necessarily represent the effective molecular size and the effective molecular radius may be a better way to determine the degree of glomerular filtration. Drug molecules in group 2 may be eliminated mainly by non-specific proteolysis or receptor mediated degradation. Other physicochemical properties such as lipophilicity, charge and functional groups may further influence the distribution and elimination mechanisms (Braeckman, 2000).

In summary, human clearance of macro-molecule drugs may be predicted using single-species allometric scaling with an optimal component value of "0.80' or using multiple-species simple allometry scaling. No correction by MLP or BRW seems needed for the scaling of macro-molecules probably due to their elimination mechanism. The therapeutic proteins are mainly eliminated by non-specific proteolysis that is very different compared to the complicated oxidative metabolic pathways of the small-molecules. In general, human clearance of small-molecule drugs may be predicted (AFE value of 2.0) using monkey body weight scaling and an optimal allometry exponent value of "0.65". However, the prediction appears less accurate when mouse, rat or dog data are used for single species allometric scaling. Human clearance is also well predicted using SA method with AFE < 2.0 for small-molecules renally excreted. The prediction error is higher for small-molecules hepatically excreted, and correction using MLP or BRW (ROE, MA and SA+MA methods) could help to reduce the prediction error. Human clearance of both small- and macro-molecule drugs could also be predicted using the monkey liver blood flow method, but the prediction using liver blood flow from other species did not work as well especially for the small molecules.

For small molecule drugs with complicated oxidative metabolic pathway and significant cross-species differences in hepatic metabolism, the simple allometry power equation may not work well for the estimation of human clearance, and in addition to MLP and BRW, other correction factors (e.g. liver blood blow, in vitro metabolic clearance, free fraction in blood, binding affinity to receptors or subcellular components, etc.) have been proposed to enhance the accuracy of prediction. Each of these techniques mentioned above has its own merits and drawbacks, and some of them have had only partial success in predicting human clearance. Research work using in vitro, in vivo, and in silico models are still ongoing to further improve the estimation accuracy of human pharmacokinetic profiles to help reducing the risk and the tremendous financial costs associated with failed clinical trials.